CHALMERS
UNIVERSITY OF TECHNOLOGY

Chiral Effective Theory of Spin-1 Dark Matter - Nucleon Scattering.

Master's thesis in Physics

Arvid Ryberg

DEPARTMENT OF SUB-ATOMIC, HIGH ENERGY AND PLASMA PHYSICS
CHALMERS UNIVERSITY OF TECHNOLOGY
Gothenburg, Sweden 2025
www.chalmers.se

Master's thesis 2025

Chiral Effective Theory of Spin-1 Dark Matter - Nucleon Scattering.

ARVID RYBERG

Department of Physics
Division Sub-atomic, High Energy and Plasma Physics
Chalmers University of Technology
Gothenburg, Sweden 2025

Chiral Effective Theory of Spin-1 Dark Matter - Nucleon Scattering
ARVID RYBERG

Supervisor: Riccardo Catena, Department of Physics
Examiner: Riccardo Catena, Department of Physics

Master's Thesis 2025
Department of Physics
Division of Sub-atomic, High Energy and Plasma Physics
Chalmers University of Technology
SE-412 96 Gothenburg
Telephone +46 31 772 1000

Typeset in LaTeX
Printed by Chalmers Reproservice
Gothenburg, Sweden 2025

Chiral Effective Theory of Spin-1 Dark Matter - Nucleon Scattering.
ARVID RYBERG
Department of Physics
Chalmers University of Technology

Abstract

This thesis aims to investigate the elusive dark matter via formulation of its interaction with normal matter. This approach is commonly known as direct detection which is an active field of dark matter research, both theoretically and experimentally. We treat the dark matter as a heavy complex vector field, corresponding to a massive spin-1 particle, which weakly interacts with a nucleus. The thesis utilizes effective field theory and chiral perturbation theory to create a general interaction Lagrangian. Starting in a relativistic approach, quantum mechanical interaction operators are found which in turn can be used to calculate scattering amplitudes. The thesis assumes non-relativistic and heavy dark matter to perform a non-relativistic reduction which aims to investigate what constraints and bounds created in the relativistic regime that lives on in the non-relativistic limit. The results are compared to previous work within the field which leads to a comprehensive analysis of the situation.

Acknowledgements

I would like to take this opportunity to give my outmost and sincere thanks to some truly wonderful people who all, in different ways, have been huge contributors to this thesis. First and foremost, I thank my supervisor professor Riccardo Catena for his guidance and his invaluable support. Even in busy times, with many master's students to look after, you always found time and energy to help me, for that I am very grateful. Your expertise within the field is a remarkable asset for any student working for you.

Secondly, I want to thank all the wonderful people at the High energy, Sub-atomic and Plasma physics department at Chalmers. It has been a joy to get a glimpse of the inspiring and complex work that you all do.

Finally, I am lucky to have amazing friends and family around me. Thank you to my partner Gabriella, my brother Olof and my parents. You always make me the best possible version of myself, and I'm grateful to share my life with you.

Arvid Ryberg, Gothenburg, 2025

Contents

List of Figures

List of Tables

1

Introduction

Even to this day the scientific community has a vanishingly small knowledge about the majority of our Universe. One of these unknown areas regards the so called dark matter (DM), which is the name given to all mass that so far has avoided the scientists eyes. Many of the properties of DM are unknown, but there is a general acceptance of its existence. This idea, that a huge part of the total mass in the Universe is unobserved, was originally concretized by astronomer Fritz Zwicky in 1933 when he observed a ”gravitational anomaly” regarding galaxies in clusters [11, 12]. Zwicky credited this anomaly to some unseen mass which he labeled ”Dunkle Materie” (german, dark matter). Although this observation is now almost 100 years old it still holds one of the more profound evidences for the existence of DM, namely that the gravitational effects of the visible matter is far from enough to create the dynamics of galaxies that we quite clearly observe.

In the decades following Zwicky's paper, numerous additional measurements and observations on different cosmological scales have left little doubt over the existence, and effects, of DM. However DM is still avoiding detection on a microscopic level and the attempts to understand more about its nature are one of the most active and prominent fields of modern theoretical physics [13].

Since DM has not been observed in our traditional ways of detection it has been concluded that DM interacts extremely weakly, or not at all, with the electromagnetic field which means that it neither emits or blocks light. Further, DM seems to interact very weakly with ordinary matter (visible matter, quarks, nucleons etc., abbreviated SM for standard model matter) since no large scale ”collisions” between DM and SM have been observed. However, since the DM carries mass, some type of exchange needs to occur when a DM particle collides with a quark or a nucleon. One can think of the interactions between DM and SM to consist of three different processes, depending on the chosen direction in the Feynman diagram. To understand this, one can consider Fig. 1.1 where the different processes *Direct detection, Indirect detection* and *particle collision* are marked. The sketch in Fig. 1.1 is rather simple, for a more detailed picture the reader is advised to see [14].

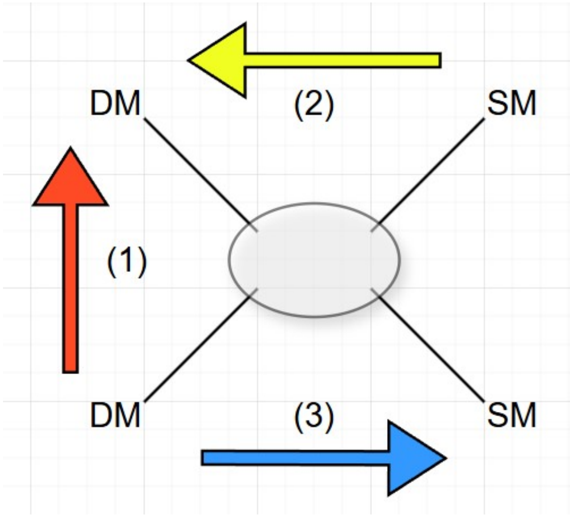

Figure 1.1: A simple sketch of a Feynman diagram showcasing the interaction between DM and SM. (1): The red arrow pointing upwards represents direct detection, i.e., the scattering of a quark/nucleon and a DM particle. (2): The yellow arrow pointing to the left is what might be observed in a collider, two SM particles annihilated to create two DM particles. (3): The blue arrow to the right shows indirect detection, the annihilation of two DM particles creating two SM particles.

In this thesis, the direct detection is studied, and a more thorough description of the process will follow in section 2.3. This thesis also gives a brief overview of the other two processes in Fig. 1.1, found in sections 2.4 and 2.5.

1.1 Outline of the thesis

The outline of this thesis is:

- Chapter 2 provides a general background to the topic of DM as well as a discussion on how to model a DM-nucleon interaction.
- Chapter 3 contains the necessary theory, with focus on explaining the interaction between DM and SM with an interaction Lagrangian.
- Chapter 4 states the theoretical methods used throughout the work.
- In chapter 5 the results are presented alongside a discussion on their importance and some noteworthy examples.
- Chapter 6 accommodates an outlook where possible continuations of the work in this thesis are discussed.
- In chapter 7 a concise conclusion is presented.

The five appendices are structured as:

- Appendix A deals with the heavy vector fields and how to model a spin-1 DM particle.
- Appendix B converts useful equations into new forms, related to the properties of the DM.

- Appendix C shows how to identify all relativistic interaction operators used in the thesis.
- In appendix D all scattering amplitudes are calculated.
- Lastly, appendix E couples the found scattering amplitudes to a new basis, where comparisons with previous work can be done.

2
Background

This chapter introduces the subject of interest, i.e.„ DM. A broad overview of the field is included, containing historic insights, descriptions of different DM models in general, and the WIMP-model specifically. Further, the three possible ways of looking for DM are introduced and described, with extra focus on the direct detection, as this is the technique used in this thesis. Finally this chapter includes a discussion on how to model DM-nucleon interactions, and how different models yield different advantages.

2.1 History of Dark Matter Theories

As it's been almost 100 years since the idea of DM was forged, naturally many different theories of its origin have fluctuated. For a more complete overview, see [24]. In this thesis only a few of the concepts are discussed.

One of the first candidates for DM were so called Massive Compact Halo Objects (MACHO). MACHO is a collective name given to objects floating through space unbounded to other large structures (such as galaxies or solar systems). On the small scale this includes brown dwarfs and unassociated planets whereas on the large scale black holes and neutron stars also are treated as MACHO candidates. These are all astronomical bodies that at first seemed to make good candidates for DM. However, after more recent observations an upper boundary on the mass of MACHO has been confirmed. It's in fact impossible that MACHO make up more than 8% of the total mass credited to DM. So even though the contribution of MACHO might be non-negligible, it became clear that the search for another DM candidate was needed [25].

The Standard Model (SM) of particle physics provides another contestant to the DM mystery. The mass of neutrinos was for a long time undetermined (thought to be massless) and it was only quite recently that scientists have been able to at least give an estimation of it [26]. This at first led to the theory that the neutrinos might be the sought DM, but quite quickly this idea was shattered thanks to cosmological constraints (the mass required by the neutrino to be eligible as a DM candidate gives a coherence length that is inconsistent with many other parameters)[27].

Moving on from the SM, there has been big hope that particles beyond the standard model (BSM), which are made possible by considering Super-Symmetry (SUSY), can be the DM. SUSY is to this day the best framework that is available, as it offers the possibility of a large variety of new, so far, undetected particles to be present in BSM. The problem is of course that these particles are still undetected. As advancements are made, both in cosmology and particle physics, the picture of how the DM "should" look like has cleared ever so slightly. One such prediction is that DM is so called Weakly Interacting Massive Particles (WIMPs) on the mass scale of > 1 GeV [13]. The framework that DM is indeed WIMPs will be used throughout this thesis and hence the phenomenology of WIMPs will be explained in more detail.

2.2 Weakly Interacting Massive Particles

WIMPS are, and have been, one of the most prominent candidates for DM. There are several reasons for the scientists fascination with this type of particle, most clearly is the so called "WIMP miracle" which refers to the fact that particles with weak interactions and non-zero masses naturally yield a relic abundance that matches the observed DM density obtained through thermal freeze out during the early universe [28]. This unexpected matching seemed too much of a coincidence for WIMPs not to be important. To render this correct density, one further has to assume that the WIMP DM is stable over the life-time of the Universe, which allows for modeling WIMP-DM without too much regard for decays [28].

The most common way to search for WIMPs is via direct detection, where the heavy DM particle (hopefully) are massive enough to render a recoil in the nucleon which can then be measured. Due to the many nice qualities of WIMPs a tremendous amount of effort and money has been put into experiments looking for them. They have all yielded null results. As a consequence, the parameter space for WIMPs is now heavily restricted, as can be seen in Fig. 2.1, which is collected from [5]. This has led to a decreasing belief within the community that WIMPs are indeed the answer to the mystery of dark matter [28]. Still, the possibility remain and further research of WIMPs is of outmost importance, especially if one are to tweak one of the more fundamental properties, such as spin. Almost all the prior works on WIMPs regards spin-0 or spin-1/2, making this study on spin-1 both interesting and very important.

2.3 Direct Detection

As stated in Fig. 1.1, direct detection (DD) is the process where a DM particle scatters on a nucleon (or a quark). This scattering would give rise to changes in momentum and energy of the nucleon, something that could be measured. A successful measurement of DD would greatly improve the knowledge of DM on the microscopic level and is therefore of high priority. Although DD experiments are seen as one of the most promising ways of finally finding DM, it is worth noting that despite tremendous efforts and many extremely advanced projects, there is still no conclusive result from any DD tests [29]. It is however still an active field of research and the hope within the community is that more and more precise equipments and a general development of detectors will prove fruitful.

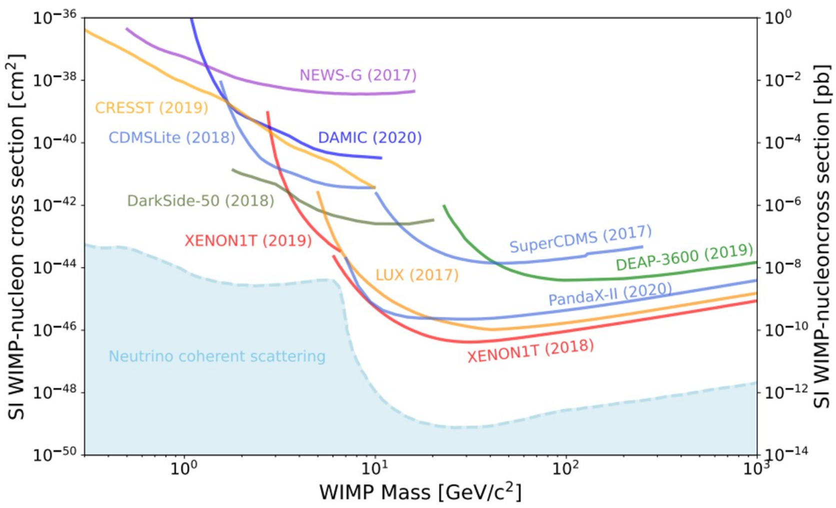

Figure 2.1: An exclusion plot showing the areas where direct detection experiments have probed for WIMP DM. The spin-independent cross-section is expressed as dependent on the DM mass, and anything above the lines is excluded by the corresponding experiment. This figure was first seen in [5].

But how could one construct such an experiment, when DM still avoids detection? Luckily, the pure volume of DM in the Universe makes things easier. From the Cosmic Microwave Background (CMB) spectrum it has been concluded that DM is responsible for roughly 85% of all mass in the Universe (the overall energy density is confirmed to be ca 68% dark energy, 27% DM and 5% SM) [31]. It is therefore easy to assume that DM particles would constantly bombard the solar system and our earth. Since DM is thought to be WIMP, it is also logical to think that this bombardment (almost) goes straight through [30]. One could further utilize the fact that DM has to be ”slow”, i.e., non-relativistic in order to be gravitationally bounded as observations imply. In fact, as argued in [8] the velocity of DM trapped in our galaxy should be of the order $v_{\text{DM}} \approx 10^{-3}c$. One can safely make the assumption that the DM that hits earth is of this non-relativistic kind, rather than the high-energy DM that would not be gravitationally bounded but instead free to roam the Universe at its own will.

One can put an upper bound on the momentum exchange q within the scattering between non-relativistic DM and nucleons. This limit has been confirmed by e.g. [33] to be roughly $q_{\text{max}} \lesssim 200$ MeV[1]. This is much less than the mass of the nucleon and hence it implies that the nucleon remain non-relativistic and intact after the scattering process. This thesis utilizes said assumptions, treats the momentum q as very small and that both the DM and SM matter remain non-relativistic throughout

[1]This limit is sought via the relation $q = 2\mu v \cos\theta$, with μ being the reduced mass, $\frac{m_X m_N}{m_X + m_N}$ for the WIMP DM m_X and the nucleon m_N, v being the initial velocity for the WIMP DM and θ being the scattering angle. Thus $q_{\text{max}} = 2\mu v$ which, with $v \approx 10^{-3}$ and appropriate estimates for m_X and m_N, gives a rough max value of 200 MeV [36].

the entire process.

2.3.1 Direct Detection. Experimental Set-Up

In this subsection, a brief overview of the experimental set-up of DD processes is given. A broader and more precise background can be found in e.g. [30].

Typically, the locations for DD experiments are chosen deep underground, as to minimize the noise from the surrounding. Since the DM discussed in this thesis is of the type WIMP it can be assumed to reach deeper into the earths surface than other particles which reduces the risk of unwanted interference. The basic idea is to let a suitable sample of nucleons be the target, placed deep underground and then wait for the DM to interact with the target in such a way that light is emitted. Often, the experiments are conducted as far down as 1.5 km underneath the surface level. It is common to use old gold mines or naturally occurring caves to host the tests [39]. An example of such a set-up is the LUX-ZEPLIN detector, which in 2019 was lowered into an abandoned gold mine in South Dakota. The detector is filled with liquid Xenon and has a total of 625 photomultiplier tubes positioned at the edge of the cryostat where they hope to catch the flashes of light emitted from the DM-SM interactions [39].

Liquid noble-gases are indeed the most common form of nucleons used in DD experiments, more specifically liquid Argon (LAr) and liquid Xenon (LXe). LAr is suitable for WIMP detection since its time-characteristics makes a clear difference between nuclear recoil (which emits light with a time constant of order nanoseconds) and gamma- and/or beta excitations (time constants of order microsecond). It is thus easy to effectively discriminate the background noise and single out the emissions that are linked to WIMP-nucleon interaction [34]. LXe exhibits the same positive properties as LAr and in addition the scattering is weighted by atomic mass of the target, as per [35] which of course means that the scattering cross section would be larger from LXe than from LAr. Overall both LAr and LXe are prime substances for DD of DM of the WIMP-type.

2.4 Indirect Detection

From Fig. 1.1 one concludes that Indirect Detection (ID) is the process where two DM particles annihilate to create two SM particles. However, in most literature the term ID also includes DM decay, not just annihilation (see for example [37]). The search for DM via ID is hence a bit more complicated, as one needs to confirm that a pear of SM particles that might be observed are in fact the result of a DM annihilation.

Usually, the particles created via ID are categorized into one of three groups: *gamma-ray photons, neutrinos* and *cosmic rays* [37]. Each of these groups have several different research-projects linked to them, both past and planned.

2.4.1 Gamma-Ray Telescopes

From the assumed mass of WIMP DM it is believable that a large portion of the energy emitted in an annihilation (or a decay) ends up in the gamma-ray spectra. Further, the properties of gamma-rays allow them to travel through space without any larger deflections, which enables the telescope that observes them to also gain information about its source [37]. Seeing how the atmosphere blocks gamma-rays, the observing telescope needs to be launched into space. An example of such a telescope is the Fermi Large Area Telescope (LAT) which, since its launch in 2008, looks for gamma-rays in the range of 20 MeV to approximately 300 MeV [38]. However, gamma-rays are a frequently occurring phenomena in space, and to separate the gamma-rays of interest (from DM) from other types proves a difficult task.

2.4.2 Neutrino Detectors

Just as for gamma-rays, neutrinos are almost interaction-free which allows them to carry information about its source all the way to the detectors. In contrast to gamma-rays however, they don´t mind the atmosphere at all and can thus easily be observed on earth. This detection is usually done in very large bodies of ice or water, up to a cubic-kilometer in volume [37]. The range for detection via these kind of experiments is usually around $\sim$ 10 GeV. A natural downside to Neutrino detectors is that since the observations occur on surface level, a large background noise is expected and difficult to deal with.

2.4.3 Cosmic-Rays Detectors

One could also find traces of DM creation/annihilation in charged cosmic-ray fluxes. These searches are highly sensitive, thanks to the low background of similar looking radiations [37]. However the cosmic-rays diffuse on their travel through the galaxy, and hence it is much more difficult to determine a signals origin than for the two processes described above in 2.4.1 and 2.4.2. The search for cosmic-rays is performed in space, e.g. the so called Alpha Magnetic Spectrometer (AMS-02) which was installed on the International Space Station (ISS). The AMS-02 uses a permanent magnet to determine both sign and charge of particles passing through and it is sensitive in the range of a few hundred MeV to TeV [32, 37].

2.5 Collider Processes

Collider searches are most commonly used when looking for sub-GeV DM, i.e., when the energy is deemed to low to cause a measurable scattering via direct detection [41]. Hence, WIMPs are not mainly the sort of DM one would expect to find here. For collider processes to yield WIMP-related results, it would have to be at the LHC or similar to reach the required energies. However, as this sections focus is to introduce the reader to the general search tools for DM, the fact that the following subsections does not apply to WIMPs can be ignored.

From Fig. 1.1, collider processes revolve around having two SM particles interact and studying the outcome. This can be done in several different ways, but the main aspects is the ”fixed target” approach where a beam of high energy SM particles (usually protons or electrons) are launched into a target at rest in the lab frame (the target should consist of a proton-dense element). A brief overview of the field will follow below but as it lays outside of the scope of this thesis the reader is advised to see [41] for a much more comprehensive study.

What is sought in fixed target experiments is the DM flux that could be produced through the beam-target interaction. This flux would then be noticeable either as lost momentum for the outgoing SM particles, or in a more ”direct-detection way” downstream from the interaction (where electrons are used as targets instead of nucleons, since the lower energy would make observations of momentum change in a big, heavy, nucleon difficult). There are several ways that this DM flux could be created, two of which is explained in more detail. These are called *meson decay* and *dark Bremsstrahlung*.

2.5.1 Meson Decay

One product of the interaction between the beam of high energy particles and a target would be a bunch of mesons (lightest color-neutral object in the SM, consisting of a quark and an anti-quark, e.g the *pion*, $\pi^+ = u\bar{d}$). These mesons could then decay into *dark photons* (denoted A' [41] or γ' [43]) which are hypothetical DM particles with great potential for detection. The scope of this thesis does not allow any in depth discussion about the dark photon and the reader is therefore strongly encouraged to see [42] for more information about this intriguing subject. In the case of mesons, the decay line for a fixed target experiment would look like this

$$pp \to \alpha\pi^0; \pi^0 \to \gamma A'; A' \to \bar{X}X. \tag{2.1}$$

Here, X is a DM particle, α are rest products of the proton scattering and γ is an ordinary photon.

2.5.2 Dark Bremsstrahlung

The ordinary Bremsstrahlung process consists of a charged particle (usually an electron) losing energy due to interaction with another charged object (usually a nucleus). In introductory courses in QFT it is common to use Bremsstrahlung to investigate the scattering of electrons, see for example [6].

For the case of dark Bremsstrahlung, one simply lets a dark photon be the carrier of the lost energy for the electron scattering. A decay line can be seen below (each particles momentum is put in parentheses)

$$e(p) + N(P) \to e(p') + N(P') + A'(k), \tag{2.2}$$

where N is the nucleus that the electron scatters against.

2.6 Modeling a DM-nucleon scattering

The modeling of nuclei-DM interactions can generally be done in three different ways, either from a non-relativistic approach, from a relativistic one or from a so called simplified model [21].

The non-relativistic approach means that the DoF are the DM and the nucleons. The interaction is considered to obey Galilean symmetry and can be described by a set of non-relativistic basis quantum operators.
The relativistic approach instead considers Effective Field Theory (EFT) (see section 3.3) to build a general quark/gluon-DM interaction Lagrangian which obeys Lorentz symmetry.
The simplified model expands the SM to include a DM particle as well as a mediator which is responsible for the interaction (see Fig. 3.1). These three models are all related to each other, and a big part of this thesis is to observe how constraints from one model might be carried over to another one. The line of thought to connect the three approaches is as follow:

- When the momentum transferred in the interaction is less than the mass of the mediator, the simplified model reduces to the EFT of the relativistic model.
- When the momentum transfer is also less than the masses of the DM and the nucleon while the DM is moving at non-relativistic velocities, the relativistic quark/gluon-DM interaction operators simplifies into a linear combination of the non-relativistic quantum operators of the non-relativistic approach [21].

It has already been established that this thesis considers momentum transfers much less than the DM and nucleon mass. It has also been stated that the DM is considered to move slow and thus it would be logical to immediately consider the non-relativistic approach. However, as is found out in the results of this thesis, by using the relativistic approach and then evaluating it in the non-relativistic limit unexpected constraints occur. For one thing, it will turn out that not all the quantum operators of the non-relativistic approach are needed (at leading order). Further, the simplified model is needed in order to describe the interaction mediated by a meson i.e., the right panel of Fig. 3.1.

2.6.1 The Models Used in This Thesis

Instead of going straight to the non-relativistic approach, this thesis starts in the simplified model, identifying two leading order Feynman diagrams. Via the assumption of $q \ll m_G$ the relativistic EFT is built. Later, by the non-relativistic property of DM one can move into the same basis as the non-relativistic approach. This procedure (moving from the simplified model to the relativistic approach into the non-relativistic approach) has been done rigorously for spin-0 and spin-1/2, but much less so for spin-1 [21].

3

Theory

This chapter will present the necessary theory needed to understand the work of the thesis. It begins with a preliminary background to Quantum Chromo Dynamics (QCD), the associated symmetries and some discussions about Pseudo-Nambu-Goldstone-Bosons (PNGBs). It then discusses the expansion of QCD with external currents via the inclusion of spurions. The chapter also includes an introduction to Effective Field Theory (EFT) as well as Chiral Perturbation Theory (ChPT). Further a section is devoted to the dark matter field, and how applying heavy quark effective theory splits the DM field into two parts, which enables a smoother analysis of its properties. From there one moves on to the concept of QCD-DM interaction Lagrangians where the terms of the most general form of $\mathcal{L}_{\text{int}}$ will be ordered based on their relevance. This interaction Lagrangian is then expressed in terms of quark/gluon and DM currents, something that will prove useful in the subsequent section, which discusses the scattering process and the framework of finding the scattering amplitude. This section also defines the two Feynman diagrams which will be used in this work. Lastly, this chapter analyses the non-relativistic effective Lagrangian and how the scattering amplitudes found in this thesis can be matched onto a set of non-relativistic basis operators which will enable comparisons of the current work to what has been done previously.

3.1 Quantum Chromodynamics

When describing the quarks in the SM it is enough to consider their interaction through the strong force, which is about 100 times stronger than the other three fundamental forces (gravity, electromagnetism and the weak force). This assumption leads to the theory of QCD, which encodes the quarks and their interactions into a Lagrangian $\mathcal{L}_{\text{QCD}}$. Quarks are fermions meaning that their field is a Dirac field which depends on the covariant derivative D_μ. The carrier of the strong force is called a gluon and its field strength tensor is denoted by $\mathcal{G}_{\mu\nu}$. One writes the QCD Lagrangian as

$$\mathcal{L}_{\text{QCD}} = \sum_{f=u,d,c,s,t,b} i\bar{q}_f \left(\gamma^\mu D_\mu - m_f\right) q_f - \frac{1}{4}\mathcal{G}_{\mu\nu}\mathcal{G}^{\mu\nu}, \tag{3.1}$$

where, $\bar{q} = q^\dagger\gamma^0$.

Thanks to experiments, e.g., at the Large Hadron Collider (LHC), one now has a very precise knowledge of the different quark masses. The latest measurements from the Particle Data Group (PDG) at CERN give the following values [7]:

- Up-quark, $m_u = 2.16$ MeV. Down-quark, $m_d = 4.67$ MeV.
- Charm-quark, $m_c = 1.27$ GeV. Strange-quark, $m_s = 97$ MeV.
- Top-quark, $m_t = 173$ GeV. Bottom-quark, $m_b = 4.18$ GeV.

In the aspects of DM detection, the focus is on the low-energy QCD (as stated in section 2.3 one assumes the DM that do interact with SM to be non-relativistic) and it is therefor reasonable to neglect the three heavy quarks, c, t, b and instead put all attention to the lighter trio, u, d, s. This is done in many DM direct detection studies, for example in [8]. In this thesis one later moves on to the framework of ChPT where said light quarks are taken to be massless, with their mass entering as a perturbation rather than an analytical factor. More on that later, first one needs to address the relevant symmetries of QCD.

3.1.1 Symmetries of QCD

Quarks, and their interactions through gluons, exhibits a local $SU(3)$ color symmetry. The group $SU(3)$ is defined as the set of all special, unitary, unimodular, 3×3 matrices obeying $U^\dagger U = \mathbb{1}$ and $\det(U) = 1$. From group theory one can conclude that such a symmetry has 8 generators (linearly independent matrices) called Gellman matrices and which usually are denoted by λ_a, $a = 1, 2, ..., 8$ [3]. This allows any element in the $SU(3)$ group to be written in the exponential form

$$U(\Theta) = \exp\left(-i \sum_{a=1}^{8} \Theta_a \frac{\lambda_a}{2}\right), \tag{3.2}$$

where Θ_a are real numbers.

Apart from this local $SU(3)$ symmetry, QCD also allows for two types of global transformations that need to be studied. These symmetries are called $SU(3)_A$ and $SU(3)_V$ with elements Λ_V and Λ_A which affects only the flavor index f on the quark-spinor field q_f. This consequently means that $G_{\mu\nu}$ is trivially left invariant. The subscripts V (A) stands for Vector (Axial) and represents how their respective currents (arising from Noether's theorem) transform under parity. The vector current is positive under such transformation, while the γ^5 in the axial current renders it to transform as a pseudo-vector. The transformations are

$$\Lambda_V: \quad q \to e^{-i\Theta_a \frac{\lambda_a}{2}} q \simeq \left(1 - i\Theta_a \frac{\lambda_a}{2}\right) q, \tag{3.3a}$$

$$\bar{q} \to \bar{q} e^{+i\Theta_a \frac{\lambda_a}{2}} \simeq \bar{q}\left(1 + i\Theta_a \frac{\lambda_a}{2}\right) \quad \text{and} \tag{3.3b}$$

$$\Lambda_A: \quad q \to e^{-i\gamma^5 \Theta_a \frac{\lambda_a}{2}} q \simeq \left(1 - i\gamma^5 \Theta_a \frac{\lambda_a}{2}\right) q, \tag{3.4a}$$

$$\bar{q} \to \bar{q} e^{-i\gamma^5 \Theta_a \frac{\lambda_a}{2}} \simeq \bar{q} \left(1 - i\gamma^5 \Theta_a \frac{\lambda_a}{2}\right). \tag{3.4b}$$

The transformation of $\bar{q}$ via Λ_A is slightly more complicated than the others, the anti-commutation relations of the γ-matrices yields an extra minus sign.

It is fairly trivial to see that both Λ_V and Λ_A leave the kinetic term of $\mathcal{L}_{\text{QCD}}$ invariant. However, the mass term transforms. As a result of that one can only treat $\mathcal{L}_{\text{QCD}}$ as truly invariant under Λ_V and Λ_A in the limit of massless quarks (i.e., $m_u \approx m_d \approx m_s \approx 0$). This is not a big problem for the system relevant in this thesis as nucleons are the matter of interest, and a nucleons mass is far greater than those of the light quarks u, d, s ($m_{\text{Nucleon}} \approx 1$ GeV $\gg m_{u,d,s}$). It is therefor safe to let the quark mass go to zero, which is called the *Chiral limit* [3]. Later, these masses will come back as a perturbation. In the Chiral limit one says that QCD has an *approximate* $SU_V(3) \times SU_A(3)$ symmetry.

3.1.1.1 Chiral Symmetry

For massless quarks, the QCD Lagrangian simplifies into

$$\mathcal{L}_{\text{QCD, Ch}} = \sum_f i\bar{q}_f \gamma^\mu D_\mu q_f - \frac{1}{4} \mathcal{G}_{\mu\nu} \mathcal{G}^{\mu\nu}. \tag{3.5}$$

The spinor q_f can be split up to a "left-handed" and a "right-handed" spinor by applying the *chiral projectors* (also called Weyl operators)

$$P_L \equiv \frac{1 - \gamma^5}{2} \implies P_L q = q_L, \tag{3.6a}$$

$$P_R \equiv \frac{1 + \gamma^5}{2} \implies P_R q = q_R. \tag{3.6b}$$

Since $(\gamma^5)^2 = 1$ it is trivial to see the following properties of $P_{L/R}$:

$$\begin{aligned} P_L P_L = P_L, \quad P_R P_R &= P_R, \\ P_L P_R = P_R P_L &= 0, \\ P_L + P_R &= 1. \end{aligned} \tag{3.7}$$

Here, the notation $q_{L/R}$ can be understood via the decomposition of q as

$$q = \begin{pmatrix} q_L \\ q_R \end{pmatrix} \implies \begin{cases} P_L \begin{pmatrix} q_L \\ q_R \end{pmatrix} = \begin{pmatrix} q_L \\ 0 \end{pmatrix} = q_L, \\ P_R \begin{pmatrix} q_L \\ q_R \end{pmatrix} = \begin{pmatrix} 0 \\ q_R \end{pmatrix} = q_R. \end{cases} \tag{3.8}$$

This type of decomposition will, regardless of which representation of the γ-matrices one uses, render the nice result that the kinetic part of the Lagrangian splits into a left-handed and a right-handed term *which can be treated/transformed separately.* Problems would arise with the mass term, as this becomes a mixed term under the decomposition in Eq. (3.8), but as stated previously the quark masses are set to zero and the mass term vanishes. One is thus free to perform the split of the quark spinors which leads to a Lagrangian in the form

$$\mathcal{L}_{\text{QCD, Ch}} = i\bar{q}_L\gamma^\mu D_\mu q_L + i\bar{q}_R\gamma^\mu D_\mu q_R - \frac{1}{4}\mathcal{G}_{\mu\nu}\mathcal{G}^{\mu\nu}. \tag{3.9}$$

Building on the structure of Eqs. (3.3) and (3.4) the transformation operators Λ_L and Λ_R can be defined as

$$\begin{aligned} q_L &\to \Lambda_L q_L = \exp{(-i\Theta^L_a\lambda_a)}q_L, \\ q_R &\to \Lambda_R q_R = \exp{(-i\Theta^R_a\lambda_a)}q_R, \end{aligned} \tag{3.10}$$

which shows that $\mathcal{L}_{\text{QCD, Ch}}$ has a global $SU_L(3)\times SU_R(3)$ symmetry. This symmetry is in fact equivalent to the $SU_V(3) \times SU_A(3)$ discussed before.

There remain one more symmetry of the QCD that is yet to be addressed. In the transformations of Eq. (3.10) one is free to add a phase $e^{i\Theta}$ which leaves the Lagrangian invariant. Such a phase corresponds to a $U(1)$ symmetry and hence it can be concluded that a QCD Lagrangian in the chiral limit exhibits a $SU_L(3) \times SU_R(3) \times U_L(1) \times U_R(1)$ symmetry. The new transformations $V_{L/R}$ is given by

$$q_L \to V_L q_L = \exp{(-i\Theta^L_a\lambda_a - i\Theta^L)}q_L, \tag{3.11a}$$

$$q_R \to V_R q_R = \exp{(-i\Theta^R_a\lambda_a - i\Theta^R)}q_R. \tag{3.11b}$$

3.1.2 Symmetry Breaking of $SU_A(3)$ and Goldstone Bosons

Before advancing further, a quick side-step into the interesting properties of the axial symmetry and its associated current is needed. As stated previously the group $SU_A(3)$ has eight generators and the axial current has negative parity.
As it happens, the lightest color-neutral objects that consist of quarks are pions (π), kaons (k) and eta-mesons (η) [15]. These three types of mesons include a total of eight different particles, all with roughly the same mass and with negative parity. Further, from Goldstones theorem of symmetry breaking [16], it is known that every generator of a (spontaneously) broken symmetry corresponds to one massless Goldstone boson. It would therefore be reasonable to assume that the eight mesons correspond to the eight generators of the $SU_A(3)$ group.

The fact that the Goldstone bosons created this way are massless might be cause to doubt the linking of $SU_A(3)$ to mesons. However, it is important to remember that the $SU_A(3)$ symmetry was only approximate in QCD, since it revolved around the quark masses being approximated as zero. Goldstone bosons with roughly zero mass (all eight mesons are light in comparison to e.g. the proton [15]) are a consequence of breaking an approximate symmetry and called PNGB [3]. This will be discussed further later on in the thesis, for now it suffice to state the eight PNGBs in a compact field form $U(x) \equiv \exp\left(\frac{i\sqrt{2}}{f}\Pi\right)$, with Π being a matrix containing the eight PNGBs . A more detailed analysis on the PNGBs written in this form will follow in section 3.4.

3.2 Expanding the QCD Lagrangian with External Currents

As far as QCD is concerned, both the quark masses and the DM-interactions can be added to the Lagrangian as currents corresponding to external classical fields. This discussion leads to the introduction of symmetry currents and spurions which will be used to in the end express the full Lagrangian.

3.2.1 Symmetry currents

To be able to grasp the concept of symmetry current one needs first to refresh the understanding of *Noether's theorem.* Although this is mostly viewed as a fundamental part of basic QFT, a short summary is adequate and will simplify the work later on.

3.2.1.1 Noether's Theorem

The work in this subsection is mostly based on [3] but many other papers and books exists in which Noether´s theorem is discussed.
Starting at a general Lagrangian, expressible in terms of an arbitrary number of fields ϕ_i and derivatives of said fields, $\partial_\mu \phi_i$, i.e.,

$$\mathcal{L}(\phi_i, \partial_\mu \phi_i) \ , \quad i \in \mathbb{Z}, \tag{3.12}$$

one naturally obtains i equations of motions, on the form

$$\frac{\partial \mathcal{L}}{\partial \phi_i} - \partial_\mu \left(\frac{\partial \mathcal{L}}{\partial(\partial_\mu \phi_i)} \right) = 0. \tag{3.13}$$

Looking at a infinitesimal local transformation of the fields ϕ_i the variation of the Lagrangian can be sought via

$$\begin{aligned} \delta \mathcal{L} &= \mathcal{L}(\phi_i', \partial_\mu \phi_i') - \mathcal{L}(\phi_i, \partial_\mu \phi_i) \\ &= \frac{\partial \mathcal{L}}{\partial \phi_i} \delta \phi_i + \frac{\partial \mathcal{L}}{\partial(\partial_\mu \phi_i)} \partial_\mu (\delta \phi_i), \end{aligned} \tag{3.14}$$

with

$$\phi_i \to \phi_i' = \phi_i + \delta \phi_i. \tag{3.15}$$

The second term of the second row of Eq. (3.14) can be rewritten using the chain rule, i.e., $\frac{\partial\mathcal{L}}{\partial(\partial_\mu\phi_i)}\partial_\mu(\delta\phi_i) = \partial_\mu\left(\frac{\partial\mathcal{L}}{\partial(\partial_\mu\phi_i)}\delta\phi_i\right) - \partial_\mu\left(\frac{\partial\mathcal{L}}{\partial(\partial_\mu\phi_i)}\right)\delta\phi_i$. This yields the variation of the Lagrangian as

$$\begin{aligned}\delta\mathcal{L} &= \frac{\partial\mathcal{L}}{\partial\phi_i}\delta\phi_i + \partial_\mu\left(\frac{\partial\mathcal{L}}{\partial(\partial_\mu\phi_i)}\delta\phi_i\right) - \partial_\mu\left(\frac{\partial\mathcal{L}}{\partial(\partial_\mu\phi_i)}\right)\delta\phi_i \\ &= \partial_\mu\left(\frac{\partial\mathcal{L}}{\partial(\partial_\mu\phi_i)}\delta\phi_i\right).\end{aligned} \tag{3.16}$$

The first and the third term of the equation above vanishes due to the Euler-Lagrange equation (see Eq. (3.13)). Obviously the action needs to remain invariant under a symmetry transformation, thus one can state

$$0 = \int\delta\mathcal{L} = \int d^4x\partial_\mu\left(\frac{\partial\mathcal{L}}{\partial(\partial_\mu\phi_i)}\delta\phi_i\right). \tag{3.17}$$

The factor inside the parenthesis is referred to as the *Noether's current* and is usually denoted by J^μ. Clearly J^μ is constant, making it a *conserved current*, i.e., $\partial_\mu J^\mu = 0$.

3.2.1.2 The Conserved Currents of QCD

The QCD Lagrangian $\mathcal{L}_{\mathrm{QCD}}$ has, as shown, a global $SU_L(3)\times SU_R(3)$ symmetry. If one looks at the variation of the Lagrangian under an infinitesimal change one gets

$$\delta\mathcal{L}_{\mathrm{QCD}} = \bar{q}_L\left(\sum_{a=1}^{8}\partial_\mu\Theta_a^L\frac{\lambda_a}{2} + \partial_\mu\Theta^L\right)\gamma^\mu q_L + \bar{q}_R\left(\sum_{a=1}^{8}\partial_\mu\Theta_a^R\frac{\lambda_a}{2} + \partial_\mu\Theta^R\right)\gamma^\mu q_R. \tag{3.18}$$

Here, γ^μ contracts with the ∂_μ which arises from the infinitesimal change of the symmetry. Applying the knowledge acquired in the previous section one can then state the conserved currents associated with the left- and right-handed quarks are [3]

$$J^\mu_{L,a} = \bar{q}_L\gamma^\mu\frac{\lambda_a}{2}q_L\ , \qquad \partial_\mu J^\mu_{L,a} = 0, \tag{3.19a}$$

$$J^\mu_{R,a} = \bar{q}_R\gamma^\mu\frac{\lambda_a}{2}q_R\ , \qquad \partial_\mu J^\mu_{R,a} = 0. \tag{3.19b}$$

Just as before, $a = 1, ..., 8$ which means that $J^\mu_{L,a}$ transforms under $SU_L(3)\times SU_R(3)$ as an octet under transformations of the left-handed field and as a singlet under transformation of the right-handed field. For $J^\mu_{R,a}$ it is the other way around. It will be more convenient to define linear combinations of $J^\mu_{L,a}$ and $J^\mu_{R,a}$ such as

$$\begin{aligned}V^\mu_a &= J^\mu_{L,a} + J^\mu_{R,a} = \bar{q}_L\gamma^\mu\frac{\lambda_a}{2}q_L + \bar{q}_R\gamma^\mu\frac{\lambda_a}{2}q_R = \bar{q}\gamma^\mu\frac{\lambda_a}{2}q, \\ A^\mu_a &= J^\mu_{R,a} - J^\mu_{L,a} = \bar{q}_R\gamma^\mu\frac{\lambda_a}{2}q_R - \bar{q}_L\gamma^\mu\frac{\lambda_a}{2}q_L = \bar{q}\gamma^\mu\gamma^5\frac{\lambda_a}{2}q.\end{aligned} \tag{3.20}$$

One can also find singlet vector and singlet axial-vector currents by transforming the quark fields by the same phase, this is explained thoroughly in [3] but the end result is

$$\begin{aligned}V^\mu &= \bar{q}\gamma^\mu q, \\ A^\mu &= \bar{q}\gamma^\mu\gamma^5 q.\end{aligned} \tag{3.21}$$

Interestingly enough, the singlet vector current is conserved whereas $\partial_\mu A^\mu \neq 0$. This causes anomalies, something that probes outside the scope of this thesis.

So all in all, it would make sense to extend the original $\mathcal{L}_{\text{QCD, Ch}}$ (see Eq. (3.9)) with these four currents. A common way to do this is via

$$\mathcal{L}_{\text{QCD}} = \mathcal{L}_{\text{QCD, Ch}} + \bar{q}\gamma^\mu \left[\nu_\mu + \gamma^5 a_\mu\right] q, \tag{3.22}$$

where ν_μ (a_μ) is defined in a way to incorporate both the octet and the singlet vector (axial) currents [8]. Eq. (3.22) is the first example of the use of spurions, which will be the topic of the next section.

3.2.2 Spurions

The definition of a spurion is that it is an auxiliary field which parametrize any symmetry breaking in order to determine all operators invariant under the relevant symmetry. One could think of this as that the symmetry breaking parameter (in the case of the chiral symmetry, the breaking parameter is of course the mass of the quark) gets promoted into a spurion field, and that field is then transformed under the symmetry. In this way the symmetry breakings can be tracked and a consistent EFT can be constructed [46].
Lets apply this to quark masses, the symmetry breaking parameter of the QCD symmetries $SU_L(3) \times SU_R(3)$. This means to promote the quark mass $M_q \equiv \text{diag}(m_u, m_d, m_s)$ to an operator $\hat{M}_q$ which transforms as

$$\hat{M}_q \to V_R \hat{M}_q (V_L)^\dagger. \tag{3.23}$$

In a similar way, the PNGBs discussed in section 3.1.2, will acquire mass from their coupling to spurions, i.e., the field U needs to transform as

$$U \to V_R U (V_L)^\dagger. \tag{3.24}$$

One might have expected that all eight PNGBs masses achieved this way would be unique, but as explained in [46] there exists a non-trivial consequence of ChPT that groups the PNGBs masses into four sections, three of which have diagonal mass-matrices:

$$\begin{aligned} \pi^+ \text{ and } \pi^- : &\quad m^2 = y\Lambda(m_u + m_d), \\ K+ \text{ and } K^- : &\quad m^2 = y\Lambda(m_u + m_s), \\ K^0 \text{ and } \bar{K}^0 : &\quad m^2 = y\Lambda(m_d + m_s), \\ \eta \text{ and } \pi^0 : &\quad m^2 = y\Lambda \begin{pmatrix} m_u + m_d & m_u - m_d \\ m_u - m_d & \frac{1}{3}(m_u + m_d + 4m_s). \end{pmatrix} \end{aligned} \tag{3.25}$$

Here y is a coupling and Λ is the so called cut-off scale (will be more formally introduced in section 3.3). Although outside the scope of this thesis, it is intriguing that the seemingly independent PNGBs have masses that coincide with each others.

With a nice theoretical understanding of spurions, one can return to Eq. (3.22) and expand it to also allow for DM interactions. This means that the DM will be seen as a perturbation in the same way as the quark masses. Hence the new Lagrangian needs to include all possible ways that the DM could interact with QCD particles. These are scalar spurions (s), pseudo scalar spurions (p), vector spurions ($\hat{\nu}_\mu$), axial vector spurions ($\hat{a}_\mu$), gluon spurions (s_G) and dual gluon spurions θ. All in all, the interaction Lagrangian becomes

$$\begin{aligned}\mathcal{L} = \mathcal{L}_{\text{QCD, Ch}} + \bar{q}\gamma^\mu \left[\nu_\mu + \gamma^5 a_\mu\right] q - \bar{q}\left[s - i\gamma^5 p\right] q + \\ \bar{q}\gamma^\mu \left[\hat{\nu}_\mu + \gamma^5 \hat{a}_\mu\right] q + s_G \frac{\alpha_s}{12\pi} \mathcal{G}^{a\mu\nu}\mathcal{G}^a_{\mu\nu} + \theta \frac{\alpha_s}{8\pi}\mathcal{G}^{a\mu\nu}\tilde{\mathcal{G}}^a_{\mu\nu}.\end{aligned} \tag{3.26}$$

The expression above allows for all possible ways of DM-QCD interaction. The choice to keep both ν_μ (a_μ) and $\hat{\nu_\mu}$ ($\hat{a}_\mu$) is to emphasize the new spurions related to DM interactions, they will later be absorbed into the vector (axial vector) currents. It is worth remembering that the Lagrangian still needs to be invariant under the local chiral transformation. The quarks transforms as

$$q \rightarrow V_R \frac{1+\gamma^5}{2} q + V_L \frac{1-\gamma^5}{2} q, \tag{3.27}$$

which forces the spurions to transforms

$$\nu_\mu + a_\mu \rightarrow V_R \left(\nu_\mu + a_\mu\right) V_R^\dagger + iV_R \partial_\mu V_R^\dagger \tag{3.28a}$$

$$\nu_\mu - a_\mu \rightarrow V_L \left(\nu_\mu - a_\mu\right) V_L^\dagger + iV_L \partial_\mu V_L^\dagger \tag{3.28b}$$

$$s + ip \rightarrow V_R(s + ip)V_L^\dagger. \tag{3.28c}$$

Trivially, s_G does not transform as $\mathcal{G}^a_{\mu\nu}$ does not transform. The other gluon term, θ is a bit more tricky and related to the anomaly discussed earlier. As it is outside the scope of the current work, it will suffice in stating that:

- The θ term undergoes a shift transformation which cancels the unwanted anomaly, this results in that it moves to the axial and pseudo-scalar currents [4].

As a result, the Lagrangian can now be written as [8]

$$\mathcal{L} = \mathcal{L}_{\text{QCD, Ch}} + \bar{q}\gamma^\mu \left[\nu_\mu + \gamma^5 a'_\mu\right] q - \bar{q}\left[s + ip'\right] q + s_G \frac{\alpha_s}{12\pi}\mathcal{G}^{a\mu\nu}\mathcal{G}^a_{\mu\nu}. \tag{3.29}$$

Here the primes note the inclusion of the θ-term, as discussed above.

3.3 Effective Field Theory

A crucial part of constructing any low-energy QCD-Lagrangian is EFT. This section introduces EFT and explains why it is essential to DM studies. EFT is broadly used in many areas of physics and there exists a large variety of course books, papers and theses about it. In this section [17] and [18] are used unless something else is specified.

It is a critical first step in any EFT attempt to identify a separation of scales, that is, to find a split between the energy (or mass or time etc) of the studied system and the energy of the underlying dynamics. As a very intuitive example one can consider the construction of a bridge: here it clearly makes sense to split the length scale. No one would worry about e.g. Van der Waals interactions for the molecules within the beam that supports the bridge, the important variables are macroscopic and if one knows how to treat them one can safely forget everything on a sub-atomic level and instead focus on the length scale relevant for the beam (which would be roughly the order of m^1).

The second part of EFT is to determine what the relevant Degrees of Freedom (DoF) are. These are connected to the chosen energy scale in such a way that the particles/fields or constructions (in the example of a bridge) of interest can be described using the DoF. One would assume that the DoF relevant in low-energy QCD are quarks (and gluons). However it becomes unpractical to use color-charged objects and instead it is much more convenient to choose color-neutral particles such as mesons and nucleons as the DoF [19]. As it is desirable with low-energy states (to keep the energy scale clearly split) it is natural to choose the PNGBs as the DoF. This is such a common approach to low-energy QCD that it has its own name, *Chiral Perturbation Theory* (ChPT). Section 3.4 is devoted to this. Before exploring ChPT however, there remain some important steps of EFT-construction to be discussed.

Having identified a split in the scale and chosen adequate DoF the next step is to identify what symmetries are active and if/when they are broken. In the case at hand the symmetries and their breaking have already been discussed, see section 3.1.1.

Step four is to create the most general Lagrangian that still obeys the local symmetries. This means of course that the Lagrangian would consists of infinitely many terms, since there is no finite number of ways an interaction obeying the relevant symmetries can be constructed. One then needs a way of sorting out these terms and to determine which are the most important. This can be done via the so called low-energy (low-momentum) expansion. This process relies on step 1 (stated above), finding a separation of energy scales and then express the Lagrangian as an expansion of the (small) fraction of the light/heavy scale, this is usually denoted by Q/Λ where Q is the low-energy and Λ is the cut-off of the scale. In that way, terms of lesser importance will be filtered out via the higher order of the small fraction. With this "ordering of terms based on their importance" it is then easy to choose what degree of accuracy is desired and truncate the Lagrangian at that order.

This whole procedure, sometimes called the "EFT recipe" will now be applied to the situation of low-energy QCD relevant in this thesis.

3.4 Chiral Perturbation Theory

For low energy QCD, the DoF of interest are the PNGBs momenta Q_{PNGBs}. The natural separation in the energy scale is then where more complex and heavy mesons start to occur. This happens at roughly 1 GeV at which the ordering of terms in the Lagrangian becomes ineffective since the fraction which monitors the expansion is no longer small (if $Q \approx \Lambda$). With PNGBs one have $Q_{\text{PNGBs}}/\Lambda \approx 0.3$ [8]. Gathering all the PNGBs in the compact form of a field $U(x)$ can be done as

$$U(x) \equiv \exp\left(\frac{i\sqrt{2}}{f}\Pi\right), \tag{3.30}$$

with Π containing the eight PNGBs

$$\Pi = \sum_a \lambda_a \pi_a = \begin{pmatrix} \frac{\pi_0}{\sqrt{2}} + \frac{\eta_s}{\sqrt{6}} & \pi^+ & K^+ \\ \pi^- & \frac{-\pi^0}{\sqrt{2}} + \frac{\eta_s}{\sqrt{6}} & K^0 \\ K^- & \bar{K}^0 & -\frac{2\eta_s}{\sqrt{6}} \end{pmatrix}, \tag{3.31}$$

and f being a constant related to the pion decay [8, 10]. One can consequently express a general low-energy QCD Lagrangian in terms of increasing order of Q/Λ, which is the same as to say in terms of the field, and derivatives of, $U(x)$. It is worth noting that since the PNGBs are degenerate with the vacuum [17] the Lagrangian needs to involve derivatives of the fields. This is analogous with stating that the interactions between them would have to be zero in the case of zero momentum.

Since U transforms as $U \to V_R U V_L^\dagger$ in agreement with Eq. (3.24) the construction of a covariant derivative would be [3, 8]:

$$\nabla_\mu U = \partial_\mu U - i(\nu_\mu + a'_\mu)U + iU(\nu_\mu - a'_\nu). \tag{3.32}$$

This covariant derivative plays an important role in the ChPT Lagrangian which at leading order (which is order two in momentum p) takes the form [8, 9]

$$\mathcal{L}^{(2)}_{\text{ChPT}} = \frac{f^2}{4}\text{Tr}\left[\nabla_\mu U^\dagger \nabla^\mu U\right] + \frac{B_0 f^2}{2}\text{Tr}\left[(s - ip)U + (s + ip)U^\dagger\right]. \tag{3.33}$$

B_0 is referred to as a low-energy constant which is related to the quark condensate, numerically it is $B_0 = 2.66$ GeV [8]. Adding the DM interaction spurions and keeping the terms linear in interactions gives the final expression for the interaction

Lagrangian [8]:

$$
\begin{aligned}
\mathcal{L}_{\text{int, ChPT}} = & -\frac{if^2}{2}\mathrm{Tr}\left[\left(U\partial_\mu U^\dagger + U^\dagger\partial_\mu U\right)\nu^\mu + \left(U\partial_\mu U^\dagger - U^\dagger\partial_\mu U\right)a^\mu\right] \\
& + \frac{B_0 f^2}{2}\mathrm{Tr}\left[s\left(U+U^\dagger\right) - ip\left(U-U^\dagger\right) - \frac{i\theta}{\mathrm{Tr}\hat{M}_q^{-1}}\left(U-U^\dagger\right)\right] \\
& - \frac{if^2}{4}\frac{\partial_\mu\theta}{\mathrm{Tr}\left[\hat{M}_q^{-1}\right]}\mathrm{Tr}\left[\left(U\partial_\mu U^\dagger - U^\dagger\partial_\mu U\right)\hat{M}_q^{-1}\right] \\
& + s_G\left(\frac{f^2}{6}\mathrm{Tr}\left[\partial_\mu U^\dagger\partial^\mu U\right] + \frac{B_0 f^2}{27}\mathrm{Tr}\left[\hat{M}_q(U+U^\dagger)\right]\right).
\end{aligned}
\tag{3.34}
$$

Eq. (3.34) is a hadronized version of Eq. (3.29) where the quarks now have been promoted into mesons via chiral perturbation theory. In section 3.7 it will be made clear that two different kinds of hadronization-processes need to be accounted for in this thesis, therefore the following subsection is needed.

3.4.1 Heavy Baryon Chiral Perturbation Theory

As one will see in section 3.7, two cases of interaction diagrams are considered in this thesis. With the framework described above in section 3.4 one can nicely model the interaction between a meson (consisting of PNGBs) and a DM particle. This will correspond to the right part of Fig. 3.1. However, there is also the possibility of an interaction directly between the nucleon and the DM particle (left part of Fig. 3.1). In such a case the ChPT needs to be adapted to instead consider nucleons rather than PNGBs. This would cause some problems, as $Q_{\text{nucleon}}/\Lambda$ can not be considered small. However, the baryons are so much heavier than the PNGBs that they can, in the same way as HQET (see section 3.5.1), be treated as static. The idea is called Heavy Baryon Chiral Perturbation Theory (HBChPT) and its results are basically the same as for ChPT. To review the underlying theory of HBChPT is not relevant for the current purpose, the reader is advised to [10] for further insights. It is worth noting one big difference between ChPT and HBChPT however. In the first case the quarks and gluons of the EFT needs to be hadronized into mesons, while for the latter the same quarks should be hadronized into nucleons. This process will be described more thoroughly in section 3.7 and in Appendix D.2.
The strategy of EFT and ChPT will be used when modeling the interactions between quark/nucleons and DM particles. But to advance to that discussion, it is necessary to first introduce the mathematical foundation of DM fields, which will be done in the next section.

3.5 Dark Matter Fields

Having gained a thorough insight into the more abstract ways of dealing with the QCD Lagrangian the next natural step is to do the same with DM. As the DM is far less understood the procedure of modeling it requires a lot more generality than for QCD. The work in this section originates from the assumptions that the

DM is heavy and non-relativistic (see section 2.3) which allows for the use of what is referred to as *Heavy Dark Matter Effective Theory* (HDMET). HDMET assumes that both the DM particle and the nucleon is much heavier than the typical momentum transfer q in a scattering process, i.e., $m_X \gg q$. The SM counterpart to HDMET is *Heavy Quark Effective Theory* (HQET) and with the foundation of quarks nicely explained in previous sections it will be intuitive to explain HDMET on the base of first understanding HQET.

3.5.1 Heavy Quark Effective Theory

The main idea of HQET is to treat a baryon consisting of one heavy quark and one (or two) light quark(s). Two common examples of such baryons are the Λ_c^+, which contains one charm quark (heavy), one up quark (light) and one down quark (light), and the Λ_b^0 formed by one bottom quark and one pair of up-down quarks.

Since the heavy quark is responsible for a vast majority of the baryons mass/ momentum it is a reasonable assumption to make to consider the heavy quark as stationary inside the rest frame of the baryon (i.e., it moves in the same directions with the same velocities as the baryon). The light quarks however behave in a much more chaotic way. Even though not completely accurate, on can make the analogy between this and an atom, with the nucleus being represented by the heavy quark, while the electrons are the light quarks. This means that in the limit of the heavy quark mass going towards the baryon mass ($m_{\text{HQ}} \to m_{\text{B}}$) its DoF can be split up into *massive* DoF and *massless* DoF [44, 45]. Thus, when considering interactions between the heavy and the light quarks one needs only to concern oneself with the massless DoF, since the massive DoF will be static within the baryon rest frame. Such a "split of DoF" are highly usable in a number of areas, it will prove very fruitful in the upcoming discussion about spin-1 DM vector fields.

3.5.2 Heavy Dark Matter Effective Theory

In this thesis spin-1 DM is treated. This implies that one can consider the DM particle as corresponding to some heavy complex vector field, which will be denoted with X^μ. In a similar way to HQET (see section 3.5.1) it is suitable to split the DM vector field into massive and massless parts. How this can be done is shown in great detail in Appendix A but the overall result is also included here. Starting at the general heavy complex vector field X^μ as

$$X^\mu = e^{im_X v \cdot x} \left(\chi^\mu + X_\parallel \right), \tag{3.35}$$

one can through a series of elaborate derivations prove the following:

- The split into χ^μ ($X_\parallel$) is indeed analogous with the split into massless (massive) fields.
- The total field X^μ can be expressed as a power series of *only* the massless part χ^μ.

The second point is truly remarkable, as it allows one to ignore the massive part of the vector field and, in the case of interactions, focus purely on χ^μ. One should however note that this does not mean that the massive part is unimportant during the process. It is instead a reflection of that the massive vector field can be described in terms of the massless one. The final expression (the end result of Appendix A) is then

$$X^\mu = e^{-im_X v\cdot x}\left(\chi^\mu - \frac{iv^\mu}{m_X}\partial_\lambda\chi^\lambda + \mathcal{O}\left(\frac{1}{m_X^2}\right)\right). \tag{3.36}$$

Due to this split, it is important to note that the massless vector field χ^μ no longer carries the full momentum of X^μ (denoted by p^μ), but rather a small portion of it. Usually this is denoted by the *residual* or *soft* momenta $\tilde{p}^\mu$. This can mathematically be described as

$$p^\mu = m_X v^\mu + \tilde{p}^\mu, \qquad m_X v^\mu \gg \tilde{p}^\mu. \tag{3.37}$$

v^μ is a reference vector fulfilling $v^\mu v_\mu = 1$. It will be convenient to later on choose it to be time-like, but for now it can be kept general.

3.6 Interaction Lagrangian of QCD and DM

Now, with a profound knowledge of QCD particles and DM separate it is time to start investigating how they might interact with each other. The approach this thesis takes, in agreement with consensus within the field (see e.g. [8]), is to treat DM-quark interactions as regular chiral QCD with the DM and the quark masses applied as an external field of spurions as described in section 3.2.2. This is the essence of ChPT in DM-quark interactions, to consider the massless quarks as the base, and then add both the quark mass and the DM as perturbations.

3.6.1 Interaction Lagrangian as Terms of Currents

As stated in section 3.3 a general interaction Lagrangian includes infinitely many terms, so as to not lose generality. Hence it is of utmost importance to order these terms in a way that one quickly can decide their importance. In the case of DM-quark/gluon interaction such a parameter is conveniently chosen as the mass of the mediating particle, noted m_G. Thanks to the low-energy limit the mediator mass can be considered dominant over the momentum transfer ($q \ll m_G$), which allows for the interaction terms to be ordered depending on the inverse order of mediator mass. Typically, this is denoted as

$$\mathcal{L}_{\text{int}} = \sum_n \mathcal{Q}_{n,q}^{(d)} \hat{C}_{n,q}^{(d)}. \tag{3.38}$$

$\mathcal{Q}_{n,q}^{(d)}$ is the *relativistic interaction operator*, numerated by the number n, for the quark flavor q and in dimension of mediator mass d. $\hat{C}_{n,q}^{(d)}$ is the coupling constant,

$$\hat{C}_{n,q}^{(d)} = \frac{C_{n,q}^{(d)}}{m_G^{(d-4)}}, \tag{3.39}$$

which is supported by [8].

Up to this point the work has revolved around finding the interaction Lagrangian in terms of QCD factors and spurions. This has been done to give a profound insight into how one generally treats low-energy QCD and EFT. For the purpose of this thesis however it will be more convenient to express the interaction Lagrangian as a sum of DM/quark currents, J_χ and J_q. The schematic way interpret this is via

$$\mathcal{L}_{\text{int}} = \sum_n \sum_{q=u,d,s} \hat{C}_{n,q} \left(J_\chi^S J_q^S + J_\chi^P J_q^P + J_\chi^{V,\mu} J_{q,\mu}^V + J_\chi^{A,\mu} J_{q,\mu}^A + ... \right) \tag{3.40}$$

Here, the super-indices indicates the current type, S for scalar, P for pseudo-scalar, etc. This notation will be used in the upcoming sections where the scattering amplitude is treated. The different quark/gluon currents can then easily be accessed through identification of the terms of Eq. (3.26). The full list is printed below for the readers convenience.

$$\begin{aligned} J_q^S &= m_q \bar{q} q, & J_q^P &= m_q \bar{q} i \gamma^5 q, \\ J_q^{V,\mu} &= \bar{q} \gamma^\mu q, & J_q^{A,\mu} &= \bar{q} \gamma^\mu \gamma^5 q, \\ J^G &= \frac{\alpha_s}{12\pi} \mathcal{G}^{a\mu\nu} \mathcal{G}^a_{\mu\nu}, & J^\theta &= \frac{\alpha_s}{8\pi} \mathcal{G}^{a\mu\nu} \tilde{\mathcal{G}}^a_{\mu\nu}. \end{aligned} \tag{3.41}$$

3.7 The Scattering Process

Proceeding to the final step of the theoretical background one can now start to model the interaction of DM and nucleon. Two cases will be considered in this thesis, and their corresponding Feynman diagrams can be studied in Fig. 3.1. These two possibilities are chosen in agreement with [8] which confirms that at leading order these two diagrams are the only ones that can be produced. The first possibility (the left panel of Fig. 3.1) is that the DM scatters with the nucleon through a "direct contact". The second case (right panel of Fig. 3.1) describes the interaction through a meson-mediator. It is important to note that since the particle "interacting" with the DM is different in the two cases the hadronization will need to reflect this. In the left panel the quark currents should be hadronized into nucleons, in the right panel the quarks should instead be hadronized into mesons. How the hadronization is performed is discussed briefly in section 3.4. A more thorough explanation is found in [8] where explicit expressions for hadronized currents are stated. These are used in this thesis, see appendix D.2 for more details.

From the two diagrams in Fig. 3.1 and the list of operators presented in section 5.1 one would conclude that there is no less than a staggering 28 scattering amplitudes to calculate (14 per diagram). The workload is somewhat decreased however, as it is pointed out in [8] that not all of the currents give leading order contributions. In fact, one needs only to consider J_q^S, J_q^V, J_q^A, J^G and J^θ for the contact diagram.

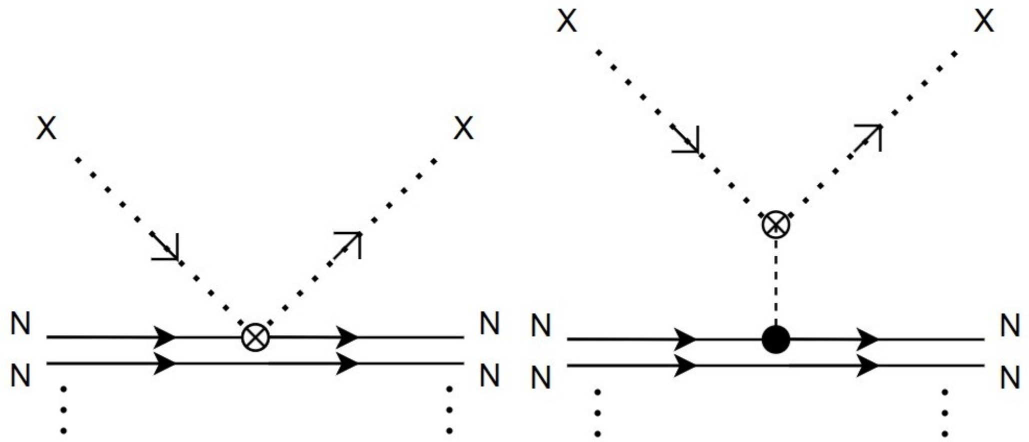

Figure 3.1: The two leading order Feynman diagrams contributing to the scattering between spin-1 DM and nucleons. X and dotted lines represents the DM, N and solid lines are the nucleons. The effective interaction is marked by the crossed circle. The left panel shows the "contact" interaction whereas the right panel represents the interaction mediated by a meson, which is marked as a dashed line. The dots below indicates additional nucleons.

For the meson mediator interaction J_q^P, J_q^A and J^θ are relevant. There is still a remarkable amount of work, but instead of 28 scattering amplitudes one can suffice in calculating 20 of them.

The momentum transfer in both processes of Fig. 3.1 can be summarized by the schematic overview of Fig. 3.2, where p (p') represents the incoming (outgoing) momentum of the DM, q is the momentum transferred in the interaction and k (k') is the momentum of the incoming (outgoing) nucleon. One can utilize momentum conservation and frame independence to find that there is in fact only two degrees of freedom, q and $v_\perp$, where the latter is defined as

$$v_\perp \equiv \frac{p+p'}{2m_X} - \frac{k+k'}{2m_N}. \tag{3.42}$$

In the efforts of calculating a scattering amplitude from the diagrams in Fig. 3.1 only the leading order of momentum is considered.

3.7.1 Theoretical Framework of the Scattering Amplitude

The scattering amplitudes are one of the main results that this thesis considers. The process of finding it is relatively straight forward if one is familiar with QFT, but since it is of immense importance for the thesis, the procedure is described below.

The truncated expansion of the matrix element of the S-matrix describing a scattering can be found from the interaction Lagrangian, i.e.,

$$S_{fi} = i \int d^4x \langle f|\mathcal{L}_{\text{int}}|i\rangle. \tag{3.43}$$

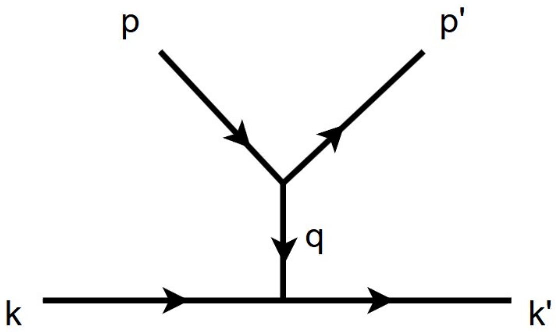

Figure 3.2: The momentum-space of a DM-SM interaction. A prime denotes the outgoing momentum (after interaction). q is the transferred momentum. Thanks to momentum conservation and frame independence there are only two degrees of freedom, q and $v_\perp$.

Here it will be very convenient to use the current-form of the interaction Lagrangian, namely Eq. (3.40). This allows for a decomposition of the above equation into one DM-current part and one SM-current part, or mathematically

$$S_{fi} = i \int d^4x \langle \mathrm{DM}_f | J_{\mathrm{DM}} | \mathrm{DM}_i \rangle \cdot \int d^4x \langle \mathrm{SM}_f | J_{\mathrm{SM}} | \mathrm{SM}_i \rangle. \tag{3.44}$$

Since the S-matrix also fulfills

$$S_{fi} = (2\pi)^4 \delta^{(4)}(E_f - E_i) \cdot i\mathcal{M}, \tag{3.45}$$

it will be straightforward to extract the scattering amplitudes for different currents. It is important to understand that the actual scattering occurs between nuclei and DM, not between quark/gluons and DM. For the DM, the Fourier expansion of the DM field will be considered, the Feynman rules needed to evaluate the vertices and in/outgoing particles are described in appendix D.1.

When expressing the scattering amplitude, it will be beneficial to do so as a product of a basis operator $Q^{(d)}_{n,N}$ and some coupling constant $c^{(d)}_{n,N}$. Here, n is an number index, N will be either proton (p) or neutron (n) to show what type of nucleon the DM scatters against and d is the order of momentum q. i.e., the scattering amplitude can be expressed as

$$i\mathcal{M} = c^{(d)}_{n,N} \cdot Q^{(d)}_{n,N}. \tag{3.46}$$

This way, a set of basis operators can be defined, which together span all possible scattering amplitudes. It is very important to note the difference between the relativistic interaction operators $\mathcal{Q}^{(d)}_{n,q}$ first defined in Eq. (3.38) (and later stated in section 5.1) and the basis operators $Q^{(d)}_{n,N}$. As much as this is bordering on abuse of notations, sometimes we are left with no choice. As a small help, the relativistic interaction operators $\mathcal{Q}$ are in this thesis *always of order six* while the basis operators, Q, spanning the amplitudes can be of *either order zero, one, two or three.* Hopefully this simplifies the distinction for the reader.

There exists a subtlety in the expression for the basis operators that needs to be discussed before moving on. Since the scattering amplitudes will be found from the non-relativistic reduction (described in section 3.5.2 and appendix A) they will be obeying Galilean symmetry even though they are written in Lorentzian notation. Consequently the underlying theory is Lorentz invariant which means that there will be terms in the scattering amplitude that breaks the Galilean symmetry. Luckily enough, these only show up at Next to Leading order (NLO) and as already stated only LO terms will be of interest due to the non-relativistic character of the DM. Therefor it will be safe to ignore the Galilean symmetry breaking terms of the scattering amplitudes (an example of this can be seen in section (5.3.2.2)).

3.7.2 Matching to the Non-Relativistic Effective Lagrangian

Once the scattering amplitude is found and expressed in the set of basis operators $Q_{n,N}^{(d)}$ one final step remains in order to get the desired results. There exist (see e.g. [21, 22]) a set of non-relativistic operators, $\mathcal{O}_{i,p/n}$ that have been found by a similar approach as the one used in this thesis, but where the modeling of the interaction starts in the non-relativistic approach instead of the simplified model (see section 2.6). These operators are enumerated by i, and denoted by either p or n for the scattering off a proton or a neutron respectively. It is desired to express the basis operators found from the simplified model-approach in this work in the basis of $\mathcal{O}_{i,p/n}$. Rewriting the basis operators would allow for nice comparisons between current work and what has been done before. It also opens the door for straightforward identification of how constraints found in the relativistic regime might inflict changes also in the non-relativistic limit. How to formulate the scattering amplitudes found in this thesis in the basis of [21] can be thoroughly studied in Appendix E.

The non-relativistic effective Lagrangian is

$$\mathcal{L}_{\text{eff}} = \sum_i \left(c_{i,p}^{\text{NR}} \mathcal{O}_{i,p} + c_{i,n}^{\text{NR}} \mathcal{O}_{i,n} \right) . \tag{3.47}$$

In previous work that establishes these non-relativistic operators the momentum transfer q is defined with a sign change to the definitions used in this thesis. For the readers convenience all operators in [21] (which in contrary to [22] also includes the operators unique to spin-1) have been rewritten using the current sign of q. These are listed in table 3.1. $\boldsymbol{S}_X$ ($\boldsymbol{S}_N$) is the spin-operator for the DM (nucleon) while $\boldsymbol{S}_{ij} = \frac{1}{2}(\boldsymbol{e}_i' \boldsymbol{e}_j + \boldsymbol{e}_i \boldsymbol{e}_j')$ where $\boldsymbol{e}$ and $\boldsymbol{e'}$ describes the polarization of the incoming and outgoing DM particle respectively. $\mathcal{O}_{17,18,19,20}$ are the spin-1 operators. In e.g. [21, 22] only operators of order 2 in momentum q are considered, in this thesis it is however necessary to include $\mathcal{O}_p^{(3)}$ which is made clear in the results (see section 5.3 and Eq. (5.45)).
With the effective Lagrangian now constructed, it will be straightforward to see if and how the constraints from the relativistic approach appears in the non-relativistic limit. This will be discussed in detail in the results (section 5).

$\mathcal{O}_{1,p} = \mathbb{1}_N \mathbb{1}_X$	$\mathcal{O}_{2,p} = \boldsymbol{v}_\perp^2 \mathbb{1}_N \mathbb{1}_X$
$\mathcal{O}_{3,p} = i\mathbb{1}_X \boldsymbol{S}_N \cdot \left(\boldsymbol{v}_\perp \times \frac{\boldsymbol{q}}{m_p}\right)$	$\mathcal{O}_{4,p} = \boldsymbol{S}_X \cdot \boldsymbol{S}_N$
$\mathcal{O}_{5,p} = i\mathbb{1}_N \boldsymbol{S}_X \cdot \left(\boldsymbol{v}_\perp \times \frac{\boldsymbol{q}}{m_p}\right)$	$\mathcal{O}_{6,p} = \left(\boldsymbol{S}_X \cdot \frac{\boldsymbol{q}}{m_p}\right)\left(\boldsymbol{S}_N \cdot \frac{\boldsymbol{q}}{m_p}\right)$
$\mathcal{O}_{7,p} = \mathbb{1}_X \left(\boldsymbol{S}_N \cdot \boldsymbol{v}_\perp\right)$	$\mathcal{O}_{8,p} = \left(\boldsymbol{S}_X \cdot \boldsymbol{v}_\perp\right)\mathbb{1}_N$
$\mathcal{O}_{9,p} = i\boldsymbol{S}_X \cdot \left(\frac{\boldsymbol{q}}{m_p} \times \boldsymbol{S}_N\right)$	$\mathcal{O}_{10,p} = -i\mathbb{1}_X \cdot \left(\boldsymbol{S}_N \cdot \frac{\boldsymbol{q}}{m_p}\right)$
$\mathcal{O}_{11,p} = -i\left(\boldsymbol{S}_X \cdot \frac{\boldsymbol{q}}{m_p}\right)\mathbb{1}_N$	$\mathcal{O}_{12,p} = \boldsymbol{S}_X \left(\boldsymbol{S}_N \times \boldsymbol{v}_\perp\right)$
$\mathcal{O}_{13,p} = -i\left(\boldsymbol{S}_X \cdot \boldsymbol{v}_\perp\right) \cdot \left(\boldsymbol{S}_N \times \frac{\boldsymbol{q}}{m_p}\right)$	$\mathcal{O}_{14,p} = -i\left(\boldsymbol{S}_X \times \frac{\boldsymbol{q}}{m_p}\right)\left(\boldsymbol{S}_N \cdot \boldsymbol{v}_\perp\right)$
$\mathcal{O}_{15,p} = -\left(\boldsymbol{S}_X \cdot \frac{\boldsymbol{q}}{m_p}\right)\left[\left(\boldsymbol{S}_N \times \boldsymbol{v}_\perp\right) \cdot \frac{\boldsymbol{q}}{m_p}\right]$	$\mathcal{O}_{17,p} = -i\frac{\boldsymbol{q}}{m_p}\boldsymbol{S} \cdot \boldsymbol{v}_\perp \mathbb{1}_N$
$\mathcal{O}_{18,p} = -i\frac{\boldsymbol{q}}{m_p}\boldsymbol{S} \cdot \boldsymbol{S}_N$	$\mathcal{O}_{19,p} = \frac{\boldsymbol{q}}{m_p} \cdot \boldsymbol{S} \cdot \frac{\boldsymbol{q}}{m_p}$
$\mathcal{O}_{20,p} = \left(\boldsymbol{S}_N \times \frac{\boldsymbol{q}}{m_p}\right) \cdot \boldsymbol{S} \cdot \frac{\boldsymbol{q}}{m_p}$	

Table 3.1: All non-relativistic quantum mechanical operators that, at leading order, contribute to the scattering between a DM particle and a proton. The four operators, $\mathcal{O}_{17,18,19,20}$ are unique to spin-1 DM [21].

4
Theoretical Methods

This chapter will be a schematic overview of the methods used to achieve the results presented in section 5. It will focus on the logical structure and overall purposes of the different steps, rather than to explain them in detail. For the more technical descriptions of the procedure, the reader should see the appendices. Each of the following subsections will have clear mentions of which appendices contain more information about the relevant topic.

4.1 Methodology

As described in e.g. section 2.6, the aim of this thesis is to construct a relativistic EFT for the interaction between spin-1 DM and nucleons and to further take it into the non-relativistic limit to see how constraints from the relativistic regime might affect the outcome in the non-relativistic case. Much of the procedure is already described within the theory section (see section 3), but here the reader is given a streamlined and schematic overview of the different steps. These steps can be summarized as

- Finding relativistic interaction operators.
- Non-relativistic reduction of the DM field vector.
- Hadronization of the quark/gluon currents.
- Calculating scattering amplitudes.
- Rewriting into a manifestly non-relativistic way.
- Matching onto basis operators of Catena et. al. [21].

4.1.1 Finding Relativistic Interaction Operators

Starting from the two Feynman diagrams in Fig. 3.1 a general Lagrangian can be built using EFT. This is described in sections 3.3 and 3.4. This Lagrangian is then treated as consisting of SM and DM currents, as seen in section 3.6.1 which allows for the creation of relativistic quantum mechanical interaction operators $\mathcal{Q}_{n,q}^{(d)}$ which incorporates both the quark/gluon current and the DM current. The quark/gluon currents are stated in Eq. (3.41) and the link between currents and operators can be seen in Eqs. (3.38) and (3.40).

These operators are found via identification of the Lagrangian in Eqs. (2.1) and (2.2) in [21] and are displayed in section 5.1. An overview of how this identification looks is presented in Appendix C. Each operator is then coupled to a coupling constant $\hat{C}_{n,q}^{(d)}$.

4.1.2 Non-Relativistic Reduction of the DM Field Vector

As stated in section 3.5.2, the spin-1 DM particle is considered as a heavy complex vector field X^μ which builds the DM currents. This vector field can, through a series of elaborate equations, be split up into a massless part χ^μ and a massive part $\not{X}$. This split depends on the common assumptions for direct detection related DM, namely that it is heavy and slow (i.e. velocities $\ll c$ and thus non-relativistic). Further, one can express the massive part as power series of the massless, rendering that the full heavy complex vector field is truncated to only include the massless part. This is explained thoroughly in Appendix A and the end result is seen in Eq. (3.36). In this thesis all terms of order $\mathcal{O}(1/m_X^2)$ and higher are discarded.

With the new form of X^μ found, one then evaluates all the DM currents in the interaction operators in 5.1 so that they only contain the massless part χ^μ. This can be seen in Appendix B, which leads to the DM current form in the interaction operators $\mathcal{Q}_{n,q}^{(d)}$ seen in section5.2.

4.1.3 Hadronization of the Quark/Gluon Currents

With the DM currents expressed in the proper form (see the section above) the next step is to fix the quark/gluon currents as well. As the interaction which is investigated regards the DM scattering either with a nucleon (left part of Fig. 3.1) or with a meson (right part of Fig. 3.1) the quark/gluon currents in Eq. (3.41) needs to be adjusted to reflect that. Following the work of F. Bishara et. al. [8] the currents in Eq. (3.41) are expressed in nucleons and mesons instead. Examples of this can be seen in Appendix D.2, e.g. in Eq. (D.9).

4.1.4 Calculating Scattering Amplitudes

With both the SM and the DM currents in $\mathcal{L}_{\text{int}}$ now correctly expressed, one can move on to calculating scattering amplitudes. How this is done is explained in section 3.7.1 and can be viewed in full in Appendix D.2. The procedure is applied to all the interaction operators in section 5.2. The work is somewhat simplified by identifying that only some of the nucleon currents give leading order contributions to the amplitude. This is more thoroughly explained in [8].

The scattering amplitudes are then split up into basis operators $Q_{n,N}^{(d)}$ and corresponding coupling constants $c_{n,N}^{(d)}$. The scattering amplitude found is of course non-relativistic since it originates from the non-relativistic reduction of the DM field, it is however still written in a Lorentzian notation. Fixing this is the next step of the methodology.

4.1.5 Rewriting Into a Manifestly Non-Relativistic Way

To be able to see how the relativistic EFT approach might affect the results even in the non-relativistic limit the basis operators found in the previous step needs to be rewritten in a way that they can be matched onto previous work starting from the non-relativistic approach. How this is done can be seen in Appendix E.1.

4.1.6 Matching Onto Basis Operators of Catena et al.

The specification of non-relativistic basis operators which span scattering amplitudes for DM interactions with nucleons has been done by several authors, in this thesis comparisons are made with the basis operators found by Catena et. al in [21] since they there also consider spin-1, something that is not done elsewhere. There are 20 in total in [21], compared to the 18 found in this thesis (see table 5.1).

Once the matching is performed, one is free to analyze and discuss the findings. This is done in section 5.5 of the results.

5

Theoretical Results and Discussion

In this chapter the theoretical results found in this work are presented. It starts with identifying all the relativistic interaction operators. Then said operators are rewritten via HDMET to be expressed solely in terms of the massless part of the DM vector field χ^μ. This chapter also states all possible scattering amplitudes arising from the suggested interactions. The amplitudes will then be expressed as a set of basis operators with corresponding coupling constants. Lastly, the basis operators will be rewritten in a manifestly non-relativistic way, which allows for an analysis on this work in comparison to previous papers within the field.

5.1 List of Interaction Operators

The full list of which DM currents (coupled to quark/gluon currents) that are possible for spin-1 DM (up to leading order) is identified in Eqs. (5.1)-(5.14). The work of finding them relies heavily on [8, 21]. Finding some of the operators is considered trivial, the rest is found through a procedure described in Appendix C. All operators must of course be Hermitian, Lorentz invariant and CPT invariant.

5.1.1 Scalar and Pseudo Scalar Operators

$$\mathcal{Q}_{1,q}^{(6)} = m_q \bar{q} q X^\mu X_\mu^*. \tag{5.1}$$

$$\mathcal{Q}_{2,q}^{(6)} = i m_q \bar{q} \gamma^5 q X^\mu X_\mu^*. \tag{5.2}$$

5.1.2 Vector Operators

5.1.2.1 Type A

$$\mathcal{Q}_{3,q}^{(6)} = i \bar{q} \gamma^\mu q X_\nu^* \overleftrightarrow{\partial}_\mu X^\nu. \tag{5.3}$$

$$\mathcal{Q}_{4,q}^{(6)} = i \bar{q} \gamma^\mu \gamma^5 q X_\nu^* \overleftrightarrow{\partial}_\mu X^\nu. \tag{5.4}$$

5.1.2.2 Type B

$$\mathcal{Q}_{5,q}^{(6)} = \bar{q} \gamma_\mu q X_\nu^* \overleftrightarrow{\partial}_\rho X_\lambda \epsilon^{\mu\nu\rho\lambda}. \tag{5.5}$$

$$\mathcal{Q}_{6,q}^{(6)} = \bar{q} \gamma_\mu \gamma^5 q X_\nu^* \overleftrightarrow{\partial}_\rho X_\lambda \epsilon^{\mu\nu\rho\lambda}. \tag{5.6}$$

5.1.2.3 Type C

$$\mathcal{Q}_{7,q}^{(6)} = i\bar{q}\gamma_\mu q \partial_\rho \Big(X_\nu^* X_\lambda \Big) \epsilon^{\mu\nu\rho\lambda}. \tag{5.7}$$

$$\mathcal{Q}_{8,q}^{(6)} = i\bar{q}\gamma_\mu \gamma^5 q \partial_\rho \Big(X_\nu^* X_\lambda \Big) \epsilon^{\mu\nu\rho\lambda}. \tag{5.8}$$

5.1.2.4 Type D

$$\mathcal{Q}_{9,q}^{(6)} = \bar{q}\gamma^\mu q \Big[X_\nu^* \partial^\nu X_\mu + \text{ c.c} \Big]. \tag{5.9}$$

$$\mathcal{Q}_{10,q}^{(6)} = \bar{q}\gamma^\mu \gamma^5 q \Big[X_\nu^* \partial^\nu X_\mu + \text{ c.c} \Big]. \tag{5.10}$$

5.1.2.5 Type E

$$\mathcal{Q}_{11,q}^{(6)} = \bar{q}\gamma^\mu q \Big[i X_\nu^* \partial^\nu X_\mu + \text{ c.c} \Big]. \tag{5.11}$$

$$\mathcal{Q}_{12,q}^{(6)} = \bar{q}\gamma^\mu \gamma^5 q \Big[i X_\nu^* \partial^\nu X_\mu + \text{ c.c} \Big]. \tag{5.12}$$

5.1.2.6 Gluons

$$\mathcal{Q}_{1,g}^{(6)} = \frac{\alpha_s}{12\pi} \mathcal{G}^{a\mu\nu} \mathcal{G}_{\mu\nu}^a X_\rho^* X^\rho. \tag{5.13}$$

$$\mathcal{Q}_{2,g}^{(6)} = \frac{\alpha_s}{8\pi} \mathcal{G}^{a\mu\nu} \tilde{\mathcal{G}}_{\mu\nu}^a X_\rho^* X^\rho. \tag{5.14}$$

5.2 HDMET Conversion of Interaction Operators

The list of interaction operators in 5.1 should be rewritten into terms of the massless vector field χ^μ before it can be put to use. Applying the many useful expressions found in Appendix B one can state the interaction operators dependent on χ^μ in next to leading order (NLO). The labels and groups follow the same scheme as in 5.1.

5.2.1 Scalar and Pseudo Scalar Operators

$$\mathcal{Q}_{1,q}^{(6)} \approx m_q \bar{q} q \chi_\mu^* \chi^\mu. \tag{5.15}$$

$$\mathcal{Q}_{2,q}^{(6)} \approx i m_q \bar{q} \gamma^5 q \chi_\mu^* \chi^\mu. \tag{5.16}$$

5.2.2 Vector Operators

5.2.2.1 Type A

$$\mathcal{Q}_{3,q}^{(6)} \approx i\bar{q}\gamma^{\mu}q\chi_{\nu}^{*}\overleftrightarrow{\partial}_{\mu}\chi^{\nu} + \left(\frac{2v_{\mu}}{m_X}\partial^{\rho}\chi_{\rho}^{*}\partial_{\lambda}\chi^{\lambda} + 2m_X v_{\mu}\chi_{\nu}^{*}\chi^{\nu}\right)\bar{q}\gamma^{\mu}q. \tag{5.17}$$

$$\mathcal{Q}_{4,q}^{(6)} \approx i\bar{q}\gamma^{\mu}\gamma^{5}q\chi_{\nu}^{*}\overleftrightarrow{\partial}_{\mu}\chi^{\nu} + \left(\frac{2v_{\mu}}{m_X}\partial^{\rho}\chi_{\rho}^{*}\partial_{\lambda}\chi^{\lambda} + 2m_X v_{\mu}\chi_{\nu}^{*}\chi^{\nu}\right)\bar{q}\gamma^{5}\gamma^{\mu}q. \tag{5.18}$$

5.2.2.2 Type B

$$\begin{aligned}\mathcal{Q}_{5,q}^{(6)} \approx\ & \bar{q}\gamma^{\mu}q\chi_{\nu}^{*}\overleftrightarrow{\partial}_{\rho}\chi_{\lambda}\epsilon^{\mu\nu\rho\lambda} + \frac{v_{\nu}}{m_X}\bar{q}\gamma_{\mu}q\left[i\chi_{\lambda}^{*}\overleftrightarrow{\partial}_{\rho}\partial_{\sigma}\chi^{\sigma} + \text{ c.c}\right]\epsilon^{\mu\nu\rho\lambda} \\ & - 2im_X\bar{q}\gamma_{\mu}qv_{\rho}\chi_{\nu}^{*}\chi_{\lambda}\epsilon^{\mu\nu\rho\lambda}.\end{aligned} \tag{5.19}$$

$$\begin{aligned}\mathcal{Q}_{6,q}^{(6)} \approx\ & \bar{q}\gamma^{\mu}\gamma^{5}q\chi_{\nu}^{*}\overleftrightarrow{\partial}_{\rho}\chi_{\lambda}\epsilon^{\mu\nu\rho\lambda} + \frac{v_{\nu}}{m_X}\bar{q}\gamma_{\mu}\gamma^{5}q\left[i\chi_{\lambda}^{*}\overleftrightarrow{\partial}_{\rho}\partial_{\sigma}\chi^{\sigma} + \text{ c.c}\right]\epsilon^{\mu\nu\rho\lambda} \\ & - 2im_X\bar{q}\gamma_{\mu}\gamma^{5}qv_{\rho}\chi_{\nu}^{*}\chi_{\lambda}\epsilon^{\mu\nu\rho\lambda}.\end{aligned} \tag{5.20}$$

5.2.2.3 Type C

$$\mathcal{Q}_{7,q}^{(6)} \approx i\bar{q}\gamma_{\mu}q\partial_{\rho}\Big(\chi_{\nu}^{*}\chi_{\lambda}\Big)\epsilon^{\mu\nu\rho\lambda} - \frac{v_{\nu}}{m_X}\bar{q}\gamma_{\mu}q\left[\partial_{\rho}\Big(\chi_{\lambda}^{*}\partial_{\sigma}\chi^{\sigma}\Big) + \text{ c.c}\right]\epsilon^{\mu\nu\rho\lambda}. \tag{5.21}$$

$$\mathcal{Q}_{8,q}^{(6)} \approx i\bar{q}\gamma_{\mu}\gamma^{5}q\partial_{\rho}\Big(\chi_{\nu}^{*}\chi_{\lambda}\Big)\epsilon^{\mu\nu\rho\lambda} - \frac{v_{\nu}}{m_X}\bar{q}\gamma_{\mu}\gamma^{5}q\left[\partial_{\rho}\Big(\chi_{\lambda}^{*}\partial_{\sigma}\chi^{\sigma}\Big) + \text{ c.c}\right]\epsilon^{\mu\nu\rho\lambda}. \tag{5.22}$$

5.2.2.4 Type D

$$\begin{aligned}\mathcal{Q}_{9,q}^{(6)} \approx\ & \bar{q}\gamma^{\mu}q\left[\partial^{\nu}\Big(\chi_{\nu}^{*}\chi_{\mu}\Big) + \text{ c.c}\right] - \frac{v_{\mu}}{m_X}\bar{q}\gamma^{\mu}q\left[i\partial^{\nu}\Big(\chi_{\nu}^{*}\partial_{\sigma}\chi^{\sigma}\Big) + \text{ c.c}\right] \\ & + \frac{1}{m_X}\bar{q}\gamma^{\mu}q\left[i\partial^{\lambda}\chi_{\lambda}^{*}v\cdot\partial\chi_{\mu} + \text{ c.c}\right].\end{aligned} \tag{5.23}$$

$$\begin{aligned}\mathcal{Q}_{10,q}^{(6)} \approx\ & \bar{q}\gamma^{\mu}\gamma^{5}q\left[\partial^{\nu}\Big(\chi_{\nu}^{*}\chi_{\mu}\Big) + \text{ c.c}\right] - \frac{v_{\mu}}{m_X}\bar{q}\gamma^{\mu}\gamma^{5}q\left[i\partial^{\nu}\Big(\chi_{\nu}^{*}\partial_{\sigma}\chi^{\sigma}\Big) + \text{ c.c}\right] \\ & + \frac{1}{m_X}\bar{q}\gamma^{\mu}\gamma^{5}q\left[i\partial^{\lambda}\chi_{\lambda}^{*}v\cdot\partial\chi_{\mu} + \text{ c.c}\right].\end{aligned} \tag{5.24}$$

5.2.2.5 Type E

$$\begin{aligned}\mathcal{Q}_{11,q}^{(6)} &\approx i\bar{q}\gamma^{\mu}q\left[\partial^{\nu}\left(\chi_{\nu}^{*}\chi_{\mu}\right)-\text{ c.c}\right]+\frac{v_{\mu}}{m_X}\bar{q}\gamma^{\mu}q\left[\partial^{\nu}\left(\chi_{\nu}^{*}\partial_{\lambda}\chi^{\lambda}\right)+\text{ c.c}\right]\\ &\quad-\frac{1}{m_X}\bar{q}\gamma^{\mu}q\left[\partial^{\lambda}\chi_{\lambda}^{*}v\cdot\partial\chi_{\mu}+\text{ c.c}\right].\end{aligned} \tag{5.25}$$

$$\begin{aligned}\mathcal{Q}_{11,q}^{(6)} &\approx i\bar{q}\gamma^{\mu}\gamma^{5}q\left[\partial^{\nu}\left(\chi_{\nu}^{*}\chi_{\mu}\right)-\text{ c.c}\right]+\frac{v_{\mu}}{m_X}\bar{q}\gamma^{\mu}\gamma^{5}q\left[\partial^{\nu}\left(\chi_{\nu}^{*}\partial_{\lambda}\chi^{\lambda}\right)+\text{ c.c}\right]\\ &\quad-\frac{1}{m_X}\bar{q}\gamma^{\mu}\gamma^{5}q\left[\partial^{\lambda}\chi_{\lambda}^{*}v\cdot\partial\chi_{\mu}+\text{ c.c}\right].\end{aligned} \tag{5.26}$$

5.2.3 Gluon Operators

$$\mathcal{Q}_{1,g}^{(6)} \approx \frac{\alpha_s}{12\pi}\mathcal{G}^{a\mu\nu}\mathcal{G}_{\mu\nu}^{a}\chi_{\sigma}^{*}\chi^{\sigma}. \tag{5.27}$$

$$\mathcal{Q}_{2,g}^{(6)} \approx \frac{\alpha_s}{8\pi}\mathcal{G}^{a\mu\nu}\tilde{\mathcal{G}}_{\mu\nu}^{a}\chi_{\sigma}^{*}\chi^{\sigma}. \tag{5.28}$$

5.3 Scattering Amplitudes

As described in 3.7.1 one can calculate the scattering amplitude for all the different possible interactions that are described by the interaction operators in section 5.2. A more detailed calculation of these amplitudes is shown in Appendix D, here only the final results are stated. As explained in section 3.7 not all interaction operators give leading order contributions for the two Feynman diagrams. Hence the work is simplified a considerable amount. It is beneficial to express the amplitudes in so called *basis operators*, which are defined and explained in Appendix D. The results are presented in two groups, one for each of the Feynman diagrams in Fig. 3.1. Note that all scattering amplitudes stated below show the interaction between DM and a proton. To instead consider the collision with a neutron, one would let $p \to n$ and $u \to d$.

5.3.1 Contact Interaction

For the contact interaction, the left panel of Fig. 3.1, the currents J_q^S, J_q^V, J_q^A, J^G and J^θ contribute [8]. As mentioned before, the currents J_q^S, J_q^V and J_q^A are hadronized into nucleons first. This has been done neatly in [8] and the procedure of evaluating it can be found in Appendix D. In the same appendix one can also find all the basis operators Q and their associated coupling constants.

5.3.1.1 Scalar Current

$$i\mathcal{M}_p^S = i\varepsilon_\mu^* \varepsilon^\mu \bar{u}_p u_p \left[\sigma_u^p \cdot \hat{C}_{1,u}^{(6)} + \sigma_d^p \cdot \hat{C}_{1,d}^{(6)} + \sigma_s \cdot \hat{C}_{1,s}^{(6)}\right]. \tag{5.29}$$

Again, the reader is strongly advised to visit Appendix D to properly understand the new notations and the procedure of expressing the scattering amplitude in such a way.

5.3.1.2 Vector Current, Type A

$$i\mathcal{M}_p^{V,a} = 2im_X \varepsilon_\mu^* \varepsilon^\mu \bar{u}_p u_p \left(2\hat{C}_{3,u}^{(6)} + \hat{C}_{3,d}^{(6)}\right). \tag{5.30}$$

5.3.1.3 Vector Current, Type B

$$\begin{aligned} i\mathcal{M}_p^{V,b} &= -2im_X V_{\perp,\mu} S_X^\mu \bar{u}_p u_p \left(2\hat{C}_{5,u}^{(6)} + \hat{C}_{5,d}^{(6)}\right) \\ &\quad - 2m_X S_X^\mu \hat{\mathcal{W}}(\hat{C}_{5,q}^{(6)}) \bar{u}_p W_\mu u_p. \end{aligned} \tag{5.31}$$

5.3.1.4 Vector Current, Type C

$$i\mathcal{M}_p^{V,c} = q \cdot S_X \bar{u}_p u_p \left(2\hat{C}_{7.u}^{(6)} + \hat{C}_{7,d}^{(6)}\right). \tag{5.32}$$

5.3.1.5 Vector Current, Type D

$$\begin{aligned} i\mathcal{M}_p^{V,d} &= -2q \cdot S \cdot V_\perp \bar{u}_p u_p \left(2\hat{C}_{9,u}^{(6)} + \hat{C}_{9,d}^{(6)}\right) \\ &\quad + 2iq^\nu S_{\mu\nu} \hat{\mathcal{W}}(\hat{C}_{9,q}^{(6)}) \bar{u}_p W^\mu u_p. \end{aligned} \tag{5.33}$$

5.3.1.6 Vector Current, Type E

$$\begin{aligned} i\mathcal{M}_p^{V,e} &= 2iq^\nu \bar{S}_{\mu\nu} v_\perp^\mu \bar{u}_p u_p \left(2\hat{C}_{11,u}^{(6)} + \hat{C}_{11,d}^{(6)}\right) \\ &\quad - \frac{i}{m_X} q \cdot S \cdot q \bar{u}_p u_p \left(2\hat{C}_{11,u}^{(6)} + \hat{C}_{11,d}^{(6)}\right) \\ &\quad + 2q^\nu \bar{S}_{\mu\nu} \hat{\mathcal{W}}(\hat{C_{11,q}^{(6)}}) \bar{u}_p W^\mu u_p. \end{aligned} \tag{5.34}$$

5.3.1.7 Axial Current, Type A

$$i\mathcal{M}_p^{A,a} = 2im_X \hat{\mathcal{A}}(\hat{C}_{4,q}^{(6)}) \varepsilon_\mu^* \varepsilon^\mu \bar{u}_p v_\perp \cdot S_N u_p. \tag{5.35}$$

5.3.1.8 Axial Current, Type B

$$i\mathcal{M}_p^{A,b} = -2m_X \hat{\mathcal{A}}(\hat{C}_{6,q}^{(6)}) S_X^\mu \bar{u}_p S_{N,\mu} u_p. \tag{5.36}$$

5.3.1.9 Axial Current, Type C

$$
\begin{aligned}
i\mathcal{M}_p^{A,c} = i\hat{\mathcal{A}}(\hat{C}_{8,q}^{(6)})\Bigg(& - q^\nu \hat{S}_{\mu\nu}\bar{u}_p S_N^\mu u_p \\
& - \frac{i}{2m_N} S_X \cdot q \bar{u}_p K \cdot S_N u_p \\
& + \epsilon^{\mu\nu\rho\lambda}\frac{v_\nu}{m_X} q_\rho \left[\bar{S}_{\lambda\sigma}\tilde{P}^\sigma + S_{\lambda\sigma}q^\sigma\right] \bar{u}_p S_{N,\mu} u_p \Bigg).
\end{aligned}
\tag{5.37}
$$

5.3.1.10 Axial Current, Type D

$$
i\mathcal{M}_p^{A,d} = 2\hat{\mathcal{A}}(\hat{C}_{10,q}^{(6)}) S_{\mu\nu} q^\nu \bar{u}_p S_N^\mu u_p. \tag{5.38}
$$

5.3.1.11 Axial Current, Type E

$$
i\mathcal{M}_p^{A,e} = -2i\hat{\mathcal{A}}(\hat{C}_{12,q}^{(6)}) q^\nu \bar{S}_{\mu\nu} \bar{u}_p S_N^\mu u_p. \tag{5.39}
$$

5.3.1.12 Gluon Current

$$
i\mathcal{M}_p^{G} = \frac{-2im_G}{27}\varepsilon_\mu^* \varepsilon^\mu \bar{u}_p u_p \hat{C}_1^{(6)}. \tag{5.40}
$$

5.3.1.13 Dual Gluon Current

$$
\begin{aligned}
i\mathcal{M}_p^{\theta} = & -i\varepsilon_\mu^* \varepsilon^\mu \bar{u}_p iq \cdot S_N u_p \hat{C}_2^{(6)} \\
& \times \left[D\left(\frac{\tilde{m}}{m_u} + \frac{\tilde{m}}{m_s}\right) + F\left(\frac{\tilde{m}}{m_u} - \frac{\tilde{m}}{m_s}\right) + G \right].
\end{aligned}
\tag{5.41}
$$

5.3.2 Meson Mediator Interaction

For the case of interaction mediated by a meson, i.e. the right panel of Fig.3.1, the currents J_q^P, J_q^A and J^θ contribute to leading order. The hadronization of the quark currents into mesons is again taken from [8] and the full expressions for this procedure and explanations of notation/constants can be found in Appendix D. The propagating meson gives the usual contribution to the amplitude, i.e. $\frac{i}{q^2 - m_{\pi/\eta}^2}$.

5.3.2.1 Pseudo Scalar Current

$$
\begin{aligned}
i\mathcal{M}_p^{P} = & \bar{u}_p iq \cdot S_N u_p \varepsilon_\mu^* \varepsilon^\mu B_0 i^2 \\
& \times \Bigg[\frac{ig_a}{q^2 - m_\pi^2}\left(\hat{C}_{2,u}^{(6)} m_u - \hat{C}_{2,d}^{(6)} m_d\right) \\
& + \frac{\Delta u + \Delta d - 2\Delta s}{3}\frac{i}{q^2 - m_\eta^2}\left(\hat{C}_{2,u}^{(6)} m_u + \hat{C}_{2,d}^{(6)} m_d - 2\hat{C}_{2,s}^{(6)} m_s\right) \Bigg].
\end{aligned}
\tag{5.42}
$$

5.3.2.2 Axial Current, Type A

As explained in Appendix D, this scattering amplitude is found to be of order three in momentum q. It is not Galilean invariant and would thus cause some problems. However, since it is coupled to the interaction operator $\mathcal{Q}^{(6)}_{4,q}$ which already gets a leading order contribution from the contact diagram (see Eq. 5.35) one can safely ignore this amplitude.

5.3.2.3 Axial Current, Type B

$$i\mathcal{M}^{A,b}_p \approx 2m_X \hat{\mathcal{B}}(\hat{C}^6_{6,q}) iq \cdot S_X \bar{u}_p iq \cdot S_N u_p. \tag{5.43}$$

5.3.2.4 Axial Current, Type C

This amplitude actually goes to zero as explained in Appendix D (see Eq. (D.50)). Thus

$$i\mathcal{M}^{A,c}_p = 0. \tag{5.44}$$

5.3.2.5 Axial Current, Type D

$$i\mathcal{M}^{A,c}_p \approx 2i\hat{\mathcal{B}}(\hat{C}^6_{10,q}) q^\nu q^\mu S_{\mu\nu} \bar{u}_p iq \cdot S_N u_p. \tag{5.45}$$

5.3.2.6 Axial Current, Type E

This amplitude gets, in similarity to type A, its leading contribution from a term that is not Galilean invariant. Again, this poses no threat as the amplitude is coupled to the interaction operator $\mathcal{Q}^{(6)}_{12,q}$ which has a leading order contribution from the contact diagram (see Eq. (D.35)).

5.4 Matching Basis Operators and Coupling Constants to the Non-Relativistic Effective Lagrangian

From the scattering amplitudes in section 5.3 18 basis operators and coupling constants are defined. These basis operators are non-relativistic but written in a Lorentzian notation. They can be viewed in table 5.1 and Eq. (5.46) but the reader is advised to visit Appendix E to get a deeper understanding. Additionally, there is one basis operator of order three:

$$Q^{(3)}_p = q \cdot S \cdot q \bar{u}_p iq \cdot S_N u_p. \tag{5.46}$$

The steps of rewriting these basis operators in a manifestly non-relativistic way (and thus compare them to the operators stated in [21]) is shown in Appendix E.1.1. The basis operators of [21] are already displayed in the theory section, see table 3.1. The relation between the basis operators $Q^{(d)}_{n,p}$ and the non-relativistic operators $\mathcal{O}_{n,p}$ in table 3.1 are shown in table E.7.

Basis operators $Q^{(d)}_{n,p}$.	
$Q^{(0)}_{1,p} = \varepsilon^*_\mu \varepsilon^\mu \bar{u}_p u_p$	$Q^{(0)}_{2,p} = S^\mu_X \bar{u}_p S_{N,\mu} u_p$
$Q^{(1)}_{1,p} = \varepsilon^*_\mu \varepsilon^\mu \bar{u}_p iq \cdot S_N u_p$	$Q^{(1)}_{2,p} = iq \cdot S_X \bar{u}_p u_p$
$Q^{(1)}_{3,p} = \varepsilon^*_\mu \varepsilon^\mu \bar{u}_p v_\perp \cdot S_N u_p$	$Q^{(1)}_{4,p} = v_{\perp,\mu} S^\mu_X \bar{u}_p u_p$
$Q^{(1)}_{5,p} = i\epsilon^{\alpha\beta\mu\nu} v_\alpha q_\beta S_{X,\mu} \bar{u}_p S_{N,\nu} u_p$	$Q^{(1)}_{6,p} = \bar{S}_{\mu\nu} q^\nu v^\mu_\perp \bar{u}_p u_p$
$Q^{(1)}_{7,p} = q^\nu \bar{S}_{\mu\nu} \bar{u}_p S^\mu_N u_p$	$Q^{(1)}_{8,p} = v_\perp \cdot S \cdot q \bar{u}_p u_p$
$Q^{(1)}_{9,p} = q^\nu S_{\mu\nu} \bar{u}_p S^\mu_N u_p$	
$Q^{(2)}_{1,p} = iq \cdot S_X \bar{u}_p iq \cdot S_N u_p$	$Q^{(2)}_{2,p} = q^\nu \bar{S}_{\mu\nu} \bar{u}_p W^\mu u_p$
$Q^{(2)}_{3,p} = q \cdot S \cdot q \bar{u}_p u_p$	$Q^{(2)}_{4,p} = q^\nu S_{\mu\nu} \bar{u}_p W^\mu u_p$
$Q^{(2)}_{5,p} = i\epsilon^{\mu\nu\rho\lambda} v_\nu q_\rho S_{\lambda\sigma} q^\sigma \bar{u}_p S_{N,\mu} u_p$	
$Q^{(2)}_{6,p} = -q_\nu \hat{S}^{\mu\nu} \bar{u}_p S_{N,\mu} u_p - \frac{i}{2m_p} S^\nu_X \cdot q \bar{u}_p K \cdot S_N u_p + \epsilon^{\mu\nu\rho\lambda} \frac{v_\nu}{m_X} q_\rho \bar{S}_{\lambda\sigma} \tilde{P}^\sigma \bar{u}_p S_{N,\mu} u_p$	

Table 5.1: All basis operators of order zero, one and two which spans all the scattering amplitudes found in section 5.3.

Expressions for $c^{\mathrm{NR}}_{n,p}$	
$c^{\mathrm{NR}}_{1,p} = -\left[\hat{c}^{(6)}_{1,u}\cdot\sigma^p_u + \hat{c}^{(6)}_{1,d}\cdot\sigma^p_d + \hat{c}^{(6)}_{1,s}\cdot\sigma^p_s\right] - 2m_X + \frac{2m_G}{27}\hat{C}^{(6)}_1$	
$c^{\mathrm{NR}}_{4,p} = -2m_X\hat{\mathcal{A}}(\hat{C}^{(6)}_{6,q}) + q^2\hat{\mathcal{W}}(\hat{C}^{(6)}_{11,q})$	$c^{\mathrm{NR}}_{5,p} = m_p\Big(2\hat{C}^{(6)}_{11,u} + \hat{C}^{(6)}_{11,d}\Big)$
$c^{\mathrm{NR}}_{6,p} = -2m_p^2 m_X\hat{\mathcal{B}}(\hat{C}^{(6)}_{6,q}) - m_p^2\hat{\mathcal{W}}(\hat{C}^{(6)}_{11,q})$	$c^{\mathrm{NR}}_{7,p} = 2m_X\hat{\mathcal{A}}(\hat{C}^{(6)}_{4,q})$
$c^{\mathrm{NR}}_{8,p} = 2m_X\Big(2\hat{C}^{(6)}_{5,u} + \hat{C}^{(6)}_{5,d}\Big)$	$c^{\mathrm{NR}}_{9,p} = 2m_p m_X\hat{\mathcal{W}}(\hat{C}^{(6)}_{5,q}) + m_p\hat{\mathcal{A}}(\hat{C}^{(6)}_{12,q})$
$c^{\mathrm{NR}}_{10,p} =$ **see Eq.** (5.47)	$c^{\mathrm{NR}}_{11,p} = -m_p\Big(2\hat{C}^{(6)}_{7,u} + \hat{C}^{(6)}_{7,d}\Big)$
$c^{\mathrm{NR}}_{14,p} = -2im_p^2\hat{\mathcal{A}}(\hat{C}^{(6)}_{8,q})$	$c^{\mathrm{NR}}_{17,p} = -2m_p\Big(2\hat{C}^{(6)}_{9,u} + \hat{C}^{(6)}_{9,d}\Big)$
$c^{\mathrm{NR}}_{18,p} = 2m_p\hat{\mathcal{A}}(\hat{C}^{(6)}_{10,q})$	$c^{\mathrm{NR}}_{19,p} = -\frac{m_p^2}{m_X}\Big(2\hat{C}^{(6)}_{11,u} + \hat{C}^{(6)}_{11,d}\Big)$
$c^{\mathrm{NR}}_{20,p} = -m_p^2\Big(2\hat{\mathcal{W}}(\hat{C}^{(6)}_{9,q}) + \frac{1}{m_X}\hat{\mathcal{A}}(\hat{C}^{(6)}_{8,q})\Big)$	$c^{\mathrm{NR}}_{(3),p} = 2m_p^3\hat{\mathcal{B}}(\hat{C}^{(6)}_{10,q})$

Table 5.2: All non-relativistic coupling constants $c^{\mathrm{NR}}_{n,p}$ associated with the basis operators $\mathcal{O}_{n,p}$ for the scattering of DM against a proton.

Their associated coupling constants are shown in table 5.2. The coupling constant $c^{\mathrm{NR}}_{10,p}$ is too long to fit in the table, and can instead be studied in Eq. (5.47).

$$
\begin{aligned}
c^{\mathrm{NR}}_{10,p} = B_0 m_p \Bigg[& g_a\left(\hat{C}^{(6)}_{2,u}m_u + \hat{C}^{(6)}_{2,d}m_d\right)\frac{1}{q^2 - m_\pi^2} + \\
& \frac{\Delta u + \Delta d - 2\Delta s}{3}\left(\hat{C}^{(6)}_{2,u}m_u + \hat{C}^{(6)}_{2,d}m_d - 2\hat{C}^{(6)}_{2,s}m_s\right)\frac{1}{q^2 - m_\eta^2}\Bigg] - \\
& \hat{C}^{(6)}_2 m_p \Bigg\{ -\left[D\left(\frac{\tilde{m}}{m_u} + \frac{\tilde{m}}{m_d}\right) + F\left(\frac{\tilde{m}}{m_u} - \frac{\tilde{m}}{m_d}\right) + G\right] + \\
& \frac{q^2}{2}\left[g_a\frac{1}{q^2 - m_\pi^2}\left(\frac{\tilde{m}}{m_u} - \frac{\tilde{m}}{m_d}\right) + \frac{\Delta u + \Delta d - 2\Delta s}{3}\frac{1}{q^2 - m_\eta^2}\left(\frac{\tilde{m}}{m_u} + \frac{\tilde{m}}{m_d} - \frac{2\tilde{m}}{m_s}\right)\right]\Bigg\}
\end{aligned}
\tag{5.47}
$$

$\hat{\mathcal{A}}, \hat{\mathcal{B}}$ and $\hat{\mathcal{W}}$ are defined in Appendix D. Numerical values and their physical connection can be viewed in appendix C of [8].

5.5 Relativistic to Non-Relativistic Matching Conditions

As can be seen in table 5.2, several of the non-relativistic operators that span the basis of scattering amplitudes (found in e.g. [21, 22]) lack a coupling constant $c^{\mathrm{NR}}_{n,p}$. This means that there exist some unused non-relativistic operators that are in fact not needed to span all possible scattering amplitudes. The unused operators are:

- Of order zero: $\mathcal{O}_{2,p}$ and $\mathcal{O}_{12,p}$.
- Of order one: $\mathcal{O}_{3,p}, \mathcal{O}_{13,p}$.
- Of order two: $\mathcal{O}_{15,p}$.

The fact that these operators are left unused is noteworthy, as (clearly indicate above) they are of different orders of momentum and have nothing in common that would suggest their unimportance.

Further attention should be brought to the operators $\mathcal{O}_4$ and $\mathcal{O}_6$ and their coupling constants. Both $c^{\mathrm{NR}}_{4,p}$ and $c^{\mathrm{NR}}_{6,p}$ contain a term with the factor $\hat{\mathcal{W}}(\hat{C}^{(6)}_{11,q})$. This originates from the relativistic interaction operator $\mathcal{Q}^{(6)}_{11,q}$ which, as seen in Eq. (5.34) (vector current, type E), yields the basis operator $Q^{(2)}_{2,p}$ (see table E.3) which rewritten into the non-relativistic notation maps onto both $\mathcal{O}_{4,p}$ and $\mathcal{O}_{6,p}$. In addition to this remarkable feature, both these constants get contributions from the relativistic coupling constant $\hat{C}^{(6)}_6$ albeit from different functions ($\hat{\mathcal{A}}$ and $\hat{\mathcal{B}}$). This also shows the importance of starting at the simplified model and then going via the relativistic approach before evaluating in the non-relativistic limit. $\hat{C}^{(6)}_{6,q}$ originates from a interaction via a meson propagator and would therefore not have been present in a purely non-relativistic approach.

There are several more examples of these noteworthy co-dependencies. Table 5.2 confirms that:

- $\mathcal{O}_{4,p}$ and $\mathcal{O}_{6,p}$ share the coupling constant $\hat{\mathcal{W}}(\hat{C}^{(6)}_{11,q})$ and are also both influenced by $\hat{C}^{(6)}_{6,q}$.
- $\mathcal{O}_{5,p}$ and $\mathcal{O}_{19,p}$ share the coupling constant $\left(2\hat{C}^{(6)}_{11,u} + \hat{C}^{(6)}_{11,d}\right)$.
- $\mathcal{O}_{14,p}$ and $\mathcal{O}_{20,p}$ both depend on $\hat{\mathcal{A}}(\hat{C}^{(6)}_{8,q})$ which stem from $\mathcal{Q}^{(6)}_{8,q}$.
- $\mathcal{O}_{8,p}$ and $\mathcal{O}_{9,p}$ depend on the coupling constant $\hat{C}^{(6)}_{5,q}$.
- $\mathcal{O}_{18,p}$ and $\mathcal{O}^{(3)}_{1,p}$ relies on $\hat{C}^{(6)}_{10,q}$.
- $\mathcal{O}_{17,p}$ and $\mathcal{O}_{20,p}$ are connected via their dependence on $\hat{C}^{(6)}_{9,q}$.

So all in all 11 of the 21 non-relativistic basis operators show some sort of co-dependence. 6 of these are only apparent if one considers the meson mediator case of interaction.

6
Outlook

This chapter will state possible continuations from the work done in this thesis. It introduces computational tools that might be used to check the theoretical conclusions stated in section 5.

6.1 The use of `DMFormFactor` by Anand et al.

In addition to the theoretical workload that spans this thesis, it would also be possible to check any new findings from the procedure described above in chapter 4 in a more computational framework. The Mathematica package `DMFormFactor`, developed by Anand et al. [22], offers such a possibility. Through use of their program, one can find e.g., event rates of DM-nucleon interactions based on the input of the coupling constants of the non-relativistic basis operators defined in table 3.1. The program is however only applicable to the operators corresponding to spin-1/2, which means that it needs to be manually adapted into considering also the operators specific to spin-1 (i.e., $\mathcal{O}_{17,18,19,20}$). A discussion on how to do this will follow later on, see section 6.2

The differential event rate $\frac{dR}{dE_R}$, where R is the event rate and E_R is the recoil energy of the nucleus related to the momentum transfer q via

$$E_R = \frac{q^2}{2m_T}, \tag{6.1}$$

with m_T being the mass of the nucleon target, is a main feature in any direct detection experiment. From $\frac{dR}{dE_R}$ it is then easy to find the actual event rate R which is the number of scattering events per unit recoil energy per unit detector mass per unit time. The differential event rate is sought via

$$\frac{dR}{dE_R} = \frac{\rho_X}{m_T m_X} \int_{v_{\min}} \frac{d\sigma}{dE_R} v f_E(\boldsymbol{v}) dv^3. \tag{6.2}$$

Here, ρ_X is the assumed density of DM in the galaxy, which has an agreed value of $\rho_X \approx 0.4\text{GeV} \cdot \text{cm}^{-3}$ [2], f_E is the velocity distribution function of the DM relative to earths frame [22] which is a Maxwell-Boltzmann distribution centered around the most probable speed $v_0 \approx 220$ km/s. It is suggested to also include the escape velocity $v_{\text{esc}} \approx 540$ km/s to truncate the distribution in order to achieve more precise answers. Further one will need the value for the detectors velocity in the rest frame of the DM halo, this is set to $v_e \approx 232$ km/s. $\frac{d\sigma}{dE_R}$ is the differential cross section.

`DMFormFactor` calculates the event rate in the following way:

- `EventRate[NT, rhoDM, qGeV, ve, v0, vesc]` where
- `NT` is the inverse of the nucleus mass. For F-19 this would mean `NT` $= \frac{1}{\texttt{19*mNucleon}}$, with `mNucleon` being the mass of one nucleon, usually set to 0.938 GeV (in agreement with [22]).
- `rhoDM, ve,v0` and `vesc` are the DM density, Earths speed relative to the DM halo, the most probable DM velocity and escape velocity respectively. Their numerical values are described in the paragraph above.
- `qGeV` is the momentum transfer, which will remain a variable for the simulations, so to get the event rate as a function depending only on the momentum transfer.

The program in [22] allows for studies of scattering of a large variety of nucleon e.g., F-19 and XE-131. What nucleon the DM scatters against actually influences the event rate, as different structures within the different nucleons causes subtle changes in how the recoil energy is transferred. A much more thorough discussion of this is found in [22]. It is also worth noting that all scattering amplitudes are be calculated in this thesis (see section 5.3 and Appendix D.2) are done so based on the interaction between DM and nucleons, not nucleus. This promotion is however built into `DMFormFactor` and thus it streamlines the usage.

6.2 Modifications to `DMFormFactor` by Anand et al.

To properly incorporate the basis operators unique to spin-1 some small adjustments to the source code of `DMFormFactor` needs to be done.

Firstly, the program is built to only accept 15 non-relativistic basis operators. It has several `If`-statements producing warnings and errors if one try to put a coupling constant related to an operator enumerated higher than 15. These needs to be modified so that they instead allow for 20 operators. By searching in the source code for strings like `<=15` one quickly finds all the lines in need of adjustment. The change is then to simply put `<=20` instead.

Secondly, the `EventRate` function writes out the effective Lagrangian used before each calculation, in order for it to also express the spin-1 operators one searches for the string `Op[1]="1"` and adds the symbolic descriptions of the new operators at the bottom off the list. This step is purely a design feature, as it will display the correct Lagrangian, it is however not important for the calculations and one could therefore see it as optional.

Thirdly, the response functions needs to be updated to include the responses which would occur from spin-1 DM. The response functions for Spin-1 DM have been defined in Eq. (4.7) in [21], these would be a suitable candidate for an updated version of the response functions of the source code. By searching for `ResponseCoeff` one finds the correct lines to adjust. This step can be expanded into excluding some operators that, in the result section (see section 5.5), are shown to lack influence. This will cut the compilation time as the program has fever inputs into the response functions to consider (which will be a high priority, the unchanged version of `EventRate` takes roughly 80 seconds to run, when unused operators are discarded the evaluation time is cut to around one fourth of that).

With these adjustments the program should then be applicable also for spin-1 interactions. The general procedure is then to set all but one of the coupling constants to zero as to isolate one specific operator and monitor its influence over the event rate. As seen in the results section (see section 5.5) there will however be times where two coupling constants c_n^{NR} originate from the same relativistic coupling constant $\hat{C}_{n,q}^{(d)}$. This is an area of interest and to investigate how two operators, sharing a constant $\hat{C}_{n,q}^{(d)}$, might interfere with each other should definitely be done.

7
Conclusion

In this work we have considered two Feynman diagrams for the interaction between the spin-1 DM and a nucleon. The two different interactions are described via either chiral perturbation theory (for the meson mediator case, right part of Fig. 3.1) or through heavy baryon chiral perturbation theory (for the contact interaction, left part of Fig. 3.1). From this simplified model we then assumed that the momentum transfer was far less than the mass of the mediating particle, which allowed us to move into the relativistic approach and construct an EFT Lagrangian. From it we found relativistic quantum mechanical interaction operators $\mathcal{Q}_{n,q}^{(d)}$ and expressed the relativistic interaction Lagrangian as a sum of different interaction operators coupled to individual coupling constants. After that, scattering amplitudes could be found and later expressed by a set of basis operators $Q_{n,p}^{(d)}$. These basis operators were then compared to the set of non-relativistic basis operators found by Catena et al. [21], $\mathcal{O}_{n,p}$. Interesting co-dependencies where found to arise between the basis operators which, from the strictly non-relativistic point of view, looked independent. This happened in no less than 11 of the 21 cases, which shows the importance of considering relativistic EFT even when operating in the non-relativistic limit. Further, we found that one basis operator of order three is necessary to include when looking at the meson mediator interaction. This operator is not included in previous work and we can thus expand the set of non-relativistic basis operators defined in [21] by our additional order three operator.

Bibliography

[1] Gustaver, M. (2020) A Chalmers University of Technology Master's thesis template for LaTeX. Unpublished.

[2] Heiles M, König M, Neubert M. Effective Field Theory for Heavy Vector Resonances Coupled to the Standard Model. 2020 Nov 16. Available from: https://arxiv.org/abs/2011.08205

[3] Stefan Scherer. "Introduction to chiral perturbation theory". In: Adv. Nucl. Phys. 27 (2003). Ed. by John W. Negele and E. W. Vogt, p. 277. arXiv: hep-ph/0210398.

[4] Georgi HG, Kaplan DB, Randall L. Manifesting the invisible axion at low energies. Phys Lett B. 1986;169(1):73–78. doi:10.1016/0370-2693(86)90688-X

[5] Workman RL, Cahn RN, Carone CD, et al. Dark matter. In: Workman RL, ed. Review of Particle Physics. Prog Theor Exp Phys. 2024;2024(8):083C01. doi:10.1093/ptep/ptae052

[6] Peskin ME, Schroeder DV. An introduction to quantum field theory. Reading, MA: Addison-Wesley; 1995.

[7] Particle Data Group. Review of Particle Physics. Prog Theor Exp Phys. 2022;2022(8):083C01. doi:10.1093/ptep/ptac097.

[8] Bishara F, Brod J, Grinstein B, Zupan J. Chiral effective theory of dark matter direct detection. J Cosmol Astropart Phys. 2017;2017(02):009. doi:10.1088/1475-7516/2017/02/009.

[9] Gasser J, Leutwyler H. Chiral perturbation theory: Expansions in the mass of the strange quark. Nucl Phys B. 1985;250(1):465–516. doi:10.1016/0550-3213(85)90492-4

[10] Jenkins E, Manohar AV. Baryon chiral perturbation theory using a heavy fermion Lagrangian. Phys Lett B. 1991;255(4):558-562. doi:10.1016/0370-2693(91)90266-S

[11] National Aeronautics and Space Administration. Dark Matter [Internet]. Washington, D.C.: NASA; 2023 Dec 20 [cited 2025 Feb 24]. Available from: https://science.nasa.gov/mission/roman-space-telescope/dark-matter/

[12] Zwicky, F. (1933), "Die Rotverschiebung von extragalaktischen Nebeln" [The red shift of extragalactic neubulae], Helvetica Physica Acta (in German)

[13] Gianfranco Bertone and Dan Hooper. "History of dark matter". In: Reviews of Modern Physics 90.4 (Oct. 2018). issn: 1539-0756. doi: 10.1103/revmodphys.90.045002.

[14] Víctor Martín Lozano, Dark Matter at Colliders: Theory. Presented at: 9th Annual Large Hadron Collider Physics. Available from: https://indico.cern.ch/event/905399/contributions/4298038/

[15] Roberts C.D., Schmidt S.M. Pseudoscalar Mesons and Emergent Mass. Few-Body Syst. 2023;64(2):42.

[16] Szymańska E. Spontaneous Symmetry Breaking and Goldstone Theorem. 2023 REYES Proceedings. 2023;9.

[17] Machleidt R, Entem DR. Chiral effective field theory and nuclear forces. Physics Reports. 2011;503(1):1-75.

[18] Petrov AA, Blechman AE. Effective Field Theories. Singapore: World Scientific; 2016.

[19] Diakonov D, Petrov V, Pobylitsa P. A chiral theory of nucleons. Nuclear Physics B. 1988;306(4):809-848.

[20] Catena R, Fridell K, Zema V. Direct detection of fermionic and vector dark matter with polarised targets. J Cosmol Astropart Phys. 2018 Nov;2018(11):018. doi: 10.1088/1475-7516/2018/11/018.

[21] Catena R, Fridell K, Krauss MB. Non-relativistic effective interactions of spin 1 dark matter. J High Energy Phys. 2019 Aug;2019(8):30. doi: 10.1007/JHEP08(2019)030.

[22] Anand N, Fitzpatrick AL, Haxton WC. Weakly interacting massive particle-nucleus elastic scattering response. Phys Rev C. 2014;89(6):065501. doi:10.1103/PhysRevC.89.065501

[23] Stephen P. Martin. “A supersymmetry primer”. In: Advanced Series on Directions in High Energy Physics (1998), pp. 1–98. issn: 1793-1339. doi: 10.1142/9789812839657_0001.

[24] Bozorgnia N, Bramante J, Cline JM, Curtin D, McKeen D, Morrissey DE, et al. Dark matter candidates and searches. Can J Phys. 2024 Sep 27; doi: 10.1139/cjp-2024-0128.

[25] Tisserand P, Le Guillou L, Afonso C, Albert JN, Andersen J, Ansari R, et al. Limits on the Macho content of the Galactic Halo from the EROS-2 Survey of the Magellanic Clouds. Astron Astrophys. 2007 Jul;469(2):387-404. doi: 10.1051/0004-6361:20066017.

[26] Nakamura K, Particle Data Group. Review of particle physics. J Phys G Nucl Part Phys. 2010 Jul;37(7A):075021. doi: 10.1088/0954-3899/37/7A/075021.

[27] S. D. M. White, C. S. Frenk, and M. Davis. “Clustering in a neutrino-dominated universe”. In: apjl 274 (Nov. 1983), pp. L1–L5. doi: 10.1086/184139

[28] Arcadi G, Dutra M, Ghosh P, Lindner M, Mambrini Y, Pierre M, Profumo S, Queiroz FS. The waning of the WIMP? A review of models, searches, and constraints. Eur Phys J C. 2018;78(3):203. doi:10.1140/epjc/s10052-018-5662-y.

[29] Misiaszek M, Rossi N. Direct detection of dark matter: A critical review. Symmetry. 2024;16(2):201. doi:10.3390/sym16020201.

[30] Teresa Marrodán Undagoitia and Ludwig Rauch. “Dark matter direct-detection experiments”. In: Journal of Physics G: Nuclear and Particle Physics 43.1 (2015), p. 013001. issn: 1361-6471. doi: 10.1088/0954-3899/43/1/013001.

[31] NASA Science. Building blocks of the universe: Dark matter [Internet]. Washington, D.C.: National Aeronautics and Space Administration; [cited 2025 Mar 3]. Available from: https://science.nasa.gov/universe/overview/building-blocks/#dark-matter

[32] Gentile S; AMS-02 Collaboration. The Alpha Magnetic Spectrometer on the International Space Station. Proceedings of the 28th International Cosmic Ray Conference; 2003 Jul 31–Aug 7; Tsukuba, Japan.

[33] Bishara F, Brod J, Grinstein B, Zupan J. From quarks to nucleons in dark matter direct detection. J High Energy Phys. 2017 Nov;2017(11):59. doi: 10.1007/JHEP11(2017)059.

[34] McDonald AB. Dark matter detection with liquid argon. Nucl Phys B. 2024;1003:116436. doi: 10.1016/j.nuclphysb.2024.116436.

[35] Hickok K. Researchers use purified liquid xenon to search for mysterious dark matter particles. Phys.org. 2022 Sep 15 [cited 2025 Mar 4]. Available from: https://phys.org/news/2022-09-purified-liquid-xenon-mysterious-dark.html

[36] Gondolo P. Recoil momentum spectrum in directional dark matter detectors [preprint]. Case Western Reserve University, Department of Physics; 2002 Sep 4. Available from: https://arxiv.org/pdf/hep-ph/0209110

[37] Gaskins J. A review of indirect searches for particle dark matter. Contemp Phys. 2016;57(4):496-525. doi:10.1080/00107514.2016.1175160.

[38] Ackermann M, Fermi-LAT Collaboration. The Fermi Large Area Telescope On Orbit: Event Classification, Instrument Response Functions, and Calibration. Astrophys J Suppl. 2012;203(4):4. doi: 10.1088/0067-0049/203/4/4.

[39] Fermi National Accelerator Laboratory. Dark matter experiments' central component takes a deep dive nearly a mile underground. Fermilab News Center. Published October 29, 2019 [cited Mar 4]. Available from: https://newscenter.lbl.gov/2019/10/29/dark-matter-experiments-central-component-takes-a-deep-dive-nearly-a-mile-underground/

[40] Baltz EA, Battaglia M, Peskin ME, Wizansky T. Determination of dark matter properties at high-energy colliders. Phys Rev D. 2006;74(3):033011. doi:10.1103/PhysRevD.74.033011.

[41] Gray TR. Producing Dark Matter at Particle Accelerators: Extending the landscape and performing global fits of Light Dark Matter theories. [Licentiate thesis]. Gothenburg: Chalmers University of Technology; 2024.

[42] Fabbrichesi M, Gabrielli E, Lanfranchi G. The dark photon. The European Physical Journal C. 2020;80(8):1-25.

[43] Gorbunov DS, Matveev VA, Pivovarov GR. Dark photon production via elastic proton bremsstrahlung with non-zero momentum transfer. Journal of High Energy Physics. 2024;2024(1):58.

[44] Manohar AV, Wise MB. Heavy Quark Physics. Cambridge: Cambridge University Press; 2000.

[45] Grozin AG. Heavy Quark Effective Theory. Berlin: Springer; 2004.

[46] Penco R. An Introduction to Effective Field Theories. arXiv preprint arXiv:2006.16285. 2020.

A

Heavy Vector Fields

In this Appendix the derivation of the decomposition of a massive complex vector field X^μ is shown. One begin by stating Eq. (3.35)

$$X^\mu = e^{-im_X v\cdot x}\left(\chi^\mu + X_\parallel^\mu\right), \tag{A.1}$$

and define

$$\chi^\mu \equiv e^{im_X v\cdot x}\mathcal{P}_\perp^{\mu\nu}X_\nu\,, \quad \mathcal{P}_\perp^{\mu\nu} \equiv g^{\mu\nu} - v^\mu v^\nu\,, \tag{A.2a}$$

$$X_\parallel^\mu \equiv e^{im_X v\cdot x}\mathcal{P}_\parallel^{\mu\nu}X_\nu\,, \quad \mathcal{P}_\parallel^{\mu\nu} \equiv v^\mu v^\nu, \tag{A.2b}$$

in agreement to [2]. v is a four-velocity, chosen to be time-like and to fulfill $v^\mu v_\mu = 1$. $\mathcal{P}_\perp$ and $\mathcal{P}_\parallel$ are projection operators who obey the usual constraints for such operators, namely $\mathcal{P}^2 = \mathcal{P}$ and $\mathcal{P}_\perp\mathcal{P}_\parallel = 0$. This can be shown:

$$\begin{aligned}\left(\mathcal{P}_\perp^2\right)^{\mu\nu} = g_{\rho\lambda}\mathcal{P}_\perp^{\mu\rho}\mathcal{P}_\perp^{\lambda\nu} &= g_{\rho\lambda}\left(g^{\mu\rho} - v^\mu v^\rho\right)\left(g^{\lambda\nu} - v^\lambda v^\nu\right)\\ &= \left(\delta_\rho^\mu - v^\mu v_\lambda\right)\left(g^{\lambda\nu} - v^\lambda v^\nu\right)\\ &= g^{\mu\nu} - v^\mu v^\nu - v^\mu v^\nu + v^\mu v_\lambda v^\lambda v^\nu\\ &= g^{\mu\nu} - v^\mu v^\nu = \mathcal{P}_\perp^{\mu\nu},\end{aligned} \tag{A.3}$$

and similarly

$$\begin{aligned}\left(\mathcal{P}_\parallel^2\right)^{\mu\nu} = g_{\rho\lambda}\mathcal{P}_\parallel^{\mu\rho}\mathcal{P}_\parallel^{\lambda\nu} &= g_{\rho\lambda}(v^\mu v^\rho)(v^\lambda v^\nu)\\ &= v^\mu v_\lambda v^\lambda v^\nu\\ &= v^\mu v^\nu = \mathcal{P}_\parallel^{\mu\nu}.\end{aligned} \tag{A.4}$$

The orthogonality also becomes obvious with this approach

$$\begin{aligned}\mathcal{P}_\perp\mathcal{P}_\parallel = g_{\rho\lambda}\mathcal{P}_\perp^{\mu\rho}\mathcal{P}^{\lambda\nu} &= g_{\rho\lambda}\left(g^{\mu\rho} - v^\mu v^\rho\right)\left(v^\lambda v^\nu\right)\\ &= \left(\delta_\lambda^\mu - v^\mu v_\lambda\right)\left(v^\lambda v^\nu\right)\\ &= v^\mu v^\nu - v^\mu v_\lambda v^\lambda v^\nu = 0.\end{aligned} \tag{A.5}$$

Moving on one should note that $v_\mu\chi^\mu = 0$, which becomes evident from

$$v_\mu\chi^\mu = v_\mu e^{im_X v\cdot x}\left(g^{\mu\nu} - v^\mu v^\nu\right)X_\nu = e^{im_X v\cdot x}\left(v^\nu X_\nu - v_\mu v^\mu v^\nu X_\nu\right) = 0. \tag{A.6}$$

For the rest of the work in this appendix, it will be convenient to use $\mathbb{X}$ instead of $X_\parallel$. Thus one define

$$X_\parallel^\mu \equiv v^\mu\mathbb{X}, \quad \mathbb{X} = e^{im_X v\cdot x}v^\nu X_\nu. \tag{A.7}$$

The description of a free massive complex vector field is encoded in the Proca Lagrangian

$$\mathcal{L}_p = -\frac{1}{2}\left(\partial_\mu X_\nu^* - \partial_\nu X_\mu^*\right)(\partial\mu X^\nu - \partial^\nu X^\mu) + m_X^2 X_\mu^* X^\mu. \tag{A.8}$$

Decomposing this Lagrangian into terms of χ and $\mathbb{X}$ can be done by evaluating each term separately. Note that all terms in Eq. (A.8) contains both X and X^*, the exponential factor of these will therefor cancel out (see Eq. (A.1)), and are thus ignored in the below derivations.

$$\begin{aligned}
\partial_\mu X_\nu^* \partial^\mu X^\nu &= \left[\partial_\mu \chi_\nu^* + v_\nu \partial_\mu \mathbb{X}^* + i m_X v_\mu \left(\chi_\nu^* + v_\nu \mathbb{X}^*\right)\right] \\
&\quad \cdot \left[\partial^\mu \chi^\nu + v^\nu \partial^\mu \mathbb{X}^* - i m_X v^\mu \left(\chi^\nu + v^\nu \mathbb{X}\right)\right] \\
&= \partial_\mu \chi_\nu^* \partial^\mu \chi^\nu + \partial_\mu \mathbb{X}^* \partial^\mu \mathbb{X} + m_X^2 \left(\chi_\nu^* \chi^\nu + \mathbb{X}^* \mathbb{X}\right) \\
&\quad - i m_X v^\mu \partial_\mu \chi_\nu^* (\chi^\nu + v^\nu \mathbb{X}^*) - i m_X v^\mu v_\nu \partial_\mu \mathbb{X}^* (\chi^\nu + v^\nu \mathbb{X}) \\
&\quad + i m_X v_\mu \partial^\mu \chi^\nu (\chi_\nu^* + v_\nu \mathbb{X}) + i m_X v_\mu v^\nu \partial^\mu \mathbb{X} (\chi_\nu^* + v_\nu \mathbb{X}^*) \\
&\quad + v^\nu \partial_\mu \chi_\nu^* \partial^\mu \mathbb{X} + v_\nu \partial^\mu \chi^\nu \partial_\mu \mathbb{X}^* \\
&= \partial_\mu \chi_\nu^* \partial^\mu \chi^\nu + \partial_\mu \mathbb{X}^* \partial^\mu \mathbb{X} + m_X^2 \left(\chi_\nu^* \chi^\nu + \mathbb{X}^* \mathbb{X}\right) \\
&\quad + \left[-i m_X \left(v \cdot \partial \chi_\nu^* \chi^\nu + v \cdot \partial \mathbb{X}^* \mathbb{X}\right) + \text{c.c}\right].
\end{aligned} \tag{A.9}$$

In the final step $v^\mu \partial_\mu = v \cdot \partial$ is used, and terms where χ is contracted with v are canceled (see Eq. (A.6)). In the same manner one can work out the other three terms of the kinetic part to be

$$\begin{aligned}
\partial_\mu X_\nu^* \partial^\nu X^\mu = \partial_\mu \chi_\nu^* \partial^\nu \chi^\mu + v \cdot \partial \mathbb{X}^* v \cdot \partial \mathbb{X} + m_X^2 \mathbb{X}^* \mathbb{X} \\
+ \left[-i m_X \left(\partial_\mu \mathbb{X}^* \chi^\mu + v \cdot \mathbb{X}^* \mathbb{X}\right) + \text{c.c}\right],
\end{aligned} \tag{A.10}$$

$$\begin{aligned}
\partial_\nu X_\mu^* \partial^\mu X^\nu = \partial_\nu \chi_\mu^* \partial^\mu \chi^\nu + v \cdot \partial \mathbb{X}^* v \cdot \partial \mathbb{X} + m_X^2 \mathbb{X}^* \mathbb{X} \\
+ \left[-i m_X \left(\partial_\nu \mathbb{X}^* \chi^\nu + v \cdot \mathbb{X}^* \mathbb{X}\right) + \text{c.c}\right],
\end{aligned} \tag{A.11}$$

$$\begin{aligned}
\partial_\nu X_\mu^* \partial^\nu X^\mu = \partial_\nu \chi_\mu^* \partial^\nu \chi^\mu + \partial_\nu \mathbb{X}^* \partial^\nu \mathbb{X} + m_X^2 \left(\chi_\mu^* \chi^\mu + \mathbb{X}^* \mathbb{X}\right) \\
+ \left[-i m_X \left(v \cdot \partial \chi_\mu^* \chi^\mu + v \cdot \partial \mathbb{X}^* \mathbb{X}\right) + \text{c.c}\right].
\end{aligned} \tag{A.12}$$

Note that in the "mixed" terms, $\partial_\nu X_\mu^* \partial^\mu X^\nu$ and $\partial_\mu X_\nu^* \partial^\nu X^\mu$ there is no mass-term coupled to the χ_μ field. Consequently the perpendicular projection of the vector field X^μ only gets mass-term contributions from the two negative terms $\partial_\mu X_\nu^* \partial^\mu X^\nu$ and $\partial_\nu X_\mu^* \partial^\nu X^\mu$ from the kinetic part of the Lagrangian. Both of these has a factor $\frac{1}{2}$ in front, yielding that the total mass-term coupled to χ^μ from the kinetic part of the Lagrangian is $-m_X^2 \chi_\mu^* \chi^\mu$.

As one might expect, the "true" mass-term in the Lagrangian is trivially $m_X^2 X_\mu^* X^\mu = m_X^2(\chi_\mu^* \chi^\mu + \mathbb{X}^* \mathbb{X})$ (see Eq. (A.8)) which means that the mass corresponding to the χ^μ part of the field disappears (two negative half's cancel one positive)! This is truly noteworthy since it implies that the decomposition of the heavy vector field leaves one of the projections massless. This consequently gives that the DoF of the original heavy vector field can be split into massless DoF coupled to χ^μ and massive DoF coupled to $\mathbb{X}$. This is one of the most useful results of this Appendix, but it should not come as a surprise since it agrees well with what have been found in similar work on HQET [44, 45]. One can add all knowledge from Eqs.(A.9)-(A.12) to state the Proca Lagrangian as

$$\begin{aligned}\mathcal{L}_p = -\frac{1}{2}\left(\partial_\mu \chi_\nu^* - \partial_\nu \chi_\mu^*\right)\left(\partial^\mu \chi^\nu - \partial^\nu \chi^\mu\right) - \partial_\mu \mathbb{X}^* \partial^\mu \mathbb{X} + m_X^2 \mathbb{X}^* \mathbb{X} \\ + v \cdot \partial \mathbb{X}^* v \cdot \partial \mathbb{X} + \left[i m_X v \cdot \partial \chi_\nu^* \chi^\nu + \text{c.c}\right].\end{aligned} \tag{A.13}$$

Using this Lagrangian, the Euler-Lagrange equation

$$\frac{\partial \mathcal{L}}{\partial X^\mu} - \partial_\nu \left(\frac{\partial \mathcal{L}}{\partial(\partial_\nu X^\mu)}\right) = 0 \tag{A.14}$$

is sought via

$$\frac{\partial \mathcal{L}}{\partial X^\mu} = m_X^2 X_\mu^*, \tag{A.15a}$$

$$\tag{A.15b}$$

$$\frac{\partial \mathcal{L}}{\partial(\partial_\nu X^\nu)} = \partial^\mu X^\nu - \partial^\nu X^\mu \qquad \Longrightarrow \qquad \partial_\nu \left(\frac{\partial \mathcal{L}}{\partial(\partial_\nu X^\nu)}\right) = \partial_\nu \left(\partial^\mu X^\nu - \partial^\nu X^\mu\right). \tag{A.15c}$$

This leads a nice and simple expression for the Euler-Lagrange equation as

$$\partial_\nu \left(\partial^\nu X^\mu - \partial^\mu X^\nu\right) + m_X^2 X^\mu = 0. \tag{A.16}$$

Decomposing into the massless vector field χ^μ and the massive vector field $\mathbb{X}$ is done by evaluating the double derivatives in Eq. (A.16).

$$\begin{aligned}\partial_\mu \partial^\mu X^\nu &= \partial_\mu \left[e^{-i m_X v \cdot x}\Big(\partial^\mu \chi^\nu + v^\nu \partial^\mu \mathbb{X} - i m_X v^\mu (\chi^\nu + v^\nu \mathbb{X})\Big)\right] \\ &= e^{-i m_X v \cdot x}\Big[\Box \chi^\nu + v^\nu \Box \mathbb{X} - 2 i m_X \left(v \cdot \partial \chi^\nu + v^\nu v \cdot \partial \mathbb{X}\right) \\ &\quad - m_X^2 \Big(\chi^\nu + v^\nu \mathbb{X}\Big)\Big].\end{aligned} \tag{A.17}$$

$$\begin{aligned}\partial_\mu \partial^\nu X^\mu &= \partial_\mu \left[e^{-i m_X v \cdot x}\Big(\partial^\nu \chi^\mu + v^\mu \partial^\nu \mathbb{X} - i m_X v^\nu (\chi^\mu + v^\mu \mathbb{X})\Big)\right] \\ &= e^{-i m_X v \cdot x}\Big[\partial_\mu \partial^\nu \chi^\mu + v \cdot \partial \partial^\nu \mathbb{X} - i m_X v^\nu \Big(\partial_\mu \chi^\mu + v \cdot \partial \mathbb{X}\Big) \\ &\quad - i m_X \partial^\nu \mathbb{X} - m_X^2 v^\nu \mathbb{X}\Big].\end{aligned} \tag{A.18}$$

Again, Eq. (A.6) is used to cancel some terms in the Eq. (A.18) which allows one to summarize the full Euler-Lagrange equation

$$\begin{aligned}&\Box \chi^\nu + v^\nu \Box \mathbb{X} - \partial_\mu \partial^\nu \chi^\mu - v \cdot \partial \partial^\nu \mathbb{X} + m_X^2 v^\nu \mathbb{X} \\ &+ i m_X \left(-2 v \cdot \partial \chi^\nu - v^\nu v \cdot \partial \mathbb{X} + \partial^\nu \mathbb{X} + v^\nu \partial_\mu \chi^\mu\right) = 0.\end{aligned} \tag{A.19}$$

As a final step of this appendix one can act with $\mathcal{P}_{\parallel,\rho\nu} = v_\rho v_\nu$ on the Euler-Lagrange equation in Eq. (A.19) to find

$$\begin{aligned} &v_\rho \Box \mathbb{X} + v_\rho m_X^2 \mathbb{X} - v_\rho (v\cdot\partial)^2 \mathbb{X} - v_\rho (v\cdot\partial)\partial_\mu \chi^\mu + i m_X v_\rho \partial_\mu \chi^\mu = 0 \quad \Longrightarrow \\ &\Longrightarrow \Big(\Box + m_X^2 - (v\cdot\partial)\Big)\mathbb{X} = \Big((v\cdot\partial) - i m_X\Big)\partial_\mu\chi^\mu . \end{aligned} \tag{A.20}$$

One can treat $\mathbb{X}$ as a plane wave, with real eigenvalues corresponding to the operators acting on it. Thus it is allowed to divide with said operators provided an imaginary perturbation $i\epsilon$ is added. This is written as

$$\mathbb{X} = \frac{1}{\Box + m_X^2 - (v\cdot\partial) + i\epsilon}\Big((v\cdot\partial) - i m_X\Big)\partial_\mu\chi^\mu . \tag{A.21}$$

It makes sense to expand this using Taylor series. Getting the denominator on the form $1/(x+1)$ with $m_X \gg 1$ can be achieved, which allows for the following expansion

$$\frac{1}{m_X^2}\frac{1}{\frac{\Box-(v\cdot\partial)^2+i\epsilon}{m_X^2}+1} = \frac{1}{m_X^2}\left(1 - \frac{\Box - (v\cdot\partial)^2 + i\epsilon}{m_X^2} + \mathcal{O}\left(\frac{1}{m_X^4}\right)\right). \tag{A.22}$$

In this work only one power of inverse mass will be considered, and hence the expansion is truncated as

$$\mathbb{X} = -\frac{-i}{m_X}\partial_\mu\chi^\mu + \mathcal{O}\left(\frac{1}{m_X^2}\right). \tag{A.23}$$

Finally one can now express the original heavy vector field X^μ purely as a function of the massless field χ^μ, since $\mathbb{X}$ can be eliminated via Eq. (A.23). This appendix concludes with stating this very useful relation

$$X^\mu = e^{-i m_X v\cdot x}\left(\chi^\mu - \frac{i v^\mu}{m_X}\partial_\lambda\chi^\lambda + \mathcal{O}\left(\frac{1}{m_X^2}\right)\right). \tag{A.24}$$

B

HDMET Conversions

Having gained the insight that the heavy vector field X^μ can be expressed solely by the massless field χ^μ one needs to apply this to a large variety of useful expressions describing the original field. These derivations are listed in this appendix, their uses are applied throughout the thesis. Recalling Eq. (A.24) one truncate it to only include terms of first order of inverse mass to state

$$X^\mu \approx e^{-im_X v\cdot x}\left(\chi^\mu - \frac{iv^\mu}{m_X}\partial_\lambda\chi^\lambda\right), \tag{B.1}$$

which is the expression used in all derivations below.

Starting simple one can look at $X^*_\mu X^\mu$:

$$X^*_\mu X^\mu \approx \left(\chi^*_\mu + \frac{iv_\mu}{m_X}\partial^\rho\chi^*_\rho\right)\left(\chi^\mu - \frac{iv^\mu}{m_X}\partial_\lambda\chi^\lambda\right) = \chi^*_\mu\chi^\mu + \frac{1}{m_X^2}\partial^\rho\chi^*_\rho\partial_\lambda\chi^\lambda. \tag{B.2}$$

In the same manner one find

$$\begin{aligned} X^*_\mu X_\nu &\approx \left(\chi^*_\mu + \frac{iv_\mu}{m_X}\partial^\rho\chi^*_\rho\right)\left(\chi_\nu - \frac{iv_\nu}{m_X}\partial^\lambda\chi_\lambda\right) \\ &= \chi^*_\mu\chi_\nu - \frac{iv_\nu}{m_X}\chi^*_\mu\partial^\lambda\chi_\lambda + \frac{iv_\mu}{m_X}\chi_\nu\partial^\rho\chi^*_\rho + \frac{v_\mu v_\nu}{m_X^2}\partial^\rho\chi^*_\rho\partial^\lambda\chi_\lambda. \end{aligned} \tag{B.3}$$

Terms including derivatives will also be useful

$$\begin{aligned} X^*_\nu\partial^\nu X_\mu &= \left(\chi^*_\nu + \frac{iv_\nu}{m_X}\partial^\rho\chi^*_\rho\right)\left[\partial^\nu\chi_\mu - \frac{iv_\mu}{m_X}\partial^\nu\partial^\lambda\chi_\lambda - im_X v^\nu\left(\chi_\mu - \frac{iv_\mu}{m_X}\partial^\lambda\chi_\lambda\right)\right] \\ &= \partial^\nu\left(\chi^*_\nu\chi_\mu\right) + \frac{v\mu}{m_X}\partial^\rho\chi_\rho v\cdot\partial\partial^\lambda\chi_\lambda - \frac{iv_\mu}{m_X}\partial^\nu\left(\chi - \nu^*\partial^\lambda\chi_\lambda\right) + \frac{i}{m_X}\partial^\rho\chi^*_\rho v\cdot\partial\chi_\mu. \end{aligned} \tag{B.4}$$

Adding the completely anti-symmetric tensor $\varepsilon^{\mu\nu\rho\lambda}$ will prove useful for some of the expressions. The two interesting properties of this tensor regarding the current framework is that

- Swapping two indices renders a sign change, i.e. $\varepsilon^{\mu\nu\rho\sigma} = -\varepsilon^{\nu\mu\rho\sigma}$.
- If two or more indices matches with vectors v one get zero. That is $v_\mu v_\nu\varepsilon^{\mu\nu\rho\lambda} = 0$.

$$\begin{aligned}
\partial_\rho \left(X_\nu^* X_\lambda\right) \varepsilon^{\mu\nu\rho\lambda} &= \Big[\partial_\rho\Big(\chi_\nu^*\chi_\lambda\Big) - \frac{iv_\lambda}{m_X}\partial_\rho\Big(\chi_\nu^*\partial^\sigma\chi_\sigma\Big) + \frac{iv_\nu}{m_X}\partial_\rho\Big(\chi_\lambda\partial^\gamma\chi_\gamma^*\Big) \\
&\quad + \frac{v_\lambda v_\nu}{m_X^2}\partial_\rho\Big(\partial^\sigma\chi_\sigma\partial^\gamma\chi_\gamma^*\Big)\Big]\varepsilon^{\mu\nu\rho\lambda} \\
&= \Big[\partial_\rho\Big(\chi_\nu^*\chi_\lambda\Big) + \frac{iv_\nu}{m_X}\partial_\rho\Big(\chi_\lambda\partial^\gamma\chi_\gamma^*\Big)\Big]\varepsilon^{\mu\nu\rho\lambda} - \frac{iv_\nu}{m_X}\partial_\rho\Big(\chi_\lambda^*\partial^\sigma\chi_\sigma\Big)\varepsilon^{\mu\lambda\rho\nu} \\
&= \Big[\partial_\rho\Big(\chi_\nu^*\chi_\lambda\Big) + \frac{iv_\nu}{m_X}\partial_\rho\Big(\chi_\lambda\partial^\gamma\chi_\gamma^*\Big) + \frac{iv_\nu}{m_X}\partial_\rho\Big(\chi_\lambda^*\partial^\sigma\chi_\sigma\Big)\Big]\varepsilon^{\mu\nu\rho\lambda}.
\end{aligned} \tag{B.5}$$

In the second row, the term containing $v_\lambda v_\nu$ was discarded due to $\varepsilon^{\mu\nu\rho\sigma}$. Also, the last term was singled out to make use of that summation indices are free to relabel. Choosing $\lambda \to \nu$ and $\nu \to \lambda$ in this term gives the expression seen in row two. In the final step the indices of ε is flipped back to its original place, rendering a sign change in the third term.

Introducing the operator $\overleftrightarrow{\partial}$, defined as

$$X_\nu^* \overleftrightarrow{\partial}_\mu X^\nu \equiv \underbrace{X_\nu^* \partial_\mu X^\nu}_{(1)} - \underbrace{\partial_\mu X_\nu^* X^\nu}_{(2)}, \tag{B.6}$$

will be of great interest. Evaluating such terms yield

$$\begin{aligned}
(1) &= \left(\chi_\nu^* + \frac{iv_\nu}{m_X}\partial^\rho\chi_\rho^*\right)\left[\partial_\mu\chi^\nu - \frac{iv^\nu}{m_X}\partial_\mu\partial_\lambda\chi^\lambda - im_X v_\mu\left(\chi^\nu - \frac{iv^\nu}{m_X}\partial^\lambda\chi_\lambda\right)\right] \\
&= \chi_\nu^*\partial_\mu\chi^\nu + \frac{1}{m_X^2}\partial^\rho\chi_\rho^*\partial_\mu\partial_\lambda\chi^\lambda - im_X v_\mu\chi_\nu^*\chi^\nu - \frac{iv_\mu}{m_X}\partial^\rho\chi_\rho^*\partial_\lambda\chi^\lambda.
\end{aligned} \tag{B.7}$$

$$(2) = \partial_\mu\chi_\nu^*\chi^\nu + \frac{1}{m_X^2}\partial_\mu\partial^\rho\chi_\rho^*\partial_\lambda\chi^\lambda + im_X v_\mu\chi_\nu^*\chi^\nu + \frac{iv_\mu}{m_X}\partial^\rho\chi_\rho^*\partial_\lambda\chi^\lambda. \tag{B.8}$$

$v^\mu\chi_\mu = 0$ was used to achieve the above expressions. Adding them together yields Eq. (B.6) as

$$\begin{aligned}
X_\nu^* \overleftrightarrow{\partial}_\mu X^\nu &= (1) - (2) \\
&= \chi_\nu^* \overleftrightarrow{\partial}_\mu \chi^\nu + \frac{1}{m_X^2}\partial^\rho\chi_\rho^* \overleftrightarrow{\partial}_\mu \partial_\lambda\chi^\lambda - \frac{2iv_\mu}{m_X}\partial^\rho\chi_\rho^*\partial_\lambda\chi^\lambda - 2im_X v_\mu\chi_\nu^*\chi^\nu.
\end{aligned} \tag{B.9}$$

Adding the knowledge from Eqs. (B.5) and (B.9) one can compute

$$\begin{aligned}
X_\nu^* \overleftrightarrow{\partial}_\rho X_\lambda \cdot \varepsilon^{\mu\nu\rho\lambda} &= \Big[\underbrace{X_\nu^* \partial_\rho X_\lambda}_{(1)} - \underbrace{\partial_\rho X_\nu^* X_\lambda}_{(2)}\Big] \cdot \varepsilon^{\mu\nu\rho\lambda} \\
&\approx \left[\chi_\nu^* \overleftrightarrow{\partial}_\rho \chi_\lambda - \frac{iv_\nu}{m_X} \chi_\lambda \overleftrightarrow{\partial}_\rho \partial^\gamma \chi_\gamma^* - 2im_X v_\rho \chi_\nu^* \chi_\lambda\right] \varepsilon^{\mu\nu\rho\lambda} \\
&\quad - \frac{iv_\nu}{m_X} \chi_\lambda^* \overleftrightarrow{\partial}_\rho \partial^\sigma \chi_\sigma \cdot \varepsilon^{\mu\lambda\rho\nu} \\
&= \Big[\chi_\nu^* \overleftrightarrow{\partial}_\rho \chi_\lambda + \frac{iv_\nu}{m_X} \chi_\lambda^* \overleftrightarrow{\partial}_\rho \partial^\sigma \chi_\sigma - \frac{iv_\nu}{m_X} \chi_\lambda \overleftrightarrow{\partial}_\rho \partial^\gamma \chi_\gamma^* \\
&\quad - 2im_X v_\rho \chi_\nu^* \chi_\lambda\Big] \varepsilon^{\mu\nu\rho\lambda}.
\end{aligned} \tag{B.10}$$

Some intermediate steps of the calculation were skipped since the same procedure can be found in previous derivations in this appendix.

C

Interaction Operators

The interaction operators in 5.1 are not trivial to find. The purpose is to describe all possible interactions between the DM and the mediator and the SM. The scalar and pseudo-scalar together with the gluon and dual gluon operators are considered trivial, but for the rest some extra care is needed. This appendix will describe how to identify all different vector and axial-vector interaction operators.

C.1 Vector and Axial-Vector Interaction Operators

To find the right operators one can consider the mediator-part of the Lagrangian for DM-quark interaction that is given in [21], Eq (2.2).

$$\mathcal{L}_{\text{Int}} = -\frac{1}{4}\mathcal{G}^{\mu\nu}\mathcal{G}_{\mu\nu} + \frac{1}{2}m_G^2 G_\mu G^\mu + G_\mu A^\mu. \tag{C.1}$$

Here G_μ is the vector field describing the mediator and $\mathcal{G}_{\mu\nu}$ is its associated field strength tensor, $\mathcal{G}_{\mu\nu} = \partial_\mu G_\nu - \partial_\nu G_\mu$. A^μ is the notation for all possible bi-linears, either for SM or for DM. In [21] they find A_μ to be

$$\begin{aligned} A_\mu = &-ib_5\Big(X_\nu^*\partial_\mu X^\nu - \partial_\mu X_\nu^* X^\nu\Big) \\ &- b_6\Big(X_\nu^*\partial^\nu X_\mu\Big) - b_6^*\Big(X_\nu\partial^\nu X_\mu^*\Big) \\ &- b_7\epsilon_{\mu\nu\rho\lambda}\Big(X^{\nu*}\partial^\rho X^\lambda\Big) - b_7^*\epsilon_{\mu\nu\rho\lambda}\Big(X^\nu\partial^\rho X^{\lambda*}\Big) \\ &- h_3\bar{q}\gamma_\mu q - h_4\bar{q}\gamma_\mu\gamma_5 q. \end{aligned} \tag{C.2}$$

The seemingly odd number-notation on the constants are made clearer in [20, 21] (more terms are present when looking at the full Lagrangian, not just the interaction of the mediator). One can take b_5 to be real, whereas b_6 and b_7 are complex, consisting of one real and one imaginary part.

Solving the Euler-Lagrange equation,

$$\begin{aligned} \frac{\partial\mathcal{L}}{\partial G_\mu} &= m_G^2 G^\mu + A^\mu \\ \partial_\nu\left(\frac{\partial\mathcal{L}}{\partial(\partial_\nu G_\mu)}\right) &= \partial_\nu\left[-\frac{1}{4}\Big(\partial^\mu G^\nu - \partial^\nu G^\mu\Big)\right], \end{aligned} \tag{C.3}$$

and assuming m_G to be large enough to overpower the derivative of the field strength tensor one find the approximate expression for the mediator vector field

$$\begin{aligned} \frac{\partial \mathcal{L}}{\partial G_\mu} - \partial_\nu \left(\frac{\partial \mathcal{L}}{\partial(\partial_\nu G_\mu)} \right) \approx m_G^2 G^\mu + A^\mu = 0 \\ \implies G^\mu \simeq -\frac{1}{m_G^2} A^\mu. \end{aligned} \tag{C.4}$$

Inserting this expression back into the interaction Lagrangian in Eq. (C.1) yields what is often referred to as the effective Lagrangian

$$\begin{aligned} \mathcal{L}_{\text{eff}} &\approx \frac{1}{2} m_G^2 \left(-\frac{1}{m_G^2} A^\mu \right) \left(-\frac{1}{m_G^2} A^\mu \right) + \left(-\frac{1}{m_G^2} A^\mu \right) A_\mu \\ &= -\frac{1}{2m_G^2} A_\mu A^\mu. \end{aligned} \tag{C.5}$$

With this simplified form of Lagrangian it is now a question of choosing the right parts of A^μ from Eq. (C.2) to build interaction operators. Looking at the Feynman diagrams in — one see that a DM bilinear (quadratic in X^μ) needs to be paired with a SM bilinear (quadratic in q). In total (as seen in the list in —) there are ten interaction operators that can be created from a vector mediator. The derivation to find five of these ($\mathcal{Q}^{(6)}_{3,q}$, $\mathcal{Q}^{(6)}_{5,q}$, $\mathcal{Q}^{(6)}_{7,q}$, $\mathcal{Q}^{(6)}_{9,q}$ and $\mathcal{Q}^{(6)}_{11,q}$) are shown in detail below. The remaining ($\mathcal{Q}^{(6)}_{4,q}$, $\mathcal{Q}^{(6)}_{6,q}$, $\mathcal{Q}^{(6)}_{8,q}$, $\mathcal{Q}^{(6)}_{10,q}$ and $\mathcal{Q}^{(6)}_{12,q}$) are found by an analogous approach (they are axial vectors, with the only difference being the factor γ^5, i.e. one only needs to take the h_4 term of A_μ instead of h_3). Note that due to the shapes of the Feynman diagrams describing the interaction one is free to ignore terms that are not quadratic in both DM and SM.

$$\begin{aligned} \boldsymbol{\mathcal{Q}^{(6)}_{3,q}}: \quad \mathcal{L}_{\text{eff}} &= -\frac{1}{2m_G^2} \underbrace{A_\mu}_{(*)} \underbrace{A^\mu}_{(**)} \\ &= -\frac{1}{\cancel{2}m_G^2} \Big[-ib_5 \Big(X_\nu^* \partial_\mu X^\nu - \partial_\mu X_\nu^* X^\nu \Big) \Big] \cdot \Big[-h_3 \bar{q} \gamma^\mu q \Big] \\ &= \frac{-b_5 h_3}{m_G^2} i\bar{q}\gamma^\mu q X_\nu^* \overleftrightarrow{\partial}_\mu X^\nu \\ &= \frac{-b_5 h_3}{m_G^2} \mathcal{Q}^{(6)}_{3,q}. \end{aligned} \tag{C.6}$$

$(*)$ =needs to be DM/SM, $(**)$ =needs to be SM/DM. The factor $\frac{1}{2}$ is crossed out in line two since there are two ways of creating the Feynman diagram (either A_μ is

DM which forces A^μ to be SM, or the other way around).

$$\begin{aligned}
\boldsymbol{\mathcal{Q}^{(6)}_{5,q}} \text{ and } \boldsymbol{\mathcal{Q}^{(6)}_{7,q}}: \quad \mathcal{L}_{\text{eff}} &= -\frac{1}{2m_G^2}A_\mu A^\mu \\
&= -\frac{1}{m_G^2}\Big[-b_7\epsilon^{\mu\nu\rho\sigma}X^*_\nu\partial_\rho X_\lambda + \text{c.c}\Big]\cdot\Big[-h_3\bar{q}\gamma_\mu q\Big] \\
&= -\frac{\Re[b_7]h_3}{m_G^2}\bar{q}\gamma_\mu q\Big[\epsilon^{\mu\nu\rho\lambda}X^*_\nu\partial_\rho X_\lambda + \epsilon^{\mu\lambda\rho\nu}X_\lambda\partial_\rho X^*_\nu\Big] \\
&\quad - i\frac{\Im[b_7]h_3}{m_G^2}\bar{q}\gamma^\mu q\Big[\epsilon^{\mu\nu\rho\lambda}X^*_\nu\partial_\rho X_\lambda - \epsilon^{\mu\lambda\rho\nu}X_\lambda\partial_\rho X^*_\nu\Big] \\
&= -\frac{\Re[b_7]h_3}{m_G^2}\bar{q}\gamma_\mu q\Big[\epsilon^{\mu\nu\rho\lambda}\left(X^*_\nu\partial_\rho X_\lambda - X_\lambda\partial_\rho X^*_\nu\right)\Big] \\
&\quad - i\frac{\Im[b_7]h_3}{m_G^2}\bar{q}\gamma^\mu q\Big[\epsilon^{\mu\nu\rho\lambda}\left(X^*_\nu\partial_\rho X_\lambda + X_\lambda\partial_\rho X^*_\nu\right)\Big] \\
&= -\frac{\Re[b_7]h_3}{m_G^2}\mathcal{Q}^{(6)}_{5,q} - \frac{\Im[b_7]h_3}{m_G^2}\mathcal{Q}^{(6)}_{7,q}\,.
\end{aligned} \tag{C.7}$$

In line three and four one applies the same trick as in appendix B and relabels dummies-index and then changes back in order, which generates a minus sign.

$$\begin{aligned}
\boldsymbol{\mathcal{Q}^{(6)}_{9,q}} \text{ and } \boldsymbol{\mathcal{Q}^{(6)}_{11,q}}: \quad \mathcal{L}_{\text{eff}} &= -\frac{1}{2m_G^2}A_\mu A^\mu \\
&= -\frac{1}{m_G^2}\Big[-b_6\Big(X^*_\nu\partial^\nu X_\mu\Big) + \text{c.c}\Big]\cdot\Big[-h_3\bar{q}\gamma^\mu q\Big] \\
&= -\frac{\Re[b_6]h_3}{m_G^2}\bar{q}\gamma^\mu q\Big[X^*_\nu\partial^\nu X_\mu + \text{c.c}\Big] \\
&\quad - \frac{\Im[b_6]h_3}{m_G^2}\bar{q}\gamma^\mu q\Big[iX^*_\nu\partial^\nu X_\mu + \text{c.c}\Big] \\
&= -\frac{\Re[b_6]h_3}{m_G^2}\mathcal{Q}^{(6)}_{9,q} - \frac{\Im[b_6]h_3}{m_G^2}\mathcal{Q}^{(6)}_{11,q}\,.
\end{aligned} \tag{C.8}$$

After applying the same procedure on the terms b_5, b_6 and b_7 but this time paring it with the h_4 term instead the Lagrangian in Eq. (C.2) has no more terms that can be combined into operators, and thus the list in 5.1 is confirmed to be complete.

D
Scattering Amplitudes

One of the main results of this thesis is the scattering amplitudes for a given DM-nucleon interaction. To find these, a considerable amount of work is required. First, the vertex coefficients for the different DM bi-linears needs to be decided which is done in section D.1. Then, one can apply that knowledge to construct a full S-matrix expansion which then is used to find the scattering amplitudes. This is done in section D.2.

D.1 DM field expansion and vertex coefficients

Expanding the massless vector field χ^μ in a Fourier series yield

$$\chi^\mu = \int \frac{d^3p}{(2\pi)^3}\frac{1}{\sqrt{2E_p}}\sum_s \left(a^s_{\vec{p}}\varepsilon^s_\nu e^{-ip\cdot x} + b^{s\dagger}_{\vec{p}}\varepsilon^{s*}_\nu e^{+ip\cdot x}\right). \tag{D.1}$$

Using this to expand the different bi-linears one can find the vertex coefficients via the expression for the S-matrix. Below the procedure is shown in detail for the case of $\mathcal{L}_{\text{int}} = J_{\text{DM}} = \chi^*_\nu \overleftrightarrow{\partial}_\mu \chi^\nu$, the rest follows analogously. Consult the diagram in Fig.3.2 for the notations of the different momenta.

$$\begin{aligned} S_{\text{fi, DM}} &= \left\langle \vec{p}\,', s' \middle| i\int d^4x \left(\chi^*_\nu\partial_\mu\chi^\nu - \partial_\mu\chi^*_\nu\chi^\nu\right) \middle| \vec{p}, s\right\rangle \\ &= (2\pi)^4\delta^{(4)}(E_{\vec{p}\,'} - E_{\vec{p}})i\mathcal{M}. \end{aligned} \tag{D.2}$$

Letting the derivatives act on the expanded form of χ^ν one find the scattering amplitude to be

$$\begin{aligned} i\mathcal{M} &= i\left(\varepsilon^{s'*}_\nu(-i\tilde{p}_\mu)\varepsilon^{s\nu} - (i\tilde{p}'_\mu)\varepsilon^{s'*}_\nu\varepsilon^{s\nu}\right) \\ &= i(-i)(\tilde{p}_\mu + \tilde{p}'_\mu)\varepsilon^{s'*}_\nu\varepsilon^{s\nu}. \end{aligned} \tag{D.3}$$

The $\tilde{p}$ is to keep the reader observant on the fact that since it is the massless field χ that gets acted on, it is the *residual momentum* (also known as the soft momentum) that falls out, rather than the full momentum p. When expressing all the scattering amplitudes in D.2 it will be useful to do so in terms of a few useful operators. These are defined as

$$S_{\mu\nu} \equiv \frac{1}{2}\left(\varepsilon^*_\mu \varepsilon_\nu + \varepsilon_\mu \varepsilon^*_\nu\right), \tag{D.4a}$$

$$\hat{S}^{\mu\nu} \equiv \varepsilon^*_\rho \varepsilon_\lambda \epsilon^{\mu\nu\rho\lambda}, \tag{D.4b}$$

$$\bar{S}_{\mu\nu} \equiv \frac{1}{2}\left(\varepsilon^*_\mu \varepsilon_\nu - \varepsilon_\mu \varepsilon^*_\nu\right). \tag{D.4c}$$

It is also beneficial to consider

$$\tilde{P}_\mu \equiv \tilde{p}_\mu + \tilde{p}'_\mu, \tag{D.5}$$

and that the momentum transfer q_μ is just $\tilde{p}'_\mu - \tilde{p}_\mu$. Other factors that will be frequently occurring in the expressions for the amplitudes are $\varepsilon_\mu \cdot \tilde{p}^\mu$ and $\varepsilon^*_\mu \cdot \tilde{p}^{\mu'}$. Thus to shorten notation one can introduce

$$p_\varepsilon \equiv \varepsilon \cdot \tilde{p}, \tag{D.6a}$$

$$p^*_\varepsilon \equiv \varepsilon^* \cdot \tilde{p}'. \tag{D.6b}$$

All Feynman rules for the different DM currents can be found analogously to Eq. (D.3) and are stated below

$$\chi^*_\nu \overleftrightarrow{\partial}_\mu \chi^\nu \rightarrow i(-i)\tilde{P}_\mu \varepsilon^*_\nu \varepsilon^\nu, \tag{D.7a}$$

$$\partial_\mu\left(\chi^*_\nu \chi^\nu\right) \rightarrow i(-i)q_\mu \varepsilon^*_\nu \varepsilon^\nu, \tag{D.7b}$$

$$\partial_\mu \chi^*_\mu \partial_\nu \chi^\nu \rightarrow i\tilde{p}'_\mu \tilde{p}_\nu \varepsilon^*_\mu \varepsilon_\nu, \tag{D.7c}$$

$$\chi^*_\lambda \overleftrightarrow{\partial}_\rho \partial_\sigma \chi^\sigma \rightarrow -i\tilde{P}_\rho \varepsilon^*_\lambda p_\varepsilon, \tag{D.7d}$$

$$\chi_\lambda \overleftrightarrow{\partial}_\rho \partial^\sigma \chi^*_\sigma \rightarrow -i\tilde{P}_\rho \varepsilon_\lambda p^*_\varepsilon, \tag{D.7e}$$

$$\partial_\rho\left(\chi^*_\lambda \partial_\sigma \chi^\sigma\right) \rightarrow -iq_\rho \varepsilon^*_\lambda p_\varepsilon, \tag{D.7f}$$

$$\partial_\rho\left(\chi_\lambda \partial^\sigma \chi^*_\sigma\right) \rightarrow iq_\rho \varepsilon_\lambda p^*_\varepsilon, \tag{D.7g}$$

$$\partial^\rho \chi^*_\rho v \cdot \partial \chi_\mu \rightarrow i(-i)p^*_\varepsilon v \cdot \tilde{p}\varepsilon_\mu, \tag{D.7h}$$

$$\partial^\rho \chi_\rho v \cdot \partial \chi^*_\mu \rightarrow i(-i)p_\varepsilon v \cdot \tilde{p}' \varepsilon^*_\mu. \tag{D.7i}$$

As a last remark before addressing the scattering amplitudes, one should note the definition

$$S^\mu_X \equiv iv_\nu \hat{S}^{\mu\nu}. \tag{D.8}$$

This will be used when expressing the amplitudes in terms of basis operators.

D.2 Scattering Amplitudes

As stated in 3.7, only the leading order in momentum is guaranteed to obey the Galilean symmetry. Since the DM that is considered is also assumed to be non-relativistic, it is safe to ignore the higher order terms. Just as in the results, section 5.3, the different amplitudes are split into two main groups, one corresponding to each of the diagrams in Fig. 3.1.

D.2.1 Contact Diagram (Left Part of Fig. 3.1)

As stated before, the currents J_q^S, J_q^V, J_q^A, J^G and J^θ contribute to this diagram [8]. The hadronization of the currents are taken from appendix C of [8].

D.2.1.1 Scalar Current

Taking the hadronization of the currents from Eq. (B.49) and Eq. (B.55) in [8],

$$J_{u,d}^S = -2b_0 m_{u,d}\bar{N}N - 2(b_D + b_F)m_{u,d}\bar{N}_{u,d}N_{u,d} + \dots, \tag{D.9a}$$

$$J_s^S = -2(b_0 + b_D - b_F)m_s\bar{N}N + \dots, \tag{D.9b}$$

where $\bar{N}N = \bar{u}_p u_p + \bar{u}_n u_n$, $N_u = u_p$ and $N_d = u_n$, one find the DM-proton interaction to be

$$\mathcal{L}_{\text{int},p}^{S,(6)} = \chi_\nu^* \chi^\nu \cdot \left[\hat{c}_{1,u}^{(6)} \cdot \sigma_u^p + \hat{c}_{1,d}^{(6)} \cdot \sigma_d^p + \hat{c}_{1,s}^{(6)} \cdot \sigma_s^p\right] \bar{u}_p u_p, \tag{D.10}$$

with constants defined as

$$\begin{aligned} \sigma_u^p &= -2(b_0 + b_D + b_F)m_u, \\ \sigma_d^p &= -2b_0 m_d, \\ \sigma_s &= -2(b_0 + b_D - b_F)m_s, \\ \sigma_u^n &= -2b_0 m_u, \\ \sigma_d^n &= -2(b_0 + b_D + b_F)m_d. \end{aligned} \tag{D.11}$$

The scattering amplitude is found from the Lagrangian in Eq. (D.10)

$$i\mathcal{M}_p^S = i\varepsilon_\nu^* \varepsilon^\nu \bar{u}_p u_p \left[\hat{c}_{1,u}^{(6)} \cdot \sigma_u^p + \hat{c}_{1,d}^{(6)} \cdot \sigma_d^p + \hat{c}_{1,s}^{(6)} \cdot \sigma_s^p\right]. \tag{D.12}$$

The corresponding interaction between DM and a neutron is achieved by letting $p \to n$ and $u \to d$.

D.2.1.2 Vector Current

The hadronized vector current is taken from Eqs. (B.47) and (B.53) in [8]:

$$J_{u,d}^{V,\mu} = \left(v^\mu + \frac{K^\mu}{2m_N}\right)\left(\bar{N}_{u,d}N_{u,d}\right) + i\left(g_4\bar{N}_{u,d}W^\mu N_{u,d} - g_4'\bar{N}W^\mu N\right) + \dots, \tag{D.13a}$$

$$J_s^{V,\mu} = -i\Big(g_4 + g_4' - g_5\Big)\bar{N}W^\mu N + \dots. \tag{D.13b}$$

Here, $W^\mu \equiv \epsilon^{\mu\alpha\beta\lambda}v_\alpha \cdot q_\lambda \cdot S_{N,\beta}$ and
$\hat{\mathcal{W}}(\hat{C}_{n,q}^d) \equiv (g_4 - g_4')\hat{C}_{n,u}^d + (-g_4')\hat{C}_{n,d}^d - (g_4 + g_4' - g_5)\hat{C}_{n,s}^d$. This means for example that

$$W^\mu v_\mu = W^\mu q_\mu = 0. \tag{D.14}$$

Also, K^μ is the sum of the nucleon momentum, i.e. $K^\mu \equiv k^\mu + k^{\mu'}$.

D.2.1.3 Type A

With the above definitions in place the scattering amplitude for the DM-proton interaction can be computed

$$\begin{aligned} i\mathcal{M}_p^{V,a} = i &\left[2m_X v_\mu \varepsilon^*_\nu \varepsilon^\nu + \frac{2iv_\mu}{m_X}\tilde{p}^{\rho'}\varepsilon^*_\rho \tilde{p}^\lambda \varepsilon_\lambda + i(-i)\tilde{P}_\mu \varepsilon^*_\nu \varepsilon^\nu\right] \cdot \\ &\left[\left(v^\mu + \frac{K^\mu}{2m_p}\right)\bar{u}_p u_p (2\hat{C}^{(6)}_{3,u} + \hat{C}^{(6)}_{3,d}) + i\hat{\mathcal{W}}(\hat{C}^6_{3,q})\bar{u}_p W^\mu u_p\right]. \end{aligned} \tag{D.15}$$

The leading order of momentum is zero (the term consisting of the first term in the first bracket multiplied by the first term in the second bracket) and thus the approximated answer is

$$i\mathcal{M}_p^{V,a} \approx 2im_X \varepsilon^*_\nu \varepsilon^\nu \bar{u}_p u_p (2\hat{C}^{(6)}_{3,u} + \hat{C}^{(6)}_{3,d}). \tag{D.16}$$

D.2.1.4 Type B

$$\begin{aligned} i\mathcal{M}_p^{V,b} = i\epsilon^{\mu\nu\rho\lambda} \cdot &\left[-2im_X v_\rho \varepsilon^*_\nu \varepsilon_\lambda - i\tilde{P}_\rho \varepsilon^*_\nu \varepsilon_\lambda - \frac{iv_\nu}{m_X}\tilde{P}_\rho\left[\varepsilon^*_\lambda p_\varepsilon - \text{ c.c}\right]\right] \cdot \\ &\left[\left(v_\mu + \frac{K_\mu}{2m_p}\right)\bar{u}_p u_p (2\hat{C}^{(6)}_{5,u} + \hat{C}^{(6)}_{5,d}) + i\hat{\mathcal{W}}(\hat{C}^6_{5,q})\bar{u}_p W_\mu u_p\right]. \end{aligned} \tag{D.17}$$

Leading order of momentum is linear which means that only the terms arising from the first and second term of the first row contribute. Expressed in terms of basis operators the amplitude becomes

$$\begin{aligned} i\mathcal{M}_p^{V,b} \approx &-2im_X v_{\perp,\mu} S^\mu_X \bar{u}_p u_p \left(2\hat{C}^{(6)}_{5,u} + \hat{C}^{(6)}_{5,d}\right) \\ &- 2m_X S^\mu_X \hat{\mathcal{W}}(\hat{C}^{(6)}_{5,q})\bar{u}_p W_\mu u_p. \end{aligned} \tag{D.18}$$

D.2.1.5 Type C

$$\begin{aligned} i\mathcal{M}_p^{V,c} = i\epsilon^{\mu\nu\rho\lambda} &\left[i(-i)q_\rho \varepsilon^*_\nu \varepsilon_\lambda v_\mu + \frac{v_\nu}{m_X}q_\rho[\varepsilon^*_\lambda p_\varepsilon - \text{ c.c}]\right] \cdot \\ &\left[\left(v_\mu + \frac{K_\mu}{2m_p}\right)\bar{u}_p u_p (2\hat{C}^{(6)}_{7,u} + \hat{C}^{(6)}_{7,d}) + i\hat{\mathcal{W}}(\hat{C}^6_{7,q})\bar{u}_p W_\mu u_p\right]. \end{aligned} \tag{D.19}$$

The leading order of momentum is linear. Thus only the term arising from the first term on the first row contribute. Expressed in basis operators the amplitude is

$$i\mathcal{M}_p^{V,c} = q \cdot S_X \bar{u}_p u_p \left(2\hat{C}^{(6)}_{7.u} + \hat{C}^{(6)}_{7,d}\right). \tag{D.20}$$

D.2.1.6 Type D

$$\begin{aligned} i\mathcal{M}_p^{V,d} = i &\left[(-i)q^\nu[\varepsilon^*_\nu \varepsilon_\mu + \text{ c.c}] + \frac{i}{m_X}q^\nu[\varepsilon_\nu p^*_\varepsilon + \text{ c.c}] + \frac{i}{m_X}[p^*_\varepsilon v \cdot \tilde{p}\varepsilon_\mu - \text{c.c}]\right] \cdot \\ &\left[\left(v_\mu + \frac{K_\mu}{2m_p}\right)\bar{u}_p u_p (2\hat{C}^{(6)}_{9,u} + \hat{C}^{(6)}_{9,d}) + i\hat{\mathcal{W}}(\hat{C}^6_{9,q})\bar{u}_p W_\mu u_p\right]. \end{aligned} \tag{D.21}$$

The leading order of momentum is quadratic (remember that $v_\mu \chi^\mu = 0$ and hence the linear term vanishes). Contribution arises from the second and the third term in the first row. Expressed in basis operators the amplitude is

$$\begin{aligned} i\mathcal{M}_p^{V,d} &= -2q \cdot S \cdot V_\perp \bar{u}_p u_p \left(2\hat{C}_{9,u}^{(6)} + \hat{C}_{9,d}^{(6)}\right) \\ &+ 2iq^\nu S_{\mu\nu} \hat{\mathcal{W}}(\hat{C}_{9,q}^{(6)}) \bar{u}_p W^\mu u_p. \end{aligned} \tag{D.22}$$

D.2.1.7 Type E

$$\begin{aligned} i\mathcal{M}_p^{V,e} = i &\left[i(-i) q^\nu [\varepsilon_\nu^* \varepsilon_\mu - \text{ c.c}] - \frac{1}{m_X} q^\nu [\varepsilon_\nu^* p_\varepsilon - \text{ c.c}] - \frac{1}{m_X} [p_\varepsilon v \cdot \tilde{p}' \varepsilon_\mu^* + \text{ c.c}] \right] \cdot \\ &\left[\left(v_\mu + \frac{K_\mu}{2m_p} \right) \bar{u}_p u_p (2\hat{C}_{11,u}^{(6)} + \hat{C}_{11,d}^{(6)}) + i\hat{\mathcal{W}}(\hat{C}_{11,q}^{6}) \bar{u}_p W_\mu u_p \right]. \end{aligned} \tag{D.23}$$

The leading order of momentum is quadratic. Thus the contribution to the amplitude comes from the first and second term of the first row. In basis operators the amplitude is

$$\begin{aligned} i\mathcal{M}_p^{V,e} &= 2iq^\nu \bar{S}_{\mu\nu} v_\perp^\mu \bar{u}_p u_p \left(2\hat{C}_{11,u}^{(6)} + \hat{C}_{11,d}^{(6)}\right) \\ &- \frac{i}{m_X} q \cdot S \cdot q \bar{u}_p u_p \left(2\hat{C}_{11,u}^{(6)} + \hat{C}_{11,d}^{(6)}\right) \\ &+ 2q^\nu \bar{S}_{\mu\nu} \hat{\mathcal{W}}(\hat{C_{11,q}^{(6)}}) \bar{u}_p W^\mu u_p. \end{aligned} \tag{D.24}$$

D.2.2 Axial Current

For the axial current, Eqs. (B.48) and (B.54) in [8] are used.

$$J_{u,d}^{A,\mu} = 2(D+F)\bar{N}_{u,d} \left(S_N^\mu - \frac{v^\mu}{2m_N} K \cdot S_N \right) N_{u,d} + 2G\bar{N} \left(S_N^\mu - \frac{v^\mu}{2m_N} K \cdot S_N \right) N + \ldots, \tag{D.25a}$$

$$J_s^{A,\mu} = 2(D-F+G)\bar{N} \left(S_N^\mu - \frac{v^\mu}{2m_N} K \cdot S_N \right) N + \ldots. \tag{D.25b}$$

S_N^μ is the spin-operator of the nucleon and it fulfills $v_\mu \cdot S_N^\mu = 0$. Just as for the vector current, it is beneficial to simplify by introducing

$$\hat{\mathcal{A}}(\hat{C}_{n,q}^d) \equiv 2(D+F+G)\hat{C}_{n,u}^d + 2G\hat{C}_{n,d}^d + 2(D-F+G)\hat{C}_{n,s}^d. \tag{D.26}$$

D.2.2.1 Type A

$$\begin{aligned} i\mathcal{M}_p^{A,a} = i\hat{\mathcal{A}}(\hat{C}_{4,q}^6) &\left[2m_X v_\mu \varepsilon_\nu^* \varepsilon^\nu + i\varepsilon_\nu^* \varepsilon^\nu \tilde{P}_\mu + \frac{2v_\mu}{m_X} i\tilde{p}^{\nu\prime} \varepsilon_\nu^* \tilde{p}^\lambda \varepsilon_\lambda \right] \cdot \\ &\left[\bar{u}_p \left(S_N^\mu - \frac{v^\mu}{2m_N} K \cdot S_N \right) u_p \right]. \end{aligned} \tag{D.27}$$

The leading order of momentum is linear and hence only the first term on the first row contribute. The amplitude expressed in basis operators becomes

$$i\mathcal{M}_p^{A,a} = 2im_X\hat{\mathcal{A}}(\hat{C}_{4,q}^{(6)})\varepsilon_\mu^*\varepsilon^\mu\bar{u}_p v_\perp \cdot S_N u_p. \tag{D.28}$$

D.2.2.2 Type B

$$\begin{aligned} i\mathcal{M}_p^{A,b} = i\hat{\mathcal{A}}(\hat{C}_{6,q}^{6})\epsilon^{\mu\nu\rho\lambda}\left[-2im_X v_\rho\varepsilon_\nu^*\varepsilon_\lambda - i\tilde{P}_\rho\varepsilon_\nu^*\varepsilon_\lambda - \frac{iv_\nu}{m_X}\tilde{P}_\rho[\varepsilon_\lambda^* p_\varepsilon - \text{ c.c}]\right]\cdot \\ \left[\bar{u}_p\left(S_{N\mu} - \frac{v_\mu}{2m_N}K\cdot S_N\right)u_p\right]. \end{aligned} \tag{D.29}$$

The leading order of momentum is zero which means that only the first term in the first row contributes. In basis operators the scattering amplitude becomes

$$i\mathcal{M}_p^{A,b} = -2m_X\hat{\mathcal{A}}(\hat{C}_{6,q}^{(6)})S_X^\mu\bar{u}_p S_{N,\mu}u_p. \tag{D.30}$$

D.2.2.3 Type C

$$\begin{aligned} i\mathcal{M}_p^{A,c} = i\hat{\mathcal{A}}(\hat{C}_{8,q}^{6})\epsilon^{\mu\nu\rho\lambda}\left[i(-i)q_\rho\varepsilon_\nu^*\varepsilon_\lambda + \frac{v_\nu}{m_X}q_\rho[\varepsilon_\lambda^* p_\varepsilon - \text{ c.c}]\right]\cdot \\ \left[\bar{u}_p\left(S_{N\mu} - \frac{v_\mu}{2m_N}K\cdot S_N\right)u_p\right]. \end{aligned} \tag{D.31}$$

The leading order of momentum is quadratic (at first glance it looks linear, but one can prove that $\hat{S}^{\mu\nu}q_\nu S_{N\mu} = \mathcal{O}(q^2)$, see Eq. (E.10) and (E.12)). Therefor all terms contribute and the amplitude is

$$\begin{aligned} i\mathcal{M}_p^{A,c} = i\hat{\mathcal{A}}(\hat{C}_{8,q}^{(6)})\bigg(& -q^\nu\hat{S}_{\mu\nu}\bar{u}_p S_N^\mu u_p \\ & - \frac{i}{2m_N}S_X\cdot q\bar{u}_p K\cdot S_N u_p \\ & + \epsilon^{\mu\nu\rho\lambda}\frac{v_\nu}{m_X}q_\rho\left[\bar{S}_{\lambda\sigma}\tilde{P}^\sigma + S_{\lambda\sigma}q^\sigma\right]\bar{u}_p S_{N,\mu}u_p\bigg). \end{aligned} \tag{D.32}$$

D.2.2.4 Type D

$$\begin{aligned} i\mathcal{M}_p^{A,d} = i\hat{\mathcal{A}}(\hat{C}_{10,q}^{6})\left[(-i)q^\nu[\varepsilon_\nu^*\varepsilon_\mu + \text{ c.c}] + \frac{i}{m_X}v_\mu q^\nu[\varepsilon_\nu^* p_\varepsilon - \text{c.c}] + \frac{i}{m_X}[p_\varepsilon^* v\cdot\tilde{p} - \text{ c.c}]\right]\cdot \\ \left[\bar{u}_p\left(S_{N\mu} - \frac{v_\mu}{2m_N}K\cdot S_N\right)u_p\right]. \end{aligned} \tag{D.33}$$

The leading order of momentum is linear and hence only the first term on the first row give a contribution. Expressed in basis operators one get

$$i\mathcal{M}_p^{A,d} = 2\hat{\mathcal{A}}(\hat{C}_{10,q}^{(6)})S_{\mu\nu}q^\nu\bar{u}_p S_N^\mu u_p. \tag{D.34}$$

D.2.2.5 Type E

$$i\mathcal{M}_p^{A,e} = i\hat{\mathcal{A}}(\hat{C}^6_{12,q})\Big[i(-i)q^\nu[\varepsilon^*_\nu\varepsilon_\mu - \text{ c.c}] - \frac{v_\mu}{m_X}q^\nu[\varepsilon^*_\nu p_\varepsilon - \text{ c.c}] - \frac{1}{m_X}[p^*_\varepsilon v\cdot p\varepsilon_\mu + \text{ c.c}]\Big]\cdot \\ \Big[\bar{u}_p\Big(S_{N\mu} - \frac{v_\mu}{2m_N}K\cdot S_N\Big)u_p\Big] \tag{D.35}$$

The leading order of momentum is linear and thus the contribution comes from the first term of the first row. In basis operators the amplitude reads as

$$i\mathcal{M}_p^{A,e} = -2i\hat{\mathcal{A}}(\hat{C}^{(6)}_{12,q})q^\nu\bar{S}_{\mu\nu}\bar{u}_pS^\mu_Nu_p. \tag{D.36}$$

D.2.2.6 Gluon Current

By using Eq. (B.57) of [8],

$$J^G = -\frac{2m_G}{27}\bar{N}N, \tag{D.37}$$

the scattering amplitude is found to be

$$i\mathcal{M}_p^G = \frac{-2im_G}{27}\varepsilon^*_\mu\varepsilon^\mu\bar{u}_pu_p\hat{C}^{(6)}_1. \tag{D.38}$$

D.2.2.7 Dual Gluon Current

Taking the dual gluon current from Eq. (B.58) in [8],

$$J^\theta = -\Big[D\Big(\frac{\tilde{m}}{m_u}+\frac{\tilde{m}}{m_s}\Big)+F\Big(\frac{\tilde{m}}{m_u}-\frac{\tilde{m}}{m_s}\Big)+G\Big]\bar{u}_piq\cdot S_Nu_p + \ldots, \tag{D.39}$$

the amplitude is found to be

$$i\mathcal{M}_p^\theta = -i\varepsilon^*_\mu\varepsilon^\mu\bar{u}_piq\cdot S_Nu_p\hat{C}^{(6)}_2 \\ \times\Big[D\Big(\frac{\tilde{m}}{m_u}+\frac{\tilde{m}}{m_s}\Big)+F\Big(\frac{\tilde{m}}{m_u}-\frac{\tilde{m}}{m_s}\Big)+G\Big]. \tag{D.40}$$

D.2.3 Meson Interchange Diagram (Right Part of Fig. 3.1)

This time, J_q^P, J_q^A and J^θ contributes to leading order [8]. Since the DM now interacts with a meson, the hadronization of the quark/gluon currents takes a different form. The QCD Lagrangian for the meson is taken from Eq. (B.24) in [8].

$$\mathcal{L}_{\text{HBChPT}} \supset \frac{g_a}{f}\left(\bar{u}_piq\cdot S_Nu_p - \bar{u}_niq\cdot S_Nu_n\right)\pi^0 + \\ + \frac{\Delta u + \Delta d - 2\Delta S}{\sqrt{3}\,f}\left(\bar{u}_piq\cdot S_Nu_p + \bar{u}_niq\cdot S_Nu_n\right)\eta. \tag{D.41}$$

D.2.3.1 Pseudo Scalar Current

The pseudo scalar current is given in Eq. (B.45):

$$J^P_{u,d} = B_0 f m_{u,d} \left(\pm\pi^0 + \frac{1}{\sqrt{3}}\eta\right) + \ldots, \tag{D.42a}$$

$$J^P_s = -\frac{2}{\sqrt{3}} B_= f m_s \eta + \ldots. \tag{D.42b}$$

Consequently, the interaction Lagrangian (for a DM-proton interaction) is written as

$$\mathcal{L}_{\text{int},p} = f B_0 \chi^*_\nu \chi^\nu \left[\pi^0 \left(\hat{C}^6_{2,u} \cdot m_u - \hat{C}^6_{2,d} \cdot m_d\right) + \frac{\eta}{\sqrt{3}} \left(\hat{C}^6_{2,u} \cdot m_u - \hat{C}^6_{2,d} \cdot m_d - 2\hat{C}^6_{2,s} \cdot m_s\right)\right], \tag{D.43}$$

which gives a scattering amplitude, expressed in basis operators

$$\begin{aligned} i\mathcal{M}^P_p = \bar{u}_p iq \cdot S_N u_p \varepsilon^*_\mu \varepsilon^\mu B_0 i^2 \cdot \Bigg[& \frac{ig_a}{q^2 - m_\pi^2} \left(\hat{C}^6_{2,u} \cdot m_u - \hat{C}^6_{2,d} \cdot m_d\right) + \\ & + \frac{\Delta u + \Delta d - 2\Delta s}{\sqrt{3}\sqrt{3}} \frac{i}{q^2 - m_\eta^2} \left(\hat{C}^6_{2,u} \cdot m_u - \hat{C}^6_{2,d} \cdot m_d - 2\hat{C}^6_{2,s} \cdot m_s\right)\Bigg]. \end{aligned} \tag{D.44}$$

D.2.4 Axial Current

For the axial current of the meson exchange diagram Eq. (B.44) in [8] is used.

$$J^A_{(u,d),\mu} = f\left(\mp\partial_\mu \pi^0 - \frac{\partial_\mu \eta}{\sqrt{3}}\right) + \ldots \tag{D.45a}$$

$$J^A_{s,\mu} = \frac{2f}{\sqrt{3}} \partial_\mu \eta + \ldots \tag{D.45b}$$

where $\partial_\mu \pi^0 = \partial_\mu \eta = iq_\mu$. It is beneficial to define

$$\begin{aligned} \hat{\mathcal{B}}(\hat{C}^d_{n,q}) \equiv & \frac{ig_a}{q^2 - m_\pi^2} \left(\hat{C}^6_{2,u} \cdot m_u - \hat{C}^6_{2,d} \cdot m_d\right) \\ & + \frac{\Delta u + \Delta d - 2\Delta s}{\sqrt{3}\sqrt{3}} \frac{i}{q^2 - m_\eta^2} \left(\hat{C}^6_{2,u} \cdot m_u - \hat{C}^6_{2,d} \cdot m_d - 2\hat{C}^6_{2,s} \cdot m_s\right), \end{aligned} \tag{D.46}$$

since that allows for more compressed answers for the upcoming scattering amplitudes.

D.2.4.1 Type A

$$\begin{aligned} i\mathcal{M}^{A,a}_p = i2\bar{u}_p iq \cdot S_N u_p \hat{\mathcal{B}}(\hat{C}^6_{4,q}) \cdot \Bigg[& 2m_X v_\mu \varepsilon^*_\nu \varepsilon^\nu q^\mu + \\ & + (-i) i \varepsilon^*_\nu \varepsilon^\nu \tilde{P}^\mu q_\mu + \frac{2}{m_X} v \cdot q \varepsilon^*_\nu \tilde{p}^{\nu'} \varepsilon_\lambda \tilde{p}^\lambda \Bigg]. \end{aligned} \tag{D.47}$$

The leading order of momentum is in fact cubic, since $q \cdot v = \mathcal{O}(q^2)$ (see Eq. (E.10)). So the amplitude would consist of the first two terms (which both are of order 3 in momentum), however one can quickly see that this expression is not Galilean invariant. Luckily it does not render any big problem, since the amplitude is coupled to $\mathcal{Q}^{(6)}_{4,q}$ which already has a leading contribution from the contact diagram (see Eq. (D.27)). It is thus safe to ignore the scattering amplitude that arises in this case.

D.2.4.2 Type B

$$\begin{aligned} i\mathcal{M}^{A,b}_p = i^2 \bar{u}_p iq \cdot S_N u_p \hat{\mathcal{B}}(\hat{C}^6_{6,q}) \cdot \Bigg[& -2im_X q_\mu v_\rho \varepsilon^*_\nu \varepsilon_\lambda \\ & + (-i)\tilde{P}_\rho q_\mu \varepsilon^*_\nu \varepsilon_\lambda + \frac{-iv_\nu}{m_X} \tilde{P}_\rho [\varepsilon^*_\lambda p_\epsilon - \text{ c.c}] \Bigg] \epsilon^{\mu\nu\rho\sigma}. \end{aligned} \tag{D.48}$$

The first term is quadratic in momentum and thus the only one to contribute at leading order. Expressed in basis operators one have

$$i\mathcal{M}^{A,b}_p \approx 2m_X \hat{\mathcal{B}}(\hat{C}^6_{6,q}) iq \cdot S_X \bar{u}_p iq \cdot S_N u_p. \tag{D.49}$$

D.2.4.3 Type C

$$\begin{aligned} i\mathcal{M}^{A,c}_p = & \, i^2 \bar{u}_p iq \cdot S_N u_p \hat{\mathcal{B}}(\hat{C}^6_{8,q}) \cdot \\ & \left[(-i) iq_\rho q_\mu \varepsilon^*_\nu \varepsilon_\lambda + \frac{1}{m_X} v_\nu q_\rho q_\mu [\varepsilon^*_\lambda p_\epsilon - \text{ c.c}] \right] \epsilon^{\mu\nu\rho\lambda}. \end{aligned} \tag{D.50}$$

Both terms are zero, since $q_\alpha q_\beta \epsilon^{\alpha\beta\mu\nu} = 0$ and thus this scattering amplitude vanishes.

D.2.4.4 Type D

$$\begin{aligned} i\mathcal{M}^{A,d}_p = i^2 \bar{u}_p iq \cdot S_N u_p \hat{\mathcal{B}}(\hat{C}^6_{10,q}) \cdot \Bigg[& (-i) q^\nu q^\mu [\varepsilon^*_\nu \varepsilon_\mu + \text{ c.c}] \\ & + \frac{i}{m_X} v \cdot q [q^\nu \varepsilon^*_\nu p_\epsilon + \text{ c.c}] + \frac{i}{m_X} q^\mu [p^*_\epsilon v \cdot p \varepsilon_\mu - \text{ c.c}] \Bigg]. \end{aligned} \tag{D.51}$$

The leading order of momentum is cubic and only the first term contributes. In basis operators the scattering amplitude is

$$i\mathcal{M}^{A,c}_p \approx 2i \hat{\mathcal{B}}(\hat{C}^6_{10,q}) q^\nu q^\mu S_{\mu\nu} \bar{u}_p iq \cdot S_N u_p. \tag{D.52}$$

D.2.4.5 Type E

$$\begin{aligned} i\mathcal{M}^{A,e}_p = i^2 \bar{u}_p iq \cdot S_N u_p \hat{\mathcal{B}}(\hat{C}^6_{12,q}) \cdot \Bigg[& (-i) iq^\nu q^\mu [\varepsilon^*_\nu \varepsilon_\mu - \text{ c.c}] \\ & - \frac{1}{m_X} v \cdot q [q^\nu \varepsilon^*_\nu p_\epsilon + \text{ c.c}] - \frac{1}{m_X} q^\mu [p^*_\epsilon v \cdot p \varepsilon_\mu + \text{ c.c}] \Bigg]. \end{aligned} \tag{D.53}$$

The first term is actually zero thanks to anti-symmetrization. The third term is then the leading term (order three) but it is not Galilean invariant. Just as for type A however, this is not a problem as the associated operator $\mathcal{Q}^{(6)}_{12,q}$ get the leading contribution from the contact diagram.

E

Basis Operators and Their Coupling Constants

With all scattering amplitudes calculated, it is a good time to look into the effective Lagrangian and how it is comprised of the basis operators that were used to express said amplitudes. The effective scattering Lagrangian for a DM-proton interaction is

$$\mathcal{L}_{\text{eff, p}} = \sum_i c_{i,p} Q_{i,p}. \tag{E.1}$$

To include neutron scattering as well a second similar looking term, with $p \to n$ would be added, see Eq. (3.47). Note that this Q denotes the basis operator of the scattering amplitude, *and is therefor not the same as the $\mathcal{Q}$ that was used for the interaction operator*. Looking at all the scattering amplitudes in appendix D.2 there are two basis operators of order zero:

Basis operators of momentum order 0	
$Q^{(0)}_{1,p} = \varepsilon^*_\mu \varepsilon^\mu \bar{u}_p u_p$	$Q^{(0)}_{2,p} = S^\mu_X \bar{u}_p S_{N,\mu} u_p$

Table E.1: All basis operators of order zero that span the scattering amplitudes.

There are a total of nine basis operators of momentum order 1.

Basis operators of momentum order 1	
$Q^{(1)}_{1,p} = \varepsilon^*_\mu \varepsilon^\mu \bar{u}_p iq \cdot S_N u_p$	$Q^{(1)}_{2,p} = iq \cdot S_X \bar{u}_p u_p$
$Q^{(1)}_{3,p} = \varepsilon^*_\mu \varepsilon^\mu \bar{u}_p v_\perp \cdot S_N u_p$	$Q^{(1)}_{4,p} = v_{\perp,\mu} S^\mu_X \bar{u}_p u_p$
$Q^{(1)}_{5,p} = i\epsilon^{\alpha\beta\mu\nu} v_\alpha q_\beta S_{X,\mu} \bar{u}_p S_{N,\nu} u_p$	$Q^{(1)}_{6,p} = \bar{S}_{\mu\nu} q^\nu v^\mu_\perp \bar{u}_p u_p$
$Q^{(1)}_{7,p} = q^\nu \bar{S}_{\mu\nu} \bar{u}_p S^\mu_N u_p$	$Q^{(1)}_{8,p} = v_\perp \cdot S \cdot q \bar{u}_p u_p$
$Q^{(1)}_{9,p} = q^\nu S_{\mu\nu} \bar{u}_p S^\mu_N u_p$	

Table E.2: All basis operators of order one that span the scattering amplitudes.

Further, there are six basis operators of momentum order 2.

Basis operators of momentum order 2	
$Q^{(2)}_{1,p} = iq \cdot S_X \bar{u}_p iq \cdot S_N u_p$	$Q^{(2)}_{2,p} = q^\nu \bar{S}_{\mu\nu} \bar{u}_p W^\mu u_p$
$Q^{(2)}_{3,p} = q \cdot S \cdot q \bar{u}_p u_p$	$Q^{(2)}_{4,p} = q^\nu S_{\mu\nu} \bar{u}_p W^\mu u_p$
$Q^{(2)}_{5,p} = i\epsilon^{\mu\nu\rho\lambda} v_\nu q_\rho S_{\lambda\sigma} q^\sigma \bar{u}_p S_{N,\mu} u_p$	
$Q^{(2)}_{6,p} = -q_\nu \hat{S}^{\mu\nu} \bar{u}_p S_{N,\mu} u_p - \frac{i}{2m_p} S^\nu_X \cdot q \bar{u}_p K \cdot S_N u_p + \epsilon^{\mu\nu\rho\lambda} \frac{v_\nu}{m_X} q_\rho \bar{S}_{\lambda\sigma} \tilde{P}^\sigma \bar{u}_p S_{N,\mu} u_p$	

Table E.3: All basis operators of order two that spans the scattering amplitudes.

Additionally, there is one basis operator of order three:

$$Q^{(3)}_p = q \cdot S \cdot q \bar{u}_p iq \cdot S_N u_p. \tag{E.2}$$

The constants coupled to each of these basis operators are enumerated in the same way to easier see which constants are coupled to which basis operator. One should however note that in $c^{(0)}_{1,p}$ the super-index (0) is just a notation and carries no practical information besides than to show which basis operator it is tied to. Tables E.4-E.6 showcase all these constants.

Constants of basis operators of order zero
$c^{(0)}_{1,p} = \left[\hat{c}^{(6)}_{1,u} \cdot \sigma^p_u + \hat{c}^{(6)}_{1,d} \cdot \sigma^p_d + \hat{c}^{(6)}_{1,s} \cdot \sigma^p_s\right] + 2m_X - \frac{2m_G}{27} \hat{C}^{(6)}_1$
$c^{(0)}_{2,p} = 2m_X \hat{\mathcal{A}}(\hat{C}^{(6)}_{6,q})$

Table E.4: The constants coupled to the zeroth order of basis operators

The constant $c^{(1)}_{1,p}$ is very long and unsuited to being displayed in a table, so instead it is given below as an ordinary equation, the rest of the constants related to basis operators of order one are collected in table E.5.

$$\begin{aligned} c^{(1)}_{1,p} = -B_0 \Bigg[& g_a \left(\hat{C}^{(6)}_{2,u} m_u + \hat{C}^{(6)}_{2,d} m_d\right) \frac{1}{q^2 - m_\pi^2} + \\ & \frac{\Delta u + \Delta d - 2\Delta s}{3} \left(\hat{C}^{(6)}_{2,u} m_u + \hat{C}^{(6)}_{2,d} m_d - 2\hat{C}^{(6)}_{2,s} m_s\right) \frac{1}{q^2 - m_\eta^2} \Bigg] + \\ & \hat{C}^{(6)}_2 \Bigg\{ - \left[D\left(\frac{\tilde{m}}{m_u} + \frac{\tilde{m}}{m_d}\right) + F\left(\frac{\tilde{m}}{m_u} - \frac{\tilde{m}}{m_d}\right) + G \right] + \\ & \frac{q^2}{2} \left[g_a \frac{1}{q^2 - m_\pi^2} \left(\frac{\tilde{m}}{m_u} - \frac{\tilde{m}}{m_d}\right) + \frac{\Delta u + \Delta d - 2\Delta s}{3} \frac{1}{q^2 - m_\eta^2} \left(\frac{\tilde{m}}{m_u} + \frac{\tilde{m}}{m_d} - \frac{2\tilde{m}}{m_s}\right) \right] \Bigg\} \end{aligned} \tag{E.3}$$

Constants of basis operators of order one	
$c^{(1)}_{2,p} = -\left(2\hat{C}^{(6)}_{7,u} + \hat{C}^{(6)}_{7,d}\right)$	$c^{(1)}_{3,p} = 2m_X\hat{\mathcal{A}}(\hat{C}^{(6)}_{4,q})$
$c^{(1)}_{4,p} = -2m_X\left(2\hat{C}^{(6)}_{5,u} + \hat{C}^{(6)}_{5,d}\right)$	$c^{(1)}_{5,p} = 2m_X\hat{\mathcal{W}}(\hat{C}^{(6)}_{5,q})$
$c^{(1)}_{6,p} = 2\left(2\hat{C}^{(6)}_{11,u} + \hat{C}^{(6)}_{11,d}\right)$	$c^{(1)}_{7,p} = -2\hat{\mathcal{A}}(\hat{C}^{(6)}_{12,q})$
$c^{(1)}_{8,p} = 2i\left(2\hat{C}^{(6)}_{9,u} + \hat{C}^{(6)}_{9,d}\right)$	$c^{(1)}_{9,p} = -2i\hat{\mathcal{A}}(\hat{C}^{(6)}_{10,q})$

Table E.5: The constants coupled to the first order of basis operators

Constants of basis operators of order two	
$c^{(2)}_{1,p} = 2m_X\hat{\mathcal{B}}(\hat{C}^{(6)}_{6,q})$	$c^{(2)}_{2,p} = -2i\hat{\mathcal{W}}(\hat{C}^{(6)}_{11,q})$
$c^{(2)}_{3,p} = -\frac{1}{m_X}\left(2\hat{C}^{(6)}_{11,u} + \hat{C}^{(6)}_{11,d}\right)$	$c^{(2)}_{4,p} = 2\hat{\mathcal{W}}(\hat{C}^{(6)}_{9,q})$
$c^{(2)}_{5,p} = \frac{1}{m_X}\hat{\mathcal{A}}(\hat{C}^{(6)}_{8,q})$	$c^{(2)}_{6,p} = \hat{\mathcal{A}}(\hat{C}^{(6)}_{8,q})$

Table E.6: The constants coupled to the second order of basis operators

The sole basis operator of order three has a coupling constant which is found to be

$$c^{(3)}_{1,p} = 2\hat{\mathcal{B}}(\hat{C}^{(6)}_{10,q}). \tag{E.4}$$

E.1 Comparison With the Non-Relativistic Approach

As one of the main focuses of this thesis is to investigate how the relativistic approach of DM-nucleon interaction may differ from the non-relativistic approach, it will be of importance to express the basis operators that was found in the previous section in such a way that it is comparable to what has been done in a manifestly non-relativistic way. It is important to note that the basis operators found in section E already are non-relativistic and obey Galilean symmetry even though they are written in Lorentz notation. The following procedure is therefor not to impose some sort of non-relativistic limit on the basis operators, but rather to rewrite them in a manifestly non-relativistic notation. The method for this aligns with [21].

The polarization vectors ε^μ_s are rewritten as

$$\begin{aligned} \varepsilon^{s,\mu} &\simeq \begin{pmatrix} \frac{1}{2m_X}(\boldsymbol{P}+\boldsymbol{q})\cdot\boldsymbol{e}^s \\ \boldsymbol{e}^s \end{pmatrix}, \\ \varepsilon^{s',\mu*} &\simeq \begin{pmatrix} \frac{1}{2m_X}(\boldsymbol{P}-\boldsymbol{q})\cdot\boldsymbol{e}^{s'} \\ \boldsymbol{e}^{s'} \end{pmatrix}. \end{aligned} \tag{E.5}$$

Bold symbols will from here on note the three-vector. Discarding the polarization state to simplify the notation and evaluating $\varepsilon^*_\mu \varepsilon^\mu$ in leading order of momentum (which is zero) yields

$$\begin{aligned}\varepsilon^*_\mu \varepsilon^\mu &= \frac{1}{4m_X^2}(\boldsymbol{P}-\boldsymbol{q})\cdot\boldsymbol{e}\cdot(\boldsymbol{P}-\boldsymbol{q})\cdot\boldsymbol{e'} - \boldsymbol{e}\cdot\boldsymbol{e'} \\ &\approx -\boldsymbol{e}\cdot\boldsymbol{e'}.\end{aligned} \tag{E.6}$$

An elaborate work to rewrite the rest of the relevant variables now follows. The reference vector v^ν will be chosen to be timelike, i.e. $v^\nu = (1,0,0,0)$ which allows W_μ to be expressed as

$$\begin{aligned} W_\mu &= v^\alpha q^\lambda S_N^\beta \epsilon_{\mu\alpha\beta\lambda} = q^\lambda S_N^\beta \epsilon_{\mu 0\beta\lambda} \\ &= -q^\lambda S_N^\beta \epsilon_{0\mu\beta\lambda} = q^\lambda S_N^\beta \epsilon_{0\mu\lambda\beta} \\ &= \begin{cases} 0\,, & \mu = 0 \\ (\boldsymbol{q}\times\boldsymbol{S_N})_\mu\,, & \mu = i \end{cases}. \end{aligned} \tag{E.7}$$

With $i = 1,2,3$.

In the same way, S_X^μ is evaluated.

$$\begin{aligned} S_X^\mu &= i\hat{S}^{\mu\nu} v_\nu = i\varepsilon^*_\rho \varepsilon_\lambda \epsilon^{\mu\nu\rho\lambda} v_\nu \\ &= i\varepsilon^*_\rho \varepsilon_\lambda \epsilon^{\mu 0\rho\lambda} = -i\varepsilon^*_\rho \varepsilon_\lambda \epsilon^{0\mu\rho\lambda} \\ &= \begin{cases} 0\,, & \mu = 0, \\ -i(\boldsymbol{e'}\times\boldsymbol{e})_\mu\,, & \mu = i \end{cases}. \end{aligned} \tag{E.8}$$

Hence, the notation $\boldsymbol{S_X}_i \equiv -i(\boldsymbol{e'}\times\boldsymbol{e})_i$ will be used.

One of the terms in $Q_{6,p}^{(2)}$ contains $\hat{S}_{\mu\nu}$ (see table E.3) and thus it needs to be considered as well. The full term is $-q_\nu \hat{S}^{\mu\nu}\bar{u}_p S_{N,\mu} u_p$ but it will suffice in investigating $q^\nu \hat{S}_{\mu\nu} S_{N,\mu}$. For this evaluation it is first necessary to remark on two identities that may not be obvious, first (as shortly noted during the calculations of the scattering amplitudes) q^0 actually is of order two in momentum. This is due to that the energy of the incoming and outgoing DM can be expressed as:

$$E_{\text{in}} = m_X + \frac{\boldsymbol{p}^2}{2m_X}\,, \quad E_{\text{out}} = m_X + \frac{\boldsymbol{p'}^2}{2m_X}. \tag{E.9}$$

This allows one to interpret q^0 as

$$q^0 = E_{\text{in}} - E_{\text{out}} = m_X - m_X + \frac{\boldsymbol{p}^2}{2m_X} - \frac{\boldsymbol{p'}^2}{2m_X} = \frac{\boldsymbol{P}\cdot\boldsymbol{q}}{2m_X}. \tag{E.10}$$

Further, following that $S_N \cdot v = 0$ and with v set to be time-like, S_N^0 is forced to be zero. With these two in mind, one can continue evaluating $q^\nu \hat{S}_{\mu\nu} S_{N,\mu}$.

$$\begin{aligned}
Q_{6,p}^{(2)} : q^\nu \hat{S}_{\mu\nu} S_{N,\mu} &= \varepsilon_\rho^* \varepsilon_\lambda \epsilon^{\mu\nu\rho\lambda} q_\nu S_{N,\mu} \\
&\approx e_i' e_j q_\nu S_{N,\mu} \epsilon^{\mu\nu ij} \\
&= -e_i' e_j q_0 S_{N,k} \epsilon^{ijk0} - e_i' e_j q_k S_{N,0} \epsilon^{ij0k} + e_i' e_j q_k S_{N,\ell} \cancel{\epsilon^{ijk\ell}} \\
&= +(\boldsymbol{e'} \times \boldsymbol{e}) \cdot \boldsymbol{S_N} q^0 - (\boldsymbol{e'} \times \boldsymbol{e}) \cdot \boldsymbol{q} \cancel{S_N^0} + 0 \\
&= +i \boldsymbol{S_X} \cdot \boldsymbol{S_N} q^0 - 0 \\
&= i \frac{\boldsymbol{P} \cdot \boldsymbol{q}}{2m_X} \boldsymbol{S_X} \cdot \boldsymbol{S_N}.
\end{aligned} \tag{E.11}$$

Next up, basis operators containing $\bar{S}_{\mu\nu}$ needs attending. It is clear from its definition (see Eq. (D.4c)) that both $\bar{S}_{00}$ and $\bar{S}_{0i} = 0$. Therefor it is enough to consider $\bar{S}_{ij}$

$$\bar{S}_{ij} = \frac{1}{2}\left(\varepsilon_i^* \varepsilon_j - \varepsilon_i \varepsilon_j^*\right) \approx \frac{1}{2} (\boldsymbol{e} \times \boldsymbol{e'})^k \epsilon_{ijk} = \frac{i}{2} \boldsymbol{S_X}^k \epsilon_{ijk}. \tag{E.12}$$

There are three basis operators containing $\bar{S}_{\mu\nu}$ (see tables E.2 and E.3) which now are presented as:

$$Q_{6,p}^{(1)} : \bar{S}_{\mu\nu} v_\perp^\mu q^\nu \approx \frac{i}{2} S_X^k \epsilon_{ijk} v_\perp^i q^j = \frac{i}{2} \boldsymbol{S_X} \cdot \left(\boldsymbol{v}_\perp \times \boldsymbol{q}\right). \tag{E.13}$$

$$\begin{aligned}
Q_{2,p}^{(2)} : q^\nu \bar{S}_{\mu\nu} W^\mu &\approx \frac{i}{2} S_X^k \epsilon_{ijk} \left(\left(\boldsymbol{q} \times \boldsymbol{S_N}\right) \cdot \boldsymbol{q}\right) \\
&= \frac{i}{2} S_X^k \left(S_{N,k} q^2 - q_k \left(\boldsymbol{q} \cdot \boldsymbol{S_N}\right)\right).
\end{aligned} \tag{E.14}$$

$$\begin{aligned}
Q_{6,p}^{(2)} : \epsilon^{\mu\nu\rho\lambda} \frac{v_\nu}{m_X} q_\rho \bar{S}_{\lambda\sigma} \tilde{P}^\sigma S_{N,\mu} &= \frac{1}{m_X} \epsilon^{\mu 0\rho\lambda} q_\rho \bar{S}_{\lambda\sigma} \tilde{P}^\sigma \\
&\approx -\frac{i}{2m_X} \epsilon^{0ijk} \epsilon_{i\ell m} S_X^m q_k \tilde{P}^\ell S_{N,j} \\
&= -\frac{i}{2m_X} \left[\delta_\ell^j \delta_m^k - \delta_m^j \delta_\ell^k\right] S_X^m q_k \tilde{P}^\ell S_{N,j} \\
&= -\frac{i}{2m_X} \left(\boldsymbol{S_X} \cdot \boldsymbol{q} \boldsymbol{P} \cdot \boldsymbol{S_N} - \boldsymbol{S_X} \cdot \boldsymbol{S_N} \boldsymbol{q} \cdot \boldsymbol{P} \right).
\end{aligned} \tag{E.15}$$

Lastly, there are six operators that contain $S_{\mu\nu}$. These correspond to the non-relativistic basis operators that are unique to spin-1, i.e. $\mathcal{O}_{17,18,19,20}$ as well as the order three operator $\mathcal{O}_1^{(3)}$.

E.1.1 Matching onto the basis operators of Catena et.Al

With all our basis operators expressed in a manifestly non-relativistic way, it can be matched onto the set of basis operators stated by Catena et. Al in [21]. Table 3.1 in section 3.7.2 showcase all of these operators and the relation between them and the basis operators found in this thesis are straightforward to find via identification after the work done above. These relations are seen in table E.7

Relation between $Q^{(d)}_{n,p}$ and $\mathcal{O}_{n,p}$	
$Q^{(0)}_{1,p} = -\mathcal{O}_{1,p}$	$Q^{(0)}_{2,p} = -\mathcal{O}_{4,p}$
$Q^{(1)}_{1,p} = -m_p\mathcal{O}_{10,p}$	$Q^{(1)}_{2,p} = +m_p\mathcal{O}_{11,p}$
$Q^{(1)}_{3,p} = +\mathcal{O}_{7,p}$	$Q^{(1)}_{4,p} = -\mathcal{O}_{8,p}$
$Q^{(1)}_{5,p} = +m_p\mathcal{O}_{9,p}$	$Q^{(1)}_{6,p} = +\frac{m_p}{2}\mathcal{O}_{5,p}$
$Q^{(1)}_{7,p} = -\frac{m_p}{2}\mathcal{O}_{9,p}$	$Q^{(1)}_{8,p} = +im_p\mathcal{O}_{17,p}$
$Q^{(1)}_{9,p} = +im_p\mathcal{O}_{18,p}$	
$Q^{(2)}_{1,p} = -m_p^2\mathcal{O}_{6,p}$	$Q^{(2)}_{2,p} = -\frac{i}{2}m_p^2\mathcal{O}_{6,p} + \frac{i}{2}q^2\mathcal{O}_{4,p}$
$Q^{(2)}_{3,p} = +m_p^2\mathcal{O}_{19,p}$	$Q^{(2)}_{4,p} = -m_p^2\mathcal{O}_{20,p}$
$Q^{(2)}_{5,p} = -m_p^2\mathcal{O}_{20,p}$	$Q^{(2)}_{6,p} = +m_p^2\mathcal{O}_{14,p}$
$Q^{(3)}_{1,p} = +m_p^3\mathcal{O}^{(3)}_{1,p}$	

Table E.7: The relation between the basis operators of this thesis, $Q^{(d)}_{n,p}$ and the ones established in [21].

Further one can now state the constants $c^{\mathrm{NR}}_{n,p}$ from Eq. (3.47). These will be presented in table E.8.

Relation between $c_{n,p}^{(d)}$ and $c_{n,p}^{\mathrm{NR}}$	
$c_{1,p}^{\mathrm{NR}} = -c_{1,p}^{(0)}$	$c_{4,p}^{\mathrm{NR}} = -c_{2,p}^{(0)} + \frac{iq^2}{2} c_{2,p}^{(2)}$
$c_{5,p}^{\mathrm{NR}} = \frac{m_p}{2} c_{6,p}^{(1)}$	$c_{6,p}^{\mathrm{NR}} = -m_p^2 c_{1,p}^{(2)} - \frac{im_p^2}{2} c_{2,p}^{(2)}$
$c_{7,p}^{\mathrm{NR}} = c_{3,p}^{(1)}$	$c_{8,p}^{\mathrm{NR}} = -c_{4,p}^{(1)}$
$c_{9,p}^{\mathrm{NR}} = m_p c_{5,p}^{(1)} - \frac{m_p}{2} c_{7,p}^{(1)}$	$c_{10,p}^{\mathrm{NR}} = -m_p c_{1,p}^{(1)}$
$c_{11,p}^{\mathrm{NR}} = m_p c_{2,p}^{(1)}$	$c_{14,p}^{\mathrm{NR}} = m_p^2 c_{2,p}^{(2)}$
$c_{17,p}^{\mathrm{NR}} = im_p c_{8,p}^{(1)}$	$c_{18,p}^{\mathrm{NR}} = im_p c_{9,p}^{(1)}$
$c_{19,p}^{\mathrm{NR}} = m_p^2 c_{3,p}^{(2)}$	$c_{20,p}^{\mathrm{NR}} = -m_p^2 \left(c_{4,p}^{(2)} + c_{5,p}^{(2)} \right)$
$c_{(3),p}^{\mathrm{NR}} = m_p^3 c_{1,p}^{(3)}$	

Table E.8: All non-relativistic constants $c_{n,p}^{\mathrm{NR}}$ as found from the constants $c_{n,p}^{(d)}$ (see table E.4-E.6) and the relation between $Q_{n,p}^{(d)}$ and $\mathcal{O}_{n,p}$ in table E.7.

Table E.8, together with the three tables E.4,E.5 and E.6 lies as foundation to table 5.2 shown in the results. Attention should be brought to some interesting co-dependencies in the mapping between $c_{n,p}^{(d)}$ and $c_{n,p}^{\mathrm{NR}}$ which are all discussed in detail in the results, see section 5.

$$\mathcal{L}_{\text{int}} = ... + \hat{C}^{(6)}_{3,q}\mathcal{Q}^{(6)}_{3,q} + ... = ... + \hat{C}^{(6)}_{3,q} i\bar{q}\gamma^\mu q X^*_\nu \overleftrightarrow{\partial}_\mu X^\nu + ...$$

$$\begin{aligned}\mathcal{Q}^{(6)}_{3,q} &= i\bar{q}\gamma^\mu q X^*_\nu \overleftrightarrow{\partial}_\mu X^\nu \\ &\approx i\bar{q}\gamma^\mu q \chi^*_\nu \overleftrightarrow{\partial}_\mu \chi^\nu + \left(\frac{2v_\mu}{m_X}\partial^\rho \chi^*_\rho \partial_\lambda \chi^\lambda + 2m_X v_\mu \chi^*_\nu \chi^\nu\right)\bar{q}\gamma^\mu q\end{aligned} \tag{E.16}$$

$$Q^{(2)}_{2,p} = q^\nu \bar{S}_{\mu\nu}\bar{u}_p W^\mu u_p \overset{\text{non.rel}}{\propto} \mathcal{O}_6 + \mathcal{O}_4 \tag{E.17}$$

$$\mathcal{Q}^{(6)}_{3,q} \tag{E.18}$$

$$Q^{(d)}_{n,p} \qquad\qquad c^{(d)}_{n,p} \tag{E.19}$$

$$\mathcal{Q}^{(6)}_{n,q} \tag{E.20}$$

$$\begin{aligned}Q^{(1)}_{1,p} &= \varepsilon^*_\mu \varepsilon^\mu \bar{u}_p iq \cdot S_N u_p \\ \implies \mathcal{O}^{\text{NR}}_{10,p} &= -i\mathbb{1}_X \cdot \left(\boldsymbol{S}_N \cdot \frac{\boldsymbol{q}}{m_p}\right)\end{aligned} \tag{E.21}$$

DEPARTMENT OF PHYSICS
CHALMERS UNIVERSITY OF TECHNOLOGY
Gothenburg, Sweden
www.chalmers.se

AVANCEZ
1829

CHALMERS
UNIVERSITY OF TECHNOLOGY